Calcium Release and Its Voltage Dependence in Frog Cut Muscle Fibers Equilibrated with 20 mM EGTA

PAUL C. PAPE, DE-SHIEN JONG, and W. KNOX CHANDLER

From the Department of Cellular and Molecular Physiology, Yale University School of Medicine, New Haven, Connecticut 06510-8026

ABSTRACT Sarcoplasmic reticulum (SR) Ca release was studied at 13–16°C in cut fibers (sarcomere length, 3.4–3.9 μm) mounted in a double Vaseline-gap chamber. The amplitude and duration of the action-potential stimulated free [Ca] transient were reduced by equilibration with end-pool solutions that contained 20 mM EGTA with 1.76 mM Ca and 0.63 mM phenol red, a maneuver that appeared to markedly reduce the amount of Ca complexed by troponin. A theoretical analysis shows that, under these conditions, the increase in myoplasmic free [Ca] is expected to be restricted to within a few hundred nanometers of the SR Ca release sites and to have a time course that essentially matches that of release. Furthermore, almost all of the Ca that is released from the SR is expected to be rapidly bound by EGTA and exchanged for protons with a 1:2 stoichiometry. Consequently, the time course of SR Ca release can be estimated by scaling the ΔpH signal measured with phenol red by $-\beta/2$. The value of β, the buffering power of myoplasm, was determined in fibers equilibrated with a combination of EGTA, phenol red, and fura-2; its mean value was 22 mM/pH unit. The Ca content of the SR (expressed as myoplasmic concentration) was estimated from the total amount of Ca released by either a train of action potentials or a depleting voltage step; its mean value was 2,685 μM in the action-potential experiments and 2,544 μM in the voltage-clamp experiments. An action potential released, on average, 0.14 of the SR Ca content with a peak rate of release of ~5 %/ms. A second action potential, elicited 20 ms later, released only 0.6 times as much Ca (expressed as a fraction of the SR content), probably because Ca inactivation of Ca release was produced by the first action potential. During a depolarizing voltage step to 60 mV, the rate of Ca release rapidly increased to a peak value of ~3 %/ms and then decreased to a quasi-steady level that was only 0.6 times as large; this decrease was also probably due to Ca inactivation of Ca release. SR Ca release was studied with small step depolarizations that open no more than one SR Ca channel in 7,000 and increase the value of spatially averaged myoplasmic free [Ca] by

Dr. Pape's present address is Département de Physiologie et Biophysique, Faculté de Médecine, Université de Sherbrooke, Québec, Canada J1H5N4.

Dr. Jong's current address is Department of Animal Science, National Taiwan University, Taipei, Taiwan, R.O.C.

Address correspondence to Dr. W. K. Chandler, Department of Cellular and Molecular Physiology, Yale University School of Medicine, 333 Cedar Street, New Haven, Connecticut 06510-8026.

J. GEN. PHYSIOL. © The Rockefeller University Press · 0022-1295/95/08/259/78 $2.00
Volume 106 August 1995 259–336

only 0.2 nM. With such small depolarizations, SR Ca release is steeply voltage dependent, with a mean *e*-fold factor of 3.5 mV. Under these conditions, if the spatial distribution of open release sites is random, EGTA is expected to shield each open site from any significant increase in free [Ca] produced by Ca flux through a neighboring open site. Consequently, the open state of any particular site would not be expected to have been caused by Ca from another open site. For this reason, it seems unlikely that SR Ca release itself—by Ca-induced Ca release, by the positive feedback model proposed by Pizarró, Csernoch, Uribe, Rodríguez, and Ríos (1991. *Journal of General Physiology.* 97:913–947), or by some other mechanism —was able to contribute to the steep voltage dependence of Ca release. Rather, it seems likely that the steep voltage dependence of Ca release directly reflects the activity of the voltage sensor in the membranes of the transverse tubular system that regulates a single release site. Such a site might consist of a single SR Ca channel or a collection of channels that function as a singly gated unit (for example, a single voltage-gated channel and neighboring channel[s] that are slaved to it).

INTRODUCTION

In studies on excitation-contraction coupling in intact and cut skeletal muscle fibers, activation is usually produced by depolarization of the membranes of the transverse tubular system by either an action potential or a voltage-clamp depolarization. Soon after depolarization, Ca ions are released from the sarcoplasmic reticulum (SR) into the myoplasm where the concentration of free Ca increases. This causes Ca to bind to the various intrinsic Ca buffers, such as the Ca-regulatory sites on troponin that are responsible for the activation of contraction. In addition, Ca may also influence the release process itself. Under certain conditions, an increase in myoplasmic free [Ca] can activate the release of additional Ca from the SR, a positive feedback process known as Ca-induced Ca release (Endo, Tanaka, and Ebashi, 1968; Ford and Podolsky, 1968; Fabiato, 1984). An increase in [Ca] can also reduce the ability of the SR to release additional Ca (Baylor, Chandler, and Marshall, 1983; Simon, Schneider, and Szúcs, 1985; Baylor and Hollingworth, 1988; Schneider and Simon, 1988; Simon, Klein, and Schneider, 1991). In this article, this negative feedback process is called Ca inactivation of Ca release.

The experiments described in this article were carried out with two goals in mind. The first was to reduce the increase in myoplasmic free [Ca] that occurs during stimulation and to limit it spatially to distances close to the SR Ca release sites. This should reduce the ability of Ca to regulate release and thereby should facilitate the study of voltage-dependent regulation. The second goal was to develop a method to measure SR Ca release under these conditions. Both goals can be achieved with a large concentration of an extrinsic myoplasmic Ca buffer and an optical signal that monitors the concentration of complexed Ca. The first studies of this type were carried out by Rakowski, Best, and James-Kracke (1985) with arsenazo III. Subsequent studies have been carried out by Baylor and Hollingworth (1988) with fura-2 (Grynkiewicz, Poenie, and Tsien, 1985), by Jacquemond, Csernoch, Klein, and Schneider (1991) with a combination of fura-2 and 1,2-*bis*-[*o*-aminophenoxy]ethane-*N*,*N*,*N*′,*N*′-tetraacetic acid (BAPTA) (Tsien, 1980), and by Csernoch, Jacquemond, and Schneider (1993) with a combination of fura-2 and derivatives of

BAPTA with different Ca affinities. The approach that we eventually adopted was to use a large concentration of ethyleneglycol-bis-(β-aminoethyl ether)-*N,N'*-tetraacetic acid (EGTA) for the Ca buffer and phenol red to measure the change in pH that occurs when EGTA binds Ca and releases protons.

The EGTA-phenol red method, as well as many other methods that use a large concentration of Ca buffer, offer several advantages for the estimation of SR Ca release. One is that the attenuation of the free [Ca] transient reduces mechanical activation and the associated optical movement artifacts. A second advantage is that the estimate of SR Ca release is direct and independent of the properties of the various intrinsic myoplasmic Ca buffers. In most of the methods first used to estimate SR Ca release (Baylor et al., 1983; Melzer, Ríos, and Schneider, 1984, 1987; Klein, Simon, and Schneider, 1990), free [Ca] transients were used to calculate the concentration of Ca that was expected to have been bound by the intrinsic myoplasmic Ca buffers. The total amount of myoplasmic [Ca], free and bound, was then taken as an estimate of the amount of Ca released from the SR. A third advantage of the EGTA-phenol red method is that it is extremely sensitive. As a result, very small rates of SR Ca release can be measured under conditions in which EGTA is expected to shield each open release site from any significant increase in free [Ca] produced by Ca flux through neighboring open sites.

This article describes some of the properties of Ca signals, including the voltage dependence associated with very small rates of SR Ca release, in fibers equilibrated with solutions that contain 20 mM EGTA and 1.76 mM Ca. As far as we can tell, the presence of EGTA appears to have had relatively little effect on the function of SR Ca channels and their gating by the voltage sensors in the membranes of the transverse tubular system. The principle modulatory effect of EGTA appears to be a reduction in Ca inactivation of Ca release, as described in the following article (Jong, Pape, Baylor, and Chandler, 1995). Many of the theoretical properties of the EGTA-phenol red method are described in Appendix A. The amplitude and time course of the expected changes in myoplasmic free [Ca] near SR Ca channels are described in Appendices B–D. Although the numerical examples in these appendices apply specifically to our experiments on frog cut muscle fibers, many of the ideas and equations may be applicable to other cells that contain Ca channels in either their internal or external membranes.

Preliminary reports of some of these results have appeared (Chandler, Jong, and Pape, 1992, 1994; Chandler, Hirota, Jong, and Pape, 1993; Pape, Jong, and Chandler, 1994).

MATERIALS AND METHODS

The experiments were carried out at 13–16°C on frog cut twitch fibers (Hille and Campbell, 1976) isolated from *Rana temporaria* that were adapted to 5°C. A fiber segment was mounted in a double Vaseline-gap chamber, similar to the one used by Kovács, Ríos, and Schneider (1983), at a sarcomere length of 3.4–3.9 μm. Soon after mounting, the surface membranes in the end pools were made permeable to small molecules and ions by a 2-min exposure to 0.01% saponin in a K-glutamate solution (action-potential experiments) or a Cs-glutamate solution (voltage-clamp experiments) that contained 20 mM EGTA plus 1.76 mM Ca. The end pools were then rinsed thoroughly with the same solution without saponin and the central-pool solution was changed to

Ringer's solution (action-potential experiments) or a tetraethylammonium (TEA)-gluconate solution (voltage-clamp experiments). The composition of the solutions is given below.

The chamber was then transferred to the experimental apparatus where electrical connections were made to the solutions in the two end pools and in the central pool. One of the end pools, denoted by 1, was used to measure potential and the other end pool, denoted by 2, was used to inject current. The central pool was maintained at earth potential. The potential in end pool 1 was maintained at −90 mV by passing a small holding current into end pool 2. Additional experimental details are given in Irving, Maylie, Sizto, and Chandler (1987) and Maylie, Irving, Sizto, and Chandler (1987*b*).

During the course of an experiment, for periods of time as long as 4 h, eight signals were monitored: six optical signals ($O_1, \ldots, O_6$, corresponding to three wavelengths, each at two planes of linear polarization) and two electrical signals (V_1, the voltage in the voltage-measuring end pool, and I_2, the current injected into the current-passing end pool and collected in the central pool). Each signal was amplified and filtered by a 0.6–10 kHz eight-pole Bessel filter. The output from each filter was connected to a programmable multiplexer and was sampled by a sixteen bit A/D converter. Linear interpolation was used with active signals so that a single set of sample times would apply to the data from each of the eight signals.

Composition of Internal and External Solutions

The K-glutamate solution that was used in the end pools in the action-potential experiments (except for the one in Fig. 1 *A*) contained 45 mM K-glutamate, 20 mM EGTA as a combination of K and Ca salts, 6.8 mM $MgSO_4$, 5.5 mM Na_2-ATP, 20 mM K_2-creatine phosphate, 5 mM K_3-phospho(enol)pyruvate, and 5 mM 3-[*N*-morpholino]-propanesulfonic acid (MOPS). The concentrations of Ca-complexed and Ca-free EGTA were 1.76 and 18.24 mM, respectively. The pH was adjusted to 7.0 by the addition of KOH; at this pH, the calculated concentrations of free Ca and free Mg were 0.036 μM and 1 mM, respectively.

The Cs-glutamate solution that was used in the end pools in the voltage-clamp experiments was similar to the K-glutamate solution except that Na and K ions were replaced with Cs. This solution was made by passage of a solution that contained the Na salts of ATP, creatine phosphate, and phospho(enol)pyruvate through a Cs-loaded ion exchange column (AG 50W-X8 resin, mesh size 100–200, from BIO-RAD, Richmond, CA). The concentration of Na, measured with a flame photometer (model M400 from Corning Glassworks, Medfield, MA), was <1 mM. This solution was added to the other ingredients in which K was replaced with Cs.

The composition of the Ringer's solution that was used in the central pool in the action-potential experiments is given in Table I of Irving et al. (1987).

The TEA-gluconate solution that was used in the central pool in the voltage-clamp experiments contained 110 mM TEA-gluconate, 10 mM $MgSO_4$, 1 μM tetrodotoxin (TTX), and 10 mM MOPS, pH 7.1; it was nominally Ca free.

The EGTA and phenol red were obtained from Sigma Chemical Co. (St. Louis, MO) and Flow Laboratories (Rockville, MD), respectively.

Use of EGTA and Phenol Red to Measure SR Ca Release

Except for the experiment illustrated in Fig. 1 *A*, the results described in this article were obtained from fibers that had been equilibrated with 20 mM EGTA and 1.76 mM Ca. At the values of myoplasmic pH encountered in our experiments, almost all of the EGTA, whether it is Ca-free or Ca-bound, is divalent (Appendix A). Hence, the net reaction between Ca and EGTA can be represented by the scheme,

$$Ca^{2+} + H_2EGTA^{2-} \rightleftharpoons CaEGTA^{2-} + 2H^+. \quad \text{(A1)}$$

According to this scheme, two protons are released from H_2EGTA^{2-} for each Ca that is bound. If the buffering power of myoplasm, β, is known, the change in [CaEGTA], denoted by Δ[CaEGTA], can be calculated from the change in myoplasmic pH, ΔpH, with the equation,

$$\Delta[\mathrm{CaEGTA}] = -(\beta/2)\,\Delta\mathrm{pH}. \tag{A7}$$

Additional information about the reaction between Ca and EGTA is presented in Appendix A. For example, in the absence of intrinsic myoplasmic Ca buffers such as troponin and parvalbumin, EGTA is expected to complex almost all (>99.9%) of the Ca released from the SR and to do so rapidly (within <0.1 ms). For the reasons given in the Discussion, even with troponin and parvalbumin present, it seems likely that almost all (~96%) of the Ca released by an action potential is complexed by EGTA. During SR Ca release, the changes in myoplasmic free [Ca] are most pronounced near the release sites. The spatial spread of these changes and the rapid speed with which they occur are described in Appendices B–D.

Estimation of Myoplasmic pH with Phenol Red

The value of myoplasmic pH at the optical recording site was estimated from the absorbance of phenol red. For this purpose, a 50-μm diam spot of quasi-white light was focused on the middle of the fiber in the central-pool region. The transmitted light was split into three beams of different wavelengths (λ), selected with 30 nm bandpass filters: 480 nm, the isosbestic wavelength of phenol red; 570 nm, a wavelength at which phenol red absorbance is sensitive to pH; and 690 nm, a wavelength not absorbed by phenol red. At the beginning of each experiment, with the K-glutamate or Cs-glutamate solution in the end pools, intensities were measured with the fiber in the field of view (to give the intensity of transmitted light, $I_t[\lambda]$) and with the fiber removed (to give the intensity of incident light, $I_i[\lambda]$). The apparent intrinsic absorbance of the fiber at each wavelength was calculated from the formula $\log_{10}[I_i(\lambda)/I_t(\lambda)]$. After this measurement was completed, the solution in the end-pools was exchanged for one that had the same ionic composition plus 0.63 mM phenol red. After the indicator had diffused into the optical recording site and reached a concentration of at least 0.15 mM, the apparent absorbance of the fiber was determined at the same wavelengths used previously. The values of absorbance, $A(\lambda)$, were corrected for the values of intrinsic absorbance and for small drifts in the intensity of the light source to give the indicator-related absorbance, $A_{ind}(\lambda)$, as described on pages 44–45 of Maylie et al. (1987*b*).

The concentration of indicator at the optical site was estimated from $A_{ind}(480)$. For this purpose, the value of the molar extinction coefficient of phenol red at 480 nm, $\varepsilon(480)$, was taken to be $1.1 \times 10^4\ M^{-1}cm^{-1}$ (Lisman and Strong, 1979). For protonated and nonprotonated indicator, a small correction was applied to the value of $\varepsilon(480)$ to allow for the slight difference between the wavelength of light passed by the 480-nm filter and the exact isosbestic wavelength of phenol red in a calibration solution. Additional information about the determination of $A_{ind}(\lambda)$ and indicator concentration is given in Irving et al. (1987) and Maylie et al. (1987*b*). All measurements of optical absorbance are expressed as 1:2 averages of the absorbance of light linearly polarized along the fiber axis and perpendicular to the fiber axis, as described in Irving et al. (1987).

The value of the fractional amount of phenol red in the nonprotonated form, f, can be estimated from

$$f = \frac{r - r_{min}}{r_{max} - r_{min}}, \tag{1}$$

in which $r = A_{ind}(570)/A_{ind}(480)$ (Irving, Maylie, Sizto, and Chandler, 1989). The value of r_{max} was 3.2 or 3.9, depending on which 480 nm filter was used, and that of r_{min} was 0.03–0.04, which is ~0. Because Eq. 1 applies to the case in which the wavelength of light passed by the 480 nm filter is ex-

actly the same as the isosbestic wavelength of phenol red, the equation was modified slightly to make use of the two values of $\varepsilon(480)$ that were measured with protonated and nonprotonated indicator; these two values were similar but not exactly the same. The value of pH was then calculated from the value of f with the usual expression,

$$\mathrm{pH} = \mathrm{pK} + \log\left(\frac{f}{1-f}\right), \tag{2}$$

with a value of 7.7 for pK (Lisman and Strong, 1979).

After stimulation, Ca is released from the SR and is complexed by H_2EGTA. Protons then dissociate from CaH_2EGTA and the value of myoplasmic pH is decreased. Phenol red is expected to track this change in pH rapidly because, in temperature-jump experiments at pH 7.4 and 25°C, the delay between a change in pH and a change in optical absorbance was found to be <10 μs (Fig. 4.11A in Hammes, 1974). Myoplasmic ΔpH signals were estimated from changes in fiber absorbance recorded simultaneously at 480, 570, and 690 nm. The procedure described on pages 44–45 and in Fig. 4 in Maylie et al. (1987*b*) was used to scale the intrinsic 690 nm signal for subtraction from the raw 570 nm signal to give the indicator-related 570-nm signal. Before the intrinsic correction was done, the noise in the slowly changing $\Delta A(690)$ signal was reduced by use of a 0.05 kHz digital Gaussian filter (Colquhoun and Sigworth, 1983).

Changes in f, denoted by Δf, were estimated from changes in r, denoted by $\Delta r = \Delta A_{ind}(570)/A_{ind}(480)$, and the differential form of Eq. 1,

$$\Delta f = \frac{\Delta \mathrm{r}}{\mathrm{r}_{max} - \mathrm{r}_{min}}. \tag{3}$$

Similar to the situation with Eq. 1, Eq. 3 was modified slightly to allow for the fact that the wavelength of light passed by the 480 nm filter was not exactly the same as the isosbestic wavelength of phenol red.

If the resting values of pH and f at the optical site are denoted by $\mathrm{pH_R}$ and f_R, respectively, $\mathrm{pH} = \mathrm{pH_R} + \Delta\mathrm{pH}$ and $f = f_R + \Delta f$. Substitution of these values of pH and f into Eq. 2 followed by subtraction of the resting values gives,

$$\Delta\mathrm{pH} = \log\left(\frac{f_R + \Delta f}{f_R}\right) - \log\left(\frac{1 - f_R - \Delta f}{1 - f_R}\right). \tag{4}$$

In the experiments described in this article, the ΔpH signal was filtered with a digital Gaussian filter (Colquhoun and Sigworth, 1983) to improve the signal-to-noise. The filter frequency was usually 0.5 kHz for an action-potential experiment and 0.15 kHz for a voltage-clamp experiment.

In Results, evidence is presented that about two-thirds of the phenol red inside a cut fiber is bound to myoplasmic constituents or sequestered inside intracellular compartments. Baylor and Hollingworth (1990) have studied the effects of this binding in intact fibers and have shown that the estimates of $\mathrm{pH_R}$ may be in error because the binding can alter the apparent pK of the indicator. Pape (1990) found that the phenol red estimates of $\mathrm{pH_R}$ were too small by 0.1–0.4 pH units in cut fibers studied under conditions similar to those used here, except that only 0.1 mM EGTA was used in the end-pool solutions in his experiments. The last section in Appendix A discusses some of the consequences of an error in the estimate of $\mathrm{pH_R}$. The main consequence is the introduction of an error into the estimate of $[\mathrm{Ca}]_R$.

Although the estimates of $\mathrm{pH_R}$ may be unreliable, Eq. 4 shows that the estimate of ΔpH is independent of both the value of $\mathrm{pH_R}$ and that of the pK of phenol red, which may be different in myoplasm than in a calibration solution (Irving et al., 1989). A reliable estimate of ΔpH requires only that (*a*) phenol red behave as a homogeneous population of indicator, so that there is some value of pK that satisfies the relation between pH and f given by Eq. 2, and (*b*) the values of A(570)/A(480) for protonated and nonprotonated indicator be known. For this reason, although the esti-

mates of pH_R may be subject to a small error (preceding paragraph), the estimates of ΔpH are expected to be reliable. Additional support for the reliability of the phenol red ΔpH signal is provided by the experiments of Baylor and Hollingworth (1990) and Pape (1990).

In any event, because the same phenol red calibration was used to estimate ΔpH during periods of SR Ca release and to estimate the value of β, any errors in the calibration are cancelled by the use of Eq. A7. As a result, the determination of Δ[CaEGTA] from the value of ΔpH depends mainly on the calibration of the Δ[Cafura-2] signals that were used for the determination of β rather than on the calibration of the phenol red absorbance signals.

Statistical Tests of Significance

Student's two-tailed *t* test was sometimes used to determine the statistical significance of the difference between two sets of results. The difference was considered to be significant if $P < 0.05$.

In Fig. 7, the data x_i, y_i were least-squares fitted by the function

$$Y = \langle y \rangle + b(X - \langle x \rangle). \tag{5}$$

x_i represents the independent variable (time or pH_R) and y_i represents the dependent variable (β). $\langle x \rangle$ and $\langle y \rangle$ represent the mean values of x_i and y_i, respectively. The slope of the straight line is given by *b*.

In these fits, Student's two-tailed *t* test was used to determine whether the value of *b* was significantly different from 0. For this purpose, the residual variance of *y*, denoted by var(*y*), for *n* values of y_i was estimated from

$$\text{var}(y) = \frac{\Sigma(y_i - Y)^2}{(n-2)}. \tag{6}$$

The variance of *b*, var(*b*), was calculated from

$$\text{var}(b) = \frac{\text{var}(y)}{\Sigma(x_i - \langle x \rangle)^2} \tag{7}$$

(Eq. 12.4.2 in Colquhoun, 1971). The value of *b* was considered to be significantly different from zero if the value of *P* determined with Student's two-tailed *t* test was <0.05. For this test, the value of *t* was set equal to $b/\sqrt{\text{var}(b)}$.

RESULTS

The Concentration of EGTA at the Optical Recording Site Is Expected to Equilibrate with That in the End-Pool Solutions within 1 h

In the experiments reported in this article (except for those used for Fig. 1 and Table I), the EGTA-phenol red method was used to estimate SR Ca release. For this estimate to be reliable, a large concentration of EGTA must be present at the optical recording site, several millimolar more than the amount of Ca released from the SR (see, for example, Eq. A5). It is therefore important to estimate the time required for EGTA to diffuse from the end-pool solutions to the optical recording site in the middle of the fiber in the central-pool region. Although the diffusion coefficient of EGTA has not been measured inside a muscle fiber, a 1-h equilibration time is expected to be adequate for its free concentration at the optical recording site to reach a value nearly equal to that in the end-pool solutions.

This expectation follows from the reasonable assumption that the diffusion coefficient of EGTA, with a molecular weight of 378 (Ca-free divalent form), has a value

that is slightly less than that of sucrose, which has a molecular weight of 342. Kushmerick and Podolsky (1969) estimated the diffusion coefficient of sucrose in frog skinned muscle fibers to be 2.1×10^{-6} cm^2/s at 20°C; at 13–16°C, the temperature used in our experiments, the value would be expected to be about 1.8×10^{-6} cm^2/s. If the diffusion coefficient of EGTA is taken to be slightly less than that of sucrose, for example 1.7×10^{-6} cm^2/s at 13–16°C, the mathematical solution of the diffusion equation indicates that, in the absence of binding or sequestration, the equilibration of EGTA at the optical recording site should be 99% complete within 1 h.

If myoplasmic binding or sequestration of EGTA occurs, as has been observed with the Ca indicators arsenazo III and antipyrylazo III (Maylie, Irving, Sizto, and Chandler, 1987*b*,*c*), the apparent diffusion coefficient for EGTA would be $<1.7 \times 10^{-6}$ cm^2/s and the extent of equilibration after 1 h would be <99%. For example, if the apparent diffusion coefficient of EGTA were $0.5 \times 1.7 \times 10^{-6}$ cm^2/s, as would be expected if the concentration of bound or sequestered EGTA were exactly equal to that of freely diffusible EGTA, the extent of equilibration after 1 h would be 90%. In this case, the concentrations of freely diffusible EGTA and of bound or sequestered EGTA would each be 90% of that in the end-pool solutions. Even if the bound or sequestered EGTA were unable to react with Ca, Eq. A5 shows that the concentration of freely diffusible EGTA should be more than adequate to capture almost all of the Ca that moves from the SR into the myoplasm after stimulation, at least in the absence of intrinsic myoplasmic Ca buffers such as troponin and parvalbumin.

EGTA Reduces Both the Amplitude and Duration of the Myoplasmic Free [Ca] Transient Elicited by an Action Potential

The top trace in Fig. 1 *A* shows an action potential in a fiber that had been equilibrated for 80 min with a solution that contained 0.1 mM EGTA. This concentration of EGTA is usually used in cut fiber experiments and is not expected to alter the free [Ca] transient to any significant extent. The bottom trace shows the accompanying change in spatially averaged free [Ca]. In the Results and Appendix A, this is denoted by Δ[Ca] (whereas in Appendices B–D, Δ[Ca] refers to local increases in free [Ca] that occur near SR Ca release sites). The Δ[Ca] signal was measured with the low affinity Ca indicator purpurate-3,3′ diacetic acid (PDAA), which is expected to provide a reliable estimate of both the time course and amplitude of the free [Ca] transient (Hirota, Chandler, Southwick, and Waggoner, 1989; Konishi, Hollingworth, Harkins, and Baylor, 1991). The Δ[Ca] signal in Fig. 1 *A* is typical of those obtained previously in cut fibers with PDAA (Hirota et al., 1989; Pape, Jong, Chandler, and Baylor, 1993). Its time to half-peak (after that of the action potential) is 2.6 ms, its peak amplitude is 14.3 μM (with respect to the prestimulus baseline), and its half-width is 7.8 ms.

Fig. 1 *B* shows a similar set of traces from another fiber that had been equilibrated for 67 min with an internal solution that contained 20 mM EGTA and 1.76 mM Ca. According to the arguments presented in the preceding section, the concentration of free EGTA at the optical site is expected to have been similar to that in the end-pool solutions, 18.24 mM. The composition of the internal solution is the same as that used in the action-potential experiments described below except

that phenol red was omitted. The reason for the omission is that the absorbance spectrum of PDAA overlaps that of phenol red, with the result that neither the PDAA Δ[Ca] signal nor the phenol red ΔpH signal can be measured if both indicators are present. The PDAA Δ[Ca] signal has a time to half-peak of 1.56 ms, a peak amplitude of 4.13 μM, and a half-width of 2.30 ms. Five other measurements of the Δ[Ca] signal were made in this fiber and the mean values from all six measurements were 1.64 ms for the time to half-peak, 4.38 μM for the peak amplitude, and 2.15 ms for the half-width. The amplitude and time course of the Δ[Ca] signal are similar to those observed in the presence of 0.5–1 mM fura-2 (Baylor and Hollingworth, 1988; Pape et al., 1993).

Δ[Ca] signals were measured with PDAA in a total of four fibers. The measurements were made 62–103 min after saponin treatment, similar to the equilibration time that was used in the fibers studied with EGTA-phenol red. Columns 2–4 in Ta-

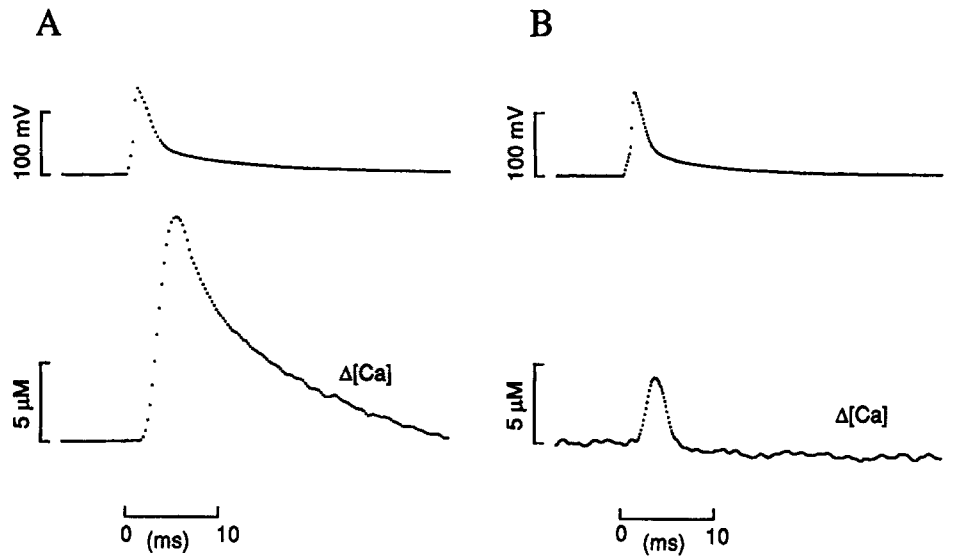

FIGURE 1. Effect of equilibration with 20 mM EGTA on the PDAA Δ[Ca] signal elicited by an action potential. (*A*) The fiber had been equilibrated with a K-glutamate solution that contained only 0.1 mM EGTA. The top trace shows the action potential and the bottom trace shows the Δ[Ca] signal estimated from the change in PDAA absorbance at 570 nm, as described in Hirota et al. (1989). Fiber reference, 323921; time after saponin treatment, 80 min; sarcomere length, 4.0 μm; fiber diameter, 94 μm; holding current, −27 nA; action potential amplitude, 135 mV; PDAA concentration at the optical site, 2.80 mM. From the experiment illustrated in Fig. 8 *A* in Pape et al. (1993), which should be consulted for additional information. (*B*) A similar set of traces from a fiber equilibrated with the K-glutamate solution that contained 20 mM EGTA plus 1.76 mM Ca and ~3 mM PDAA. Fiber reference, 519921; time after saponin treatment, 67 min; sarcomere length, 3.9 μm; fiber diameter, 71 μm; holding current, −61 nA; action potential amplitude, 132 mV; PDAA concentration at the optical site, 2.83 mM. Ringer's solution at 14°C was used in the central pool in both experiments; the interval of time between data points was 0.24 ms in *A* and 0.12 ms in *B*. In this and subsequent figures, 0 ms on the time axis corresponds to the start of the stimulus.

TABLE I
PDAA Ca Transients after a Single Action Potential in Fibers Equilibrated with 20 mM EGTA

(1)	(2)	(3)	(4)
		Δ[Ca]	
Fiber reference	Time to half-peak	Peak	Half-width
	ms	*μM*	*ms*
515922	1.76	5.20	2.14
518921	1.79	1.84	2.74
519921	1.64	4.38	2.15
522921	1.69	1.95	2.94
Mean	1.72	3.34	2.49
SEM	0.03	0.85	0.20

Column 1 gives the fiber reference. Columns 2–4 give the times to half-peak (after that of the action potential), the peak values, and the half-widths of the Δ[Ca] signal estimated with PDAA. Each value represents the mean value obtained from 4–7 runs. Time after saponin treatment, 62–103 min; sarcomere length, 3.4–3.9 μm; fiber diameter 69–133 μm; holding current, −32 to −65 nA; action potential amplitude, 131–137 mV; action potential half-width, 1.7–2.1 ms; temperature, 14°C; concentration of PDAA at the optical site, 2.616–3.171 mM. Ringer's solution was used in the central pool; the K-glutamate solution with 20 mM EGTA plus 1.76 mM Ca and 0.63 mM phenol red was used in the end pools.

ble I give the results. On average, the Δ[Ca] signals had a time to half-peak of 1.72 ms, a peak amplitude of 3.34 μM, and a half-width of 2.49 ms. For comparison, in eight fibers in which the Δ[Ca] signal had not been attenuated by a large concentration of EGTA, similar to the experiment illustrated in Fig. 1 *A*, the mean amplitude and half-width of the signal measured with PDAA were 21 μM and 7 ms, respectively, and the time to half-peak was 2.4 ms (Hirota et al., 1989). Thus, equilibration with 20 mM EGTA reduces the time to half-peak, the amplitude, and the duration of the Δ[Ca] signal elicited by an action potential.

After the transient increase in the Δ[Ca] signal in Fig. 1 *B*, the signal undershot the baseline and appeared to reach a final level of ~−1 μM. This undershoot was a consistent finding in our experiments with PDAA and EGTA and is reminiscent of the undershoot observed with tetramethylpurpurate (Maylie, Irving, Sizto, Boyarski, and Chandler, 1987*a*) and with PDAA in the presence of millimolar concentrations of fura-2 (Jong, Pape, Chandler, and Baylor, 1993). Although the origin of this undershoot is unknown, it seems unlikely that it represents a genuine negative value of myoplasmic Δ[Ca]. Its presence, however, introduces an uncertainty into the estimate of the peak amplitude of the Δ[Ca] signal, with a maximal uncertainty of ~1 μM or 25%.

The Time Course of the Δ[Ca] Signal Elicited by an Action Potential in a Fiber Equilibrated with 20 mM EGTA Is Expected to Be Similar to That of SR Ca Release

The purpose of this section is to give a qualitative description of Ca complexation by EGTA during the Δ[Ca] signal in Fig. 1 *B*. Appendix A shows that, in the pres-

ence of 20 mM EGTA and in the absence of intrinsic myoplasmic Ca buffers, almost all (>99.9%) of the Ca that is released from the SR, denoted by $\Delta[Ca_T]$, is expected to be captured by EGTA (Eq. A5). Evidence is presented below, in connection with Fig. 11 and Table III, that a similar conclusion is expected to hold with troponin and parvalbumin present at normal myoplasmic concentrations. In this case, EGTA is expected to capture about 96% of the Ca released by an action potential.

The capture of Ca by EGTA is expected to be rapid, with a rate constant that is equal to $k_1([EGTA] + [Ca]_R) + k_{-1} \cong k_1[EGTA] \cong k_1[EGTA]_R$ (Eq. A4 and subsequent discussion in Appendix A). k_1 and k_{-1} are the association and dissociation rate constants, respectively, for the reaction between Ca and EGTA, and $[Ca]_R$ and $[EGTA]_R$ are the resting values of free [Ca] and [EGTA]. The mean time required for EGTA at its resting concentration to bind Ca is $(k_1[EGTA]_R)^{-1}$, denoted by τ_{Ca}. The value of τ_{Ca} is expected to be independent of pH because, in stopped-flow experiments, the value of k_1 is independent of pH between pH 5.8 and 7.3 (Smith, Liesegang, Berger, Czerlinski, and Podolsky, 1984). Under the conditions of our experiments, the value of τ_{Ca} is estimated to be 22 μs. Although this estimate may be subject to some unertainty, as discussed in Appendix A, it seems highly unlikely that the true value of τ_{Ca} is more than two or three times 22 μs. Consequently, it seems safe to conclude that EGTA is expected to capture the Ca released from the SR in <0.1 ms.

Appendix A shows that the value of myoplasmic free [Ca] is expected to be equal to the sum of two terms,

$$[Ca] = K_{Dapp}\frac{[CaEGTA]}{[EGTA]} + (k_1[EGTA])^{-1} \cdot (d[CaEGTA]/dt), \qquad (A8)$$

in which K_{Dapp} represents the apparent dissociation constant of the reaction between Ca and EGTA. The first term is equal to the equilibrium value of [Ca] associated with the value of [CaEGTA]/[EGTA]. The second term is proportional to the rate of SR Ca release, $d[Ca_T]/dt$, because $d[Ca_T]/dt \cong d[CaEGTA]/dt$. When several hundred micromolar Ca is released rapidly from the SR, such as occurs after an action potential, the second term increases much more than the first term during the period of release. In this case, the change in myoplasmic free [Ca], $\Delta[Ca]$, is approximately given by,

$$\Delta[Ca] \cong (k_1[EGTA])^{-1} \cdot (d\Delta[CaEGTA]/dt). \qquad (A10)$$

Because $[EGTA] \cong [EGTA]_R$ in our experiments, the proportionality constant is approximately equal to τ_{Ca}. Fig. 8 *A* (below) shows an example of a $\Delta[Ca]$ signal that is approximately proportional to the rate of SR Ca release.

The Spatial Variation of Free [Ca] in the Myoplasm near Release Sites in the Presence of 20 mM EGTA

In the description of Ca complexation by EGTA that is presented in Appendix A, spatial variations in the concentrations of Ca, EGTA, and CaEGTA were neglected.

Appendices B–D, however, show that such variations are expected to occur. The purpose of this section is to describe some of their properties and to show how local changes in [Ca] are expected to contribute to a spatially averaged Δ[Ca] signal such as the one shown in Fig. 1 *B*.

One of the properties of the Δ[Ca] signals that are described in Appendices B–D is that EGTA restricts the increase of free [Ca] to within a few hundred nanometers of the release sites. This is illustrated in Figs. 15, *A* and *B*, and 17 *A*. Another property is that changes in [CaEGTA] and [EGTA] also occur near the sites, as illustrated in Fig. 15 *B* (Δ[EGTA] = −Δ[CaEGTA]). Although these changes extend further from the release sites than do the changes in [Ca], their magnitude is small compared with the value of $[EGTA]_R$ (Fig. 15 *B*) so that, to a good approximation, the value of [EGTA] may be taken to be $[EGTA]_R$ (as is done in Appendices C and D). Another property of the Δ[Ca] signals is that the amplitude of any local change in free [Ca] is directly proportional to the rate of SR Ca release. This holds throughout Appendices B–D (see, for example, Eqs. B21 and D7). The last important property of the Δ[Ca] signals is that, if the rate of Ca release is changed, Δ[Ca] changes within 0.1 ms. This is illustrated for a single channel in Fig. 16, *C* and *D*, and, from the principle of superposition, is expected to apply to the case of many channels. Thus, within the temporal accuracy of our estimates of SR Ca release, the changes in local [Ca] may be considered to occur instantaneously.

These properties of local Δ[Ca] signals can be used to understand the changes in free [Ca] that are expected to have occurred inside the fiber in the experiment illustrated in Fig. 1 *B*. Soon after the action potential, a brief period of SR Ca release began. Throughout the sarcomere, the value of free Δ[Ca] increased with essentially the same time course as Ca release. This increase was large near the release sites and progressively decreased to nearly zero at distances more than a few hundred nanometers from the sites. Since, at any particular location within the sarcomere, the amplitude of Δ[Ca] was directly proportional to the rate of SR Ca release, it follows that the amplitude of the spatially averaged Δ[Ca] signal was also directly proportional to the rate of SR Ca release.

The local Δ[Ca] signals just described should be added to the value of [Ca] that existed a few hundred nanometers from the release sites. Under resting conditions, this value is given by $[Ca]_R = K_{Dapp}[CaEGTA]_R/[EGTA]_R$. During release, the value of [CaEGTA] increases, [EGTA] decreases, and the equilibrium value of [Ca] increases according to $K_{Dapp}[CaEGTA]/[EGTA]$. During this period, small gradients in [CaEGTA] and [EGTA] are established near the release sites so that the value of [CaEGTA]/[EGTA] a few hundred nanometers from the release sites may be slightly different from the ratio of the spatially averaged values of [CaEGTA] and [EGTA]. The time t required for these gradients to dissipate should be roughly equal to the time required for CaEGTA and EGTA to diffuse along half a myofibril. This time can be estimated from the Einstein relation, $t = l^2/(2D_{EGTA})$; with $D_{EGTA} = 1.7 \times 10^{-6}$ cm^2/s and $l \cong 1.8$ μm (a typical value of half the sarcomere length in our experiments), $t \cong 10$ ms. Thus, the value of [Ca] a few hundred nanometers from the release sites is expected to follow the value of $K_{Dapp}[CaEGTA]/[EGTA]$ calculated from the spatially averaged values of [CaEGTA] and [EGTA] with a delay of about 10 ms.

In Fig. 1 *B*, when Ca release was over, the local Δ[Ca] signals are expected to have decreased to zero almost immediately, within <0.1 ms. The gradients in [CaEGTA] and [EGTA] are expected to have lasted longer, for ~10 ms (preceding paragraph). After this time, the concentrations of CaEGTA and EGTA are expected to be homogeneous throughout the fiber with $[\text{CaEGTA}] \cong [\text{CaEGTA}]_R + \Delta[\text{Ca}_T]$, $[\text{EGTA}] \cong [\text{EGTA}]_R - \Delta[\text{Ca}_T]$, and $[\text{Ca}] = K_{D\text{app}}[\text{CaEGTA}]/[\text{EGTA}]$. Unfortunately, in Fig. 1 *B*, this small increase in spatially averaged [Ca] is obscured by the undershoot in the PDAA Δ[Ca] signal.

Approximately Two Thirds of the Phenol Red inside Myoplasm Is Bound or Sequestered

In the rest of the experiments described in this article, phenol red was used in the end-pool solutions so that myoplasmic pH could be estimated. In these experiments, the concentration of phenol red at the optical recording site was estimated from measurements of the indicator's absorbance. The plots of phenol red concentration against time (not shown) were qualitatively similar to those observed with arsenazo III and other Ca indicators studied in this laboratory and could be well fitted by a solution of the one-dimensional diffusion equation with the assumption that any myoplasmic binding or sequestration of indicator is linear, rapid, and reversible (Eqs. 6 and 8 in Maylie et al., 1987*b*). If D represents the true diffusion coefficient of the indicator and R represents the ratio of bound to free indicator, the apparent diffusion coefficient of the indicator is given by $D/(R + 1)$ and the fraction of indicator that appears to be bound or sequestered is given by $R/(R + 1)$.

The time course of phenol red diffusion was analyzed in six fibers with the K-glutamate solution with 20 mM EGTA plus 1.76 mM Ca and 0.63 mM phenol red in the end pools; Ringer's solution was used in the central pool. On average, $D/(R + 1) = 0.39 \times 10^{-6}$ cm^2/s (SEM, 0.01×10^{-6} cm^2/s), $R = 1.80$ (SEM, 0.23), $D = 1.08 \times 10^{-6}$ cm^2/s (SEM, 0.09×10^{-6} cm^2/s), and $R/(R + 1) = 0.627$ (SEM, 0.04). In 19 experiments with the Cs-glutamate solution with 20 mM EGTA plus 1.76 mM Ca and 0.63 mM phenol red in the end pools, and the TEA-gluconate solution in the central pool, $D/(R + 1) = 0.40 \times 10^{-6}$ cm^2/s (SEM, 0.01×10^{-6} cm^2/s), $R = 2.11$ (SEM, 0.13), $D = 1.22 \times 10^{-6}$ cm^2/s (SEM, 0.05×10^{-6} cm^2/s), and $R/(R + 1) = 0.669$ (SEM, 0.013). The values of $D/(R + 1)$, R, D, and $R/(R + 1)$ that were obtained with the two solutions are not significantly different.

The values of $D/(R + 1)$, 0.39×10^{-6} and 0.40×10^{-6} cm^2/s, are similar to the mean value 0.37×10^{-6} cm^2/s obtained in intact fibers at 16°C by Baylor and Hollingworth (1990). The mean values of $R/(R + 1)$, 0.627 and 0.669, indicate that approximately two thirds of the phenol red inside the myoplasm appears to have been bound or sequestered. As mentioned in Methods, although such binding might lead to an underestimate of the value of resting pH by 0.1–0.4 pH units, it is expected to have little effect on the estimate of changes in pH after stimulation.

The Value of Resting pH Decreases during the Time Course of a Cut Fiber Experiment

Fig. 2 shows the value of resting myoplasmic pH, denoted by pH_R, plotted as a function of time after saponin treatment of the end-pool segments of a cut fiber. In this experiment, phenol red was introduced into the end pools 18 min after saponin

treatment. The central pool contained Ringer's solution and the end pools contained the K-glutamate solution with 20 mM EGTA plus 1.76 mM Ca and 0.63 mM phenol red.

In Fig. 2, an open circle denotes a measurement of pH_R that was made without an immediate subsequent stimulation. Open squares and diamonds denote measurements that were followed by one or two action potentials, respectively. Filled circles denote measurements that were followed by a train of 40 action potentials, which produced a pronounced acidification, to pH <6.8. These two symbols, which are not easily discernible, are marked by the second and third tick marks.

The first measurement of pH_R, with 0.152 mM phenol red, gave a value of 7.090. Thereafter, the value progressively decreased and, at the end of the experiment,

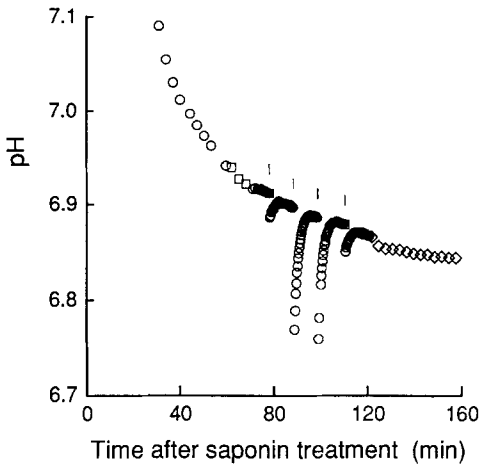

FIGURE 2. Time course of myoplasmic pH at the optical recording site plotted against time after saponin treatment of the fiber segments in the end pools. At 18 min, 0.63 mM phenol red was introduced into the end pools and allowed to diffuse into the fiber. Different symbols denote different types of stimulation after the value of pH was measured: (*open circle*) no stimulation; (*open square*) one action potential; (*open diamond*) two action potentials; (*filled circle*) 40 action potentials. The four ticks indicate four stimulations in which the time course of recovery was measured. The first tick marks the point associated with the traces in Figs. 4, 8 *A*, and 11; the third tick marks the point associated with the stimulation in Fig. 3 and the trace in Fig. 8 *B*. Fiber reference, 925911; sarcomere length, 3.4 μm; temperature, 14°C. Range of values from beginning to end of experiment: fiber diameter, 103–102 μm; holding current, −34 nA to −43 nA; action potential amplitude, 135–130 mV; concentration of phenol red at the optical site, 0.152–1.804 mM; estimated pH_R and $[Ca]_R$, 7.090–6.844 and 0.024–0.074 μM, respectively. Ringer's solution was used in the central pool; the K-glutamate solution with 20 mM EGTA plus 1.76 mM Ca and 0.63 mM phenol red was used in the end pools.

was 6.844. Between 70 and 120 min, the recovery of pH after one, 40, 40, and one action potential(s) was monitored by making measurements every 0.25 or 0.5 min (cf. Fig. 3); these stimulations are marked by the four vertical ticks. The first action-potential stimulation was used for the traces in Figs. 4 and 8 *A*. The second 40 action-potential stimulation was used for the traces in Fig. 8 *B* and the time course of recovery in Fig. 3.

The progressive decrease in pH_R in Fig. 2 was observed in all of our experiments. A similar decrease has been reported in cut fibers equilibrated with solutions that contained only 0.1 mM EGTA, in which pH was measured either with phenol red (Irving et al., 1989; Pape, 1990) or with dimethylcarboxyfluorescein (Irving et al., 1989). Thus, the decrease does not appear to be related to the concentration of

EGTA in the end-pool solutions or to the use of phenol red. It does appear to be related to the use of cut fibers, however, since similar changes were not found in intact fibers studied with phenol red (Baylor and Hollingworth, 1990).

Although the cause of the decrease in pH_R in cut fibers is unknown, it is not expected to interfere with the ability of EGTA-phenol red to measure SR Ca release and to do so rapidly (see Appendix A). Furthermore, it does not appear to directly affect the regulation of SR Ca release that is studied in this article (see below).

The Value of pH_R Varies from Fiber to Fiber

Table II tabulates results from 12 fibers that were studied with action-potential stimulation. The measurements were made at least 1 h after saponin treatment of the end-pool segments of the fibers, when the fibers were first exposed to the internal solution. Column 1 gives fiber references, arranged in order of decreasing pH_R. Column 2 gives the values of pH_R; these range from 7.08 (*top row*) to 6.69 (*bottom row*). Baylor and Hollingworth (1990) reported a somewhat larger variation in pH_R, from 6.81 to 7.51, in intact fibers in which pH_R was also estimated with phenol red. Their mean value was 7.17 (SEM, 0.08) with red-shifted calibration curves and 7.11 with unshifted curves as used here. Our mean value, 6.90 (SEM, 0.03), is significantly smaller than either one of theirs, as might be expected from the decrease in pH_R that occurs during the first 1–2 h in experiments with cut fibers (Fig. 2). As discussed in Methods, estimates of pH_R with phenol red may not be reliable and, in cut fibers studied under conditions similar to those used here, may be too small by 0.1–0.4 pH units (Pape, 1990).

Column 3 in Table II gives the values of $[Ca]_R$. Here and elsewhere in this article, these were calculated from the first term on the right-hand side of Eq. A8 on the assumption that the values of $[CaEGTA]_R$ and $[EGTA]_R$ at the optical site were the same as those in the end-pool solutions, 1.76 and 18.24 mM, respectively. The value of K_{Dapp} was determined from Eq. A9 with the values of pH_R in column 2. The values of $[Ca]_R$ increase with decreasing pH_R, from 0.025 to 0.150 μM; their mean value is 0.066 μM (SEM, 0.011 μM).

Klein, Simon, Szúcs, and Schneider (1988) estimated the value of $[Ca]_R$ with fura-2 in cut fibers equilibrated with end-pool solutions that contained Cs glutamate and only 0.1 mM EGTA. They obtained mean values of 0.049 μM (SEM, 0.008 μM) and 0.101 μM (SEM, 0.018 μM) after 60 and 90 min exposures, respectively, to internal solution. Our values of $[Ca]_R$, which were obtained at similar times after exposure to the internal solution, are similar to theirs. This agreement may be fortuitous, however: in our experiments, the actual values of $[Ca]_R$ may be smaller than the estimated values because of a possible 0.1–0.4 underestimate of pH_R (see Methods) whereas, in their experiments, they may be larger, by as much as severalfold, because of an underestimate of the dissociation constant of Ca and fura-2 (Klein et al., 1988).

It is difficult to assess whether the values of $[Ca]_R$ that we estimated in our cut fibers are similar to those measured in intact fibers, because estimates of $[Ca]_R$ in intact fibers vary widely according to the method of measurement, from <0.06 μM with ion-selective electrodes (Coray, Fry, Hess, McGuigan, and Weingart, 1980) and aequorin (Blatter and Blinks, 1991) to values as large as 0.2–0.3 μM with fura red

TABLE II

SR Ca Release after a Single Action Potential in Fibers Equilibrated with 20 mM EGTA

(1)	(2)	(3)	(4)	(5)	(6)	(7)	(8)	(9)	(10)	(11)
					$d\Delta[Ca_T]/dt$			$\Delta[Ca]$		
Fiber reference	pH_R	$[Ca]_R$	$\Delta[Ca_T]$	$[Ca_{SR}]_R$	Time to half-peak	Peak	Half-width	Time to half-peak	Peak	Half-width
		μM	*μM*	*μM*	*ms*	*μM/ms*	*ms*	*ms*	*μM*	*ms*
415911	7.08	0.025	228	1391	2.88	45	4.67	2.84	1.02	4.88
O10911	6.98	0.039	299	1781	2.71	121	2.52	2.70	2.72	2.56
420921	6.98	0.040	316	2145	2.11	109	2.87	2.11	2.45	2.88
417921	6.96	0.044	309	2223	1.97	107	2.76	1.96	2.41	2.84
923911	6.96	0.045	287	2252	2.84	116	2.35	2.83	2.61	2.40
423911	6.95	0.046	370	2456	2.08	133	2.73	2.10	3.02	2.76
425911	6.94	0.049	395	2535	1.72	142	2.92	1.71	3.21	2.96
925911	6.91	0.054	366	2777	2.89	132	2.72	2.89	2.98	2.76
406921	6.83	0.078	407	2810	1.62	178	2.25	1.62	4.05	2.30
401921	6.78	0.099	455	3568	1.99	172	2.57	1.97	3.95	2.65
402921	6.73	0.125	534	4367	1.89	226	2.28	1.89	5.23	2.33
402922	6.69	0.150	539	3912	1.82	230	2.29	1.81	5.31	2.36
Mean	6.90	0.066	375	2685	2.21	143	2.74	2.20	3.25	2.81
SEM	0.03	0.011	28	252	0.14	15	0.19	0.14	0.35	0.20

Column 1 gives the fiber references, arranged in order of decreasing pH_R. Column 2 gives the values of pH_R estimated from Eqs. 1 and 2. Column 3 gives the values of myoplasmic free $[Ca]_R$ estimated from the values of pH_R in column 2 with Eqs. A8 (first term on right-hand side) and A9; the value of [CaEGTA]/[EGTA] at the optical site was assumed to be equal to that in the end-pool solutions, 1.76/18.24. Column 4 gives the values of $\Delta[Ca_T]$, the increase in total myoplasmic [Ca] produced by a single action potential. These were taken to be equal to the values of Δ[CaEGTA] determined 30–50 ms after the action potentials. Column 5 gives values of $[CaSR]_R$ that were obtained from a depleting tetanus that was given, on average, 14 min (SEM, 5 min; range, 3–65 min) after the single action potential used for the values in columns 2–4. Columns 6–8 give the times to half-peak (after that of the action potential), the peak values, and the half-widths of the $d\Delta[Ca_T]/dt$ signals that were obtained by differentiation of the $\Delta[Ca_T]$ signals used for column 4. Columns 9–11 give similar information about the Δ[Ca] signal calculated from Eq. A8. Conditions for the single action potential trials: time after saponin treatment, 61–100 min; saromere length, 3.4–3.8 μm; fiber diameter, 86–150 μm; holding current, −19 to −76 nA; action potential amplitude, 125–139 mV; action potential half-width, 1.59–2.37 ms; temperature, 13–15°C; concentration of phenol red at the optical site, 0.755–1.453 mM. Ringer's solution was used in the central pool; the K-glutamate solution with 20 mM EGTA plus 1.76 mM Ca and 0.63 mM phenol red was used in the end pools.

and fluo-3 (Kurebayashi, Harkins, and Baylor, 1993; Harkins, Kurebayashi, and Baylor, 1993).

Recovery of pH after Stimulation Requires Several Minutes in Fibers Equilibrated with 20 mM EGTA

Because our experiments were carried out on fibers equilibrated with a large con-

centration of EGTA, the value of myoplasmic free [Ca] after stimulation is expected to have been small. For this reason and also because Ca dissociates from CaEGTA slowly, it seemed possible that a long period of time might be required for Ca to be returned to the SR by the SR Ca pump after stimulation. It was therefore important to find out how rapidly the pH signal is able to recover after stimulation so that a reasonable period of recovery could be used between successive trials.

Fig. 3 shows an experiment in which 40 action potentials at 50 Hz were used to release essentially all of the readily releasable Ca from the SR into the myoplasm. The open circles at times ≤ 0 min show the values of pH_R before stimulation. The open square at time = 0 min shows the value recorded immediately after the train of action potentials had been completed. This value corresponds to a decrease in

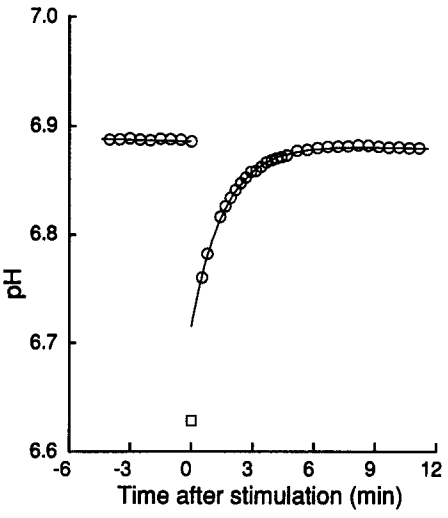

FIGURE 3. Time course of recovery of myoplasmic pH after a train of action potentials. pH (*open circles*) was sampled at 0.5-min intervals for 4 min before the fiber was stimulated. At 0 min, the fiber was stimulated to give a train of action potentials (shown in Fig. 8 *B*). The value of pH immediately after the train is plotted as an open square and subsequent values of resting pH are plotted as open circles. The line and curve show the best least-squares fit of a sloping straight line that starts at −4 min plus a decreasing exponential function that starts at 0 min; the open square was excluded from the fit. The time constant of the exponential function is 1.61 min. The half time for recovery was estimated by interpolation to be 0.51 min. Same fiber as used in Fig. 2, in which the third tick indicates the time of stimulation. See legend of Fig. 2 for additional information.

myoplasmic pH equal to −0.252 pH units. With β = 22 mM/pH unit, as determined below, this decrease in pH corresponds to an increase in total myoplasmic [Ca] of 2,772 μM (Eq. A7). The circles at times >0 min show values of "resting" pH recorded at different times after the stimulation had been stopped. The value of pH slowly increased and became approximately constant and equal to its prestimulus value ~5 min after the tetanus. The half time for recovery, $t_{1/2}$, was estimated by interpolation to be 0.51 min.

The time course of recovery in Fig. 3 was also analyzed with a least-squares fit of a sloping baseline plus a decreasing exponential function starting at 0 min. The open square was omitted from the fit. The theoretical curve, shown in the figure, provides a good fit to the open circles but lies above the open square. This indicates that there was a rapid initial phase of recovery followed by a slower, exponential phase. The rapid phase appears to have been completed by 0.52 min, the time when the first open circle was obtained. The time constant of the exponential function is 1.61 min.

Recovery of pH was studied in a similar manner in a total of four trials on three fibers. The mean values of $t_{1/2}$ and of the time constant of the exponential function were 0.57 min (SEM, 0.04 min) and 1.77 min (SEM, 0.11 min), respectively.

Recovery was also studied after a single action potential (not shown), which produced a change in pH that was 0.13–0.17 times that produced by a tetanus. In this case, for reasons unknown, the rapid phase of recovery was absent and a decreasing exponential function provided a reasonable fit to the entire time course of pH after stimulation. The mean value of the time constant was 2.14 min (SEM, 0.09 min; four trials on two fibers).

The time course of pH after a depleting voltage-clamp depolarization (not shown) was similar to that observed after a depleting tetanus (Fig. 3). In a total of three trials on two fibers, the mean values of $t_{1/2}$ and of the time constant of the exponential function were 0.45 min (SEM, 0.02 min) and 1.07 min (SEM, 0.09 min), respectively.

In principle, it might be possible to interpret the time course of pH recovery in terms of Ca reaccumulation by the SR Ca pump. We are reluctant to do this, however, because several metabolic processes might influence myoplasmic pH during a recovery period that lasts as long as several minutes. The main use of the time course of recovery was to help decide how long to wait between successive trials so that the SR could reaccumulate Ca. As a general rule, a period of 5 min was allowed after the SR had been depleted of almost all of its readily releasable Ca by either a train of action potentials or a voltage-clamp depolarization, and a period of 3 min was allowed after partial depletion by one or two action potentials or a brief voltage-clamp depolarization.

A Single Action Potential Produces a Step Decrease in Myoplasmic pH

Fig. 4 shows electrical and optical traces associated with a single action potential. The top trace shows the action potential recorded in end pool 1. The next three traces show the changes in absorbance $\Delta A(\lambda)$, with λ = 480, 570, and 690 nm, as indicated. (Throughout this article, the symbol Δ refers to changes with respect to the prestimulus level.) These traces contain contributions from changes in the intrinsic optical properties of the fiber (which can be expressed as changes in absorbance) as well as possible changes in phenol red absorbance.

Because phenol red does not absorb 690 nm light, and because its isosbestic wavelength is close to 480 nm, the $\Delta A(690)$ and $\Delta A(480)$ traces are expected to contain contributions primarily from changes in the intrinsic optical properties of the fiber. Consequently, the amplitude of these signals is much smaller than that of the ΔA(570) signal, which contains a substantial contribution from changes in phenol red absorbance. The change in indicator-related absorbance at 570 nm, $\Delta A_{ind}(570)$ (not shown), was obtained from the $\Delta A(570)$ signal by subtraction of the ΔA(690) signal, suitably scaled to match the intrinsic signal at 570 nm (see Methods). Because the amplitude of the $\Delta A(570)$ signal is ~20 times that of the ΔA(690) signal, the accuracy of the intrinsic correction is not critical to the determination of $\Delta A_{ind}(570)$.

The lowermost trace in Fig. 4 shows the ΔpH signal calculated from the $\Delta A_{ind}(570)$ trace, as described in Methods. A few milliseconds after the action potential, the

myoplasmic pH rapidly decreased 0.033 pH units from its resting level, estimated to be 6.912. Such a decrease in pH is expected when EGTA combines with Ca and releases two protons for each Ca that is bound, reaction scheme A1.

Eq. A7 can be used to convert the ΔpH signal in Fig. 4 to the Δ[CaEGTA] signal, if the value of the buffering power of myoplasm, β, is known; β has units of total proton concentration removed from (added to) the myoplasm per unit increase (decrease) in pH. The following section describes the method used to determine β.

Because the ΔpH signal in Fig. 4 represents the change in spatially averaged myoplasmic pH, it is of interest to estimate the magnitude of any gradients in pH that might develop near an open SR Ca channel. Appendix B shows that, in the steady state, local changes in proton concentration, $\Delta[H^+]$, are expected to be proportional to the local changes in CaEGTA concentration, with a proportionality constant of $\sim 10^{-4}$. Because the value of $\Delta[H^+]$ during a transient is never expected to exceed that during the steady state, and because the maximal value of local

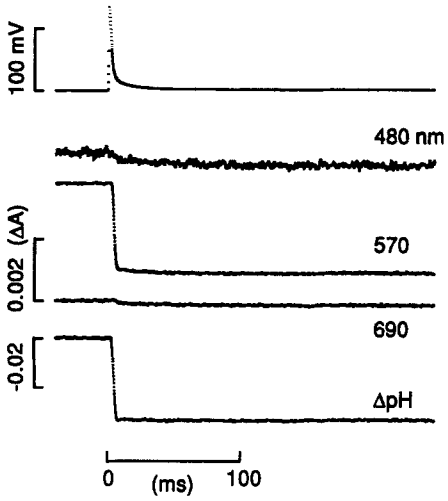

FIGURE 4. Optical changes associated with an action potential in a fiber equilibrated with 20 mM EGTA and phenol red. The top trace shows the action potential. The next three traces show the changes in absorbance at 480, 570, and 690 nm, as labeled. The bottom trace shows ΔpH, estimated from the absorbance changes at 570 and 690 nm as described in Methods. Same fiber as used for Fig. 2, in which the first tick indicates the time of stimulation. Time after saponin treatment, 78 min; holding current, −33 nA; action potential amplitude, 136 mV; phenol red concentration at the optical site just before stimulation, 1.223 mM; estimated pH_R and free $[Ca]_R$ just before stimulation, 6.912 and 0.054 μM, respectively; interval of time between data points, 0.12 ms. See legend of Fig. 2 for additional information.

Δ[CaEGTA] near a single open SR Ca channel is expected to be only ~5 μM (Fig. 15 *B*), the value of $\Delta[H^+]$ near a single open Ca channel is expected to be negligibly small, <1 nM. Although the analysis in Appendix B of the gradients of [CaEGTA] and $[H^+]$ near a single SR Ca channel has not been extended to include the case of Ca release from many channels (as was done for [Ca] in Appendix D), it seems unlikely that substantial gradients of $[H^+]$ are ever established near the SR Ca release sites.

A Description of the Method for the Determination of the Rapidly Available Buffering Power

Because SR Ca release usually lasts only a fraction of a second, it is important for the conversion of ΔpH to Δ[CaEGTA] to use a value of β that applies during this period of time. This will be called the rapidly available buffering power.

The principle of the method to measure β on this time scale is to equilibrate a

cut muscle fiber with a solution that contains EGTA, phenol red, and fura-2, and to use an action potential to rapidly release a bolus of Ca from the SR into the myoplasm. Although the apparent dissociation constants of EGTA and fura-2 are similar at the values of internal pH encountered in these experiments, the corresponding forward and backward rate constants are very different because the reaction between Ca and fura-2 is much faster than that between Ca and EGTA. Consequently, after SR Ca release is over, some of the Ca that was initially complexed by the rapidly reacting fura-2 dissociates and becomes complexed by EGTA. This leads to a decrease in internal pH. With the assumption that Δ[CaEGTA] = $-\Delta$[Cafura-2] during this time and that the stoichiometry of Ca exchange for protons by EGTA is 1:2, the relative amplitudes of the ΔpH and Δ[Cafura-2] signals can be used to estimate the value of β. This estimate depends mainly on events that occur during the first 100 ms after the action potential. In our estimates of β, the relatively small uptake of protons by fura-2 as Cafura-2 dissociates has been neglected; at pH = 7.0, for example, the stoichiometry of this exchange is $\sim$1 Ca:0.05 protons (Pape, Konishi, Hollingworth, and Baylor, 1990).

For the determination of β, fibers were first equilibrated for 58–84 min with the K-glutamate solution with 20 mM EGTA plus 1.76 mM Ca and 0.63 mM phenol red (no fura-2) in the end pools; Ringer's solution was used in the central pool. Fig. 5 *A* shows a set of traces obtained with action-potential stimulation. The top trace shows the electrical recording. The next two traces show changes in indicator-related absorbance, ΔA(420) and ΔA(570), as indicated. The contribution of the fiber's intrinsic signal to each raw absorbance signal has been removed by subtraction of the $\Delta A(690)$ signal (not shown) after suitable scaling (see Methods and Fig. 4). The $\Delta A(420)$ and $\Delta A(570)$ signals underwent abrupt changes soon after the action potential and then remained relatively constant. The negative sign of the $\Delta A(570)$ signal is similar to that observed in Fig. 4 and is consistent with an acidification of the myoplasmic solution. Because the isosbestic wavelength of phenol red is 480 nm (Lisman and Strong, 1979), the $\Delta A(420)$ signal is expected to be of opposite sign, as observed.

The first 200 ms of the $\Delta A(570)$ signal was least-squares fitted to the $\Delta A(420)$ signal, which gave a scaling factor of -0.42. The bottom trace in Fig. 5 *A* shows the $\Delta A(420)$ signal after subtraction of -0.42 times the $\Delta A(570)$ signal. The trace is flat, showing that the $\Delta A(420)$ and $\Delta A(570)$ signals had the same waveform. Two other sets of measurements gave the same value of the scaling factor, -0.42.

After these measurements were completed, 2 mM fura-2 with 0.5 mM Ca was added to the end-pool solutions. The traces in Fig. 5 *B*, plotted with the same format used in Fig. 5 *A*, were obtained 52 min later. The indicator-related $\Delta A(420)$ and $\Delta A(570)$ signals in Fig. 5 *B* are clearly different from those in Fig. 5 *A*. Because fura-2 (although not Cafura-2) absorbs 420 nm light, the indicator-related $\Delta A(420)$ signal is expected to contain contributions from both phenol red and fura-2. On the other hand, since neither fura-2 nor Cafura-2 is able to absorb 570 nm light, the indicator-related $\Delta A(570)$ signal is expected to contain contributions from only phenol red.

The initial decrease in the $\Delta A(570)$ signal in Fig. 5 *B* is smaller but otherwise similar to that in Fig. 5 *A* and is likely caused by an initial complexation by EGTA of

some of the Ca that was released from the SR. The subsequent decrease in $\Delta A(570)$, during the next 100–200 ms, is consistent with the idea that some of the Ca that was initially complexed by the rapidly reacting fura-2 dissociated during this period and combined with EGTA. If this idea is correct, [Cafura-2] should have decreased during this period and, because [fura-2] + [Cafura-2] should have remained constant, [fura-2] should have increased.

The fura-2-related $\Delta A(420)$ signal, which is the bottom trace in Fig. 5 *B*, was ob-

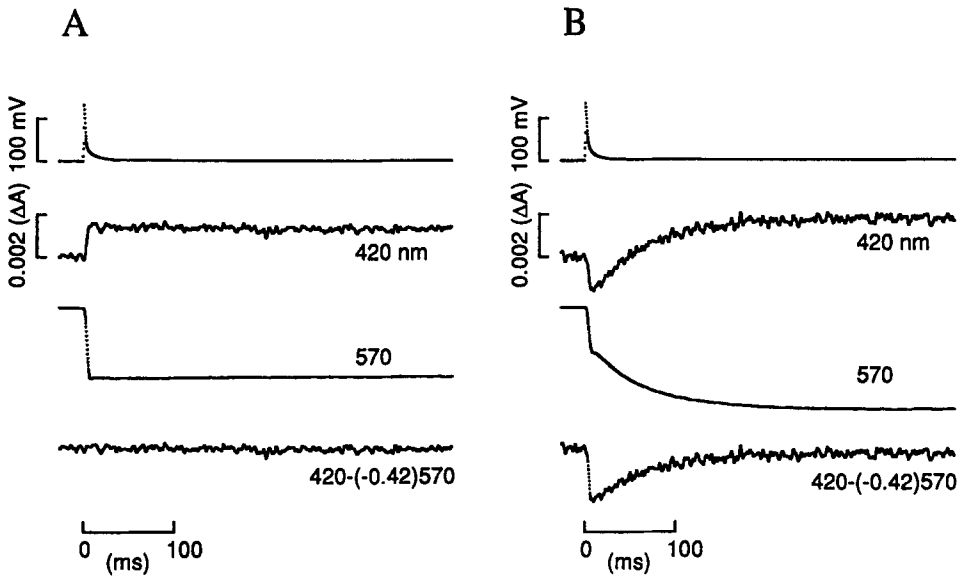

FIGURE 5. Changes in indicator-related absorbance before (*A*) and after (*B*) fura-2 had diffused into the optical recording site. (*A*) The top trace shows the action potential. The next two traces show changes in indicator-related absorbance at 420 and 570 nm, as indicated. The bottom trace shows the 420-nm trace minus the 570-nm trace scaled by −0.42. Time after saponin treatment, 64 min; time after introduction of phenol red into the end pools, 49 min; fiber diameter, 151 μm; holding current, −64 nA; action potential amplitude, 134 mV; concentration of phenol red at the optical site, 1.065 mM; estimated pH_R and $[Ca]_R$, 6.977 and 0.040 μM, respectively. (*B*) Similar to *A* except that the measurements were made 62 min later, after fura-2 had diffused into the optical site. Time after saponin treatment, 126 min; time after introduction of fura-2 into the end pools, 52 min; fiber diameter, 151 μm; holding current, −71 nA; action potential amplitude, 134 mV; concentration of phenol red at the optical site, 1.916 mM; estimated pH_R and $[Ca]_R$, 6.954 and 0.045 μM, respectively. Fiber reference, 420921; sarcomere length, 3.6 μm; temperature, 15°C; interval of time between data points, 0.24 ms.

tained from the indicator-related $\Delta A(420)$ signal (second trace) by subtraction of the contribution from phenol red. This contribution was estimated by scaling the indicator-related $\Delta A(570)$ signal (third trace) by −0.42, the scaling factor that was determined before fura-2 was added to the end pools (Fig. 5 *A*). The fura-2-related $\Delta A(420)$ signal shows an initial decrease, consistent with a reduction in [fura-2] and an increase in [Cafura-2]. The signal then returned toward baseline with a time course similar to that of the decrease of the $\Delta A(570)$ signal, as expected if Ca

dissociated from Cafura-2 and combined with EGTA. This movement of Ca from fura-2 to EGTA was initially observed in a series of unpublished experiments carried out in collaboration with Dr. Stephen Baylor. It forms the basis of the method for the estimation of β.

Because neither fura-2 nor Cafura-2 is able to appreciably absorb 480 nm light, the value of indicator-related $A(480)$ can be used to monitor the concentration of phenol red at the optical site, as was done in the absence of fura-2. In the fiber in Fig. 5, the concentration was 1.065 mM in *A* and 1.916 mM in *B*. The final ampli-

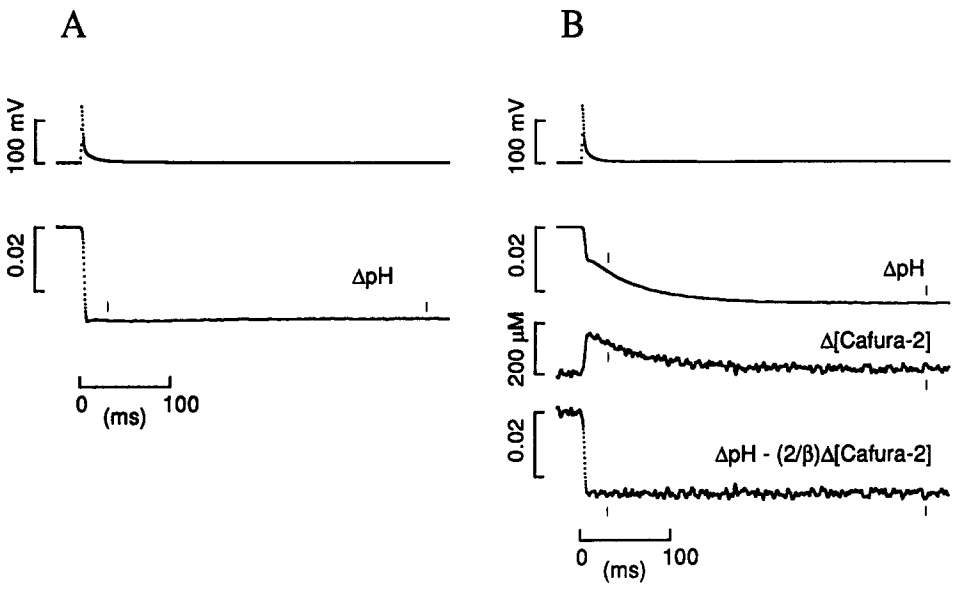

FIGURE 6. ΔpH (*A* and *B*) and Δ[Cafura-2] (*B*) signals estimated from the optical traces in Fig. 5. (*A* and *B*) The top traces in each panel repeat the corresponding action potentials in Fig. 5. The second traces in each panel show the ΔpH signals estimated from the indicator-related ΔA(570) signals. (*B*) The third trace shows the Δ[Cafura-2] signal estimated from the ΔA(420) + 0.42ΔA(570) signal in Fig. 5 *B*. The bottom trace shows ΔpH − (2/β)Δ[Cafura-2], which represents the ΔpH signal that would have been obtained with the same SR Ca release if fura-2 had not been present at the optical site. The value of β, 20.7 mM/pH unit, was obtained from a least-squares fit of the ΔpH trace to the Δ[Cafura-2] trace in the interval indicated by vertical ticks, 30–382 ms after the stimulation. See text for additional information.

tude of the indicator-related $\Delta A(570)$ signal in *B* is larger than that in *A* owing to this difference in concentration of phenol red.

Because the indicator-related $\Delta A(570)$ signals in Fig. 5 contain contributions from only phenol red, they can be converted to ΔpH signals, as described in the Methods. Similarly, the fura-2-related ΔA(420) signal at the bottom of Fig. 5 *B* can be scaled to give Δ[Cafura-2], as described in Pape et al. (1993). Fig. 6 shows the result.

Fig. 6 *A* shows the step decrease in pH (*lower trace*) that accompanied the action potential (*upper trace*) in the absence of fura-2, similar to that shown in Fig. 4. The middle two traces in Fig. 6 *B* show the ΔpH and Δ[Cafura-2] signals that were ob-

tained after fura-2 had diffused into the optical recording site. Soon after stimulation, there was an abrupt decrease in ΔpH (due to an abrupt increase in Δ[CaEGTA]) and an abrupt increase in Δ[Cafura-2]. During the next 100–200 ms, both ΔpH and Δ[Cafura-2] decreased with a similar time course. The ΔpH signal was least-squares fitted to the Δ[Cafura-2] signal in the interval 30–382 ms after stimulation, indicated by vertical ticks. The fit was good (not shown) and a value of 20.7 mM/pH unit was obtained for β from the relation $\Delta pH = (2/\beta)\Delta[\text{Cafura-2}]$. This relation assumes that, in the interval between the tick marks, (*a*) there were no sources or sinks for Ca other than EGTA and fura-2 so that the relation $\Delta[\text{CaEGTA}] = -\Delta[\text{Cafura-2}]$ would apply, (*b*) the exchange of Ca for protons by EGTA was 1:2, and (*c*) there were no sources or sinks for protons other than those associated with β. Assumptions *a* and *c* are supported by the observation that, in the absence of fura-2, the ΔpH signal was flat in the interval between the tick marks (Fig. 6 *A*), consistent with the idea that there were no sources or sinks for Ca or protons in the myoplasm during this period. Assumption *b* follows from the known values of the dissociation constants of EGTA for protons and Ca (cf. Appendix A).

According to Appendix B, in the experiment illustrated in Fig. 6 *B*, almost all of the initial complexation of Ca by EGTA and fura-2 is expected to have occurred within a few hundred nanometers of the SR Ca release sites. After Ca release was completed, the concentrations of CaEGTA, EGTA, Cafura-2, and fura-2 are expected to have equilibrated by diffusion, a process that is expected to have occurred throughout the sarcomere and to have been mostly completed by the time of the first tick mark, 30 ms after stimulation. Thus, it seems likely that there were no appreciable gradients of freely diffusible CaEGTA, EGTA, Cafura-2, and fura-2 during the period when the value of β was estimated.

The bottom trace in Fig. 6 *B* shows $\Delta pH - (2/\beta)\Delta[\text{Cafura-2}]$, with $\beta = 20.7$ mM/pH unit. This represents the ΔpH signal that would have been obtained if fura-2 had been absent and SR Ca release had been unchanged. Its steplike appearance is consistent with the observation that the fit of the ΔpH trace to the Δ[Cafura-2] trace in the interval between the tick marks was good (not shown). The mean value of the trace in this interval is −0.0256 pH units whereas that in Fig. 6 *A* is −0.0290 pH units. This difference suggests that the amount of Ca released from the SR had decreased by 12% from *A* to *B* in Fig. 6. This change is similar to that observed in experiments without fura-2 (see above) and is attributed to fiber run down during the 62-min period that separated the measurements in *A* and *B* in Fig. 6.

The Value of β Is Constant 2–4 h after Saponin Treatment

Fig. 7 *A* shows the value of β plotted as a function of time after saponin treatment of the end-pool segments, from the fiber used for Figs. 5 and 6. The straight line represents a least-squares fit of Eq. 5 with $\langle\beta\rangle = 21.5$ mM/pH unit and a slope $b = -0.0043$ mM/(pH unit × min). According to the test described in Methods, the value of *b* is not significantly different from 0. This is consistent with the idea that the freely mobile myoplasmic buffers at the optical site had equilibrated with those in the end-pool solutions by the time that the first measurement was made, and that the concentrations of the myoplasmic buffers, both mobile and immobile, remained relatively constant during the next 150 min.

The Mean Value of β is 22 mM/pH Unit and Is Approximately Independent of pH_R between 6.7 and 7.0

Fig. 7 *B* shows individual estimates of β from seven fibers, plotted as a function of pH_R. Each fiber is represented by a different symbol; an open circle represents the fiber illustrated in Figs. 5, 6, and 7 *A*. The straight line was least-squares fitted to the

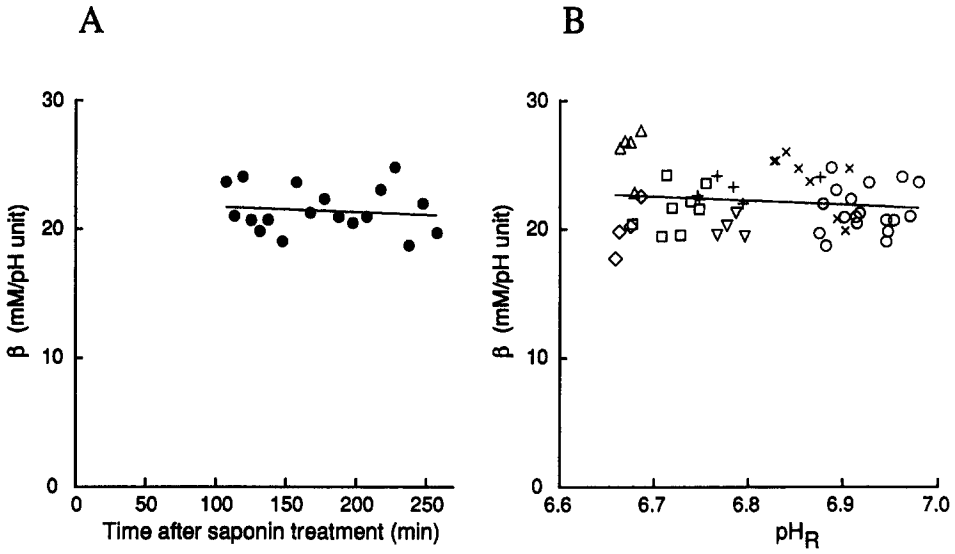

FIGURE 7. Effect of experiment duration (*A*) and pH_R (*B*) on β. (*A*) Values of β are plotted as a function of time after saponin treatment of the end-pool segments, from the experiment in Figs. 5 and 6. Each value of β was estimated from a least-squares fit of a ΔpH trace to the corresponding Δ[Cafura-2] trace in the interval 30 to 250–430 ms after stimulation, as described in connection with Fig. 6 *B*. The straight line shows the least-squares fit of Eq. 5, with ⟨time⟩ = 175.8 min, ⟨β⟩= 21.5 mM/pH unit, and $b = -0.0043$ mM/(pH unit × min). During the experiment, the fiber diameter progressively decreased from 151 to 145 μm; the holding current changed from −69 to −85 nA; the action potential amplitude remained constant at 134 mV; the concentration of phenol red at the optical site increased from 1.742 to 2.384 mM; and pH_R decreased from 6.980 to 6.875. Additional information is given in the legend of Fig. 5. (*B*) Values of β from seven fibers plotted as a function of pH_R. Each fiber is represented by a different symbol; (*open circles*) represent the fiber used in Figs. 5, 6, and 7 *A*. The straight line shows the least-squares fit of Eq. 5, with $\langle pH_R \rangle = 6.815$, ⟨β⟩ = 22.2 mM/pH unit, and $b = -3.1$ mM/(pH unit)^2. Time after the introduction of fura-2 into the end pools, 34–184 min; sarcomere length, 3.4–3.8 μm; fiber diameter, 94–151 μm; holding current, −35 to −85 nA; action potential amplitude, 124–134 mV; temperature, 14–15°C; concentration of phenol red at the optical site, 0.790–2.630 mM. Additional information is given in the text.

data (Eq. 5), with values $\langle pH_R \rangle = 6.815$, ⟨β⟩ = 22.2 mM/pH unit, and $b = -3.1$ mM/(pH unit)^2. According to the test described in Methods, the value of b is not significantly different from 0. Thus, within the scatter of the data, there is no discernible dependence of β on pH_R between 6.66 and 6.98.

In one experiment, fura-2 was added to the end pools at the same time as phenol

red, so that the value of β could be estimated as soon as possible after saponin treatment of the end-pool segments. Six values of β, plotted as crosses in Fig. 7 *B*, were determined 52–81 min after saponin treatment. They varied from 22.0 to 24.0 mM/pH unit with a mean value of 23.0 mM/pH unit (SEM, 0.4 mM/pH unit). Although these values were obtained about an hour sooner after saponin treatment than those from the other six fibers, they lie within the range of values obtained from the other fibers. This finding suggests that the freely mobile myoplasmic buffers at the optical site became equilibrated with those in the end-pool solutions within an hour after saponin treatment. This suggests that the apparent diffusion coefficient of most of these buffers is $\geq 1 \times 10^{-6}$ cm^2/s, because a substance with an apparent diffusion coefficient of 1×10^{-6} cm^2/s would be expected to be 93% equilibrated within an hour.

In all of the experiments described below, a value of 22 mM/pH unit has been used for β to convert ΔpH signals to Δ[CaEGTA].

The Value of the Dissociation Rate Constant of Cafura-2 is ~30 s^{-1}

During all of the experiments with EGTA and fura-2, the time constant associated with the transfer of Ca from fura-2 to EGTA progressively increased with the duration of the experiment (not shown). A theoretical analysis (not shown) shows that such an increase is expected from the increase in concentration of fura-2 that occurred at the same time; to a first approximation, the time constant is expected to increase linearly with fura-2 concentration. A qualitative explanation of this effect is that, after Ca ions dissociate from Cafura-2, there is a high probability that they will rapidly become either complexed by EGTA or recomplexed by fura-2. The fractional amount that becomes recomplexed by fura-2 depends on the relative concentrations of EGTA and fura-2 and increases as the concentration of fura-2 is increased. Since any Ca that is recomplexed by fura-2 must wait for a subsequent dissociation to have a chance to become complexed by EGTA and contribute to Δ[Cafura-2] and Δ[CaEGTA], the length of time that Ca is complexed by EGTA becomes progressively longer as the concentration of fura-2 is increased.

The theoretical analysis mentioned in the preceding paragraph was used to estimate the value of the dissociation rate constant of Cafura-2, k_{-2} (method not shown). The mean value of k_{-2} in seven fibers was 29 s^{-1} (SEM, 4 s^{-1}) at 14–15°C.

A Single Action Potential Releases 200–500 μM Ca from the SR into the Myoplasm

The top trace in Fig. 8 *A* shows the action potential from Fig. 4 plotted on an expanded time scale. The next trace shows $\Delta[Ca_T]$, which is defined by $\Delta[Ca_T] = \Delta[Ca] + \Delta[CaEGTA]$. Δ[CaEGTA] was obtained by scaling the ΔpH trace in Fig. 4 by the factor $-\beta/2$ (Eq. A7), with β = 22 mM/pH unit (see above). Since, except at the very beginning of a [Ca] transient, the absolute value of Δ[Ca] is expected to be much smaller than that of Δ[CaEGTA] (compare columns 4 and 10 in Table II), $\Delta[Ca_T]$ is taken to be equal to Δ[CaEGTA]. Soon after the rising phase of the action potential, $\Delta[Ca_T]$ increased rapidly to a nearly constant value of 366 μM. Just after the rapid increase, but before the trace became flat, there was a suggestion of a small overshoot.

Evidence is presented in Appendix A and the Discussion that $\Delta[Ca_T]$ is approximately equal to the total amount of Ca released from the SR into the myoplasm, expressed as myoplasmic concentration. Thus, within a few milliseconds after the action potential, sufficient Ca was released from the SR into the myoplasm to increase its total concentration by approximately 366 μM. Thereafter, the value of $\Delta[Ca_T]$ was essentially constant. This constancy is consistent with the idea that there were little or no movements of protons or Ca either into or out of the myo-

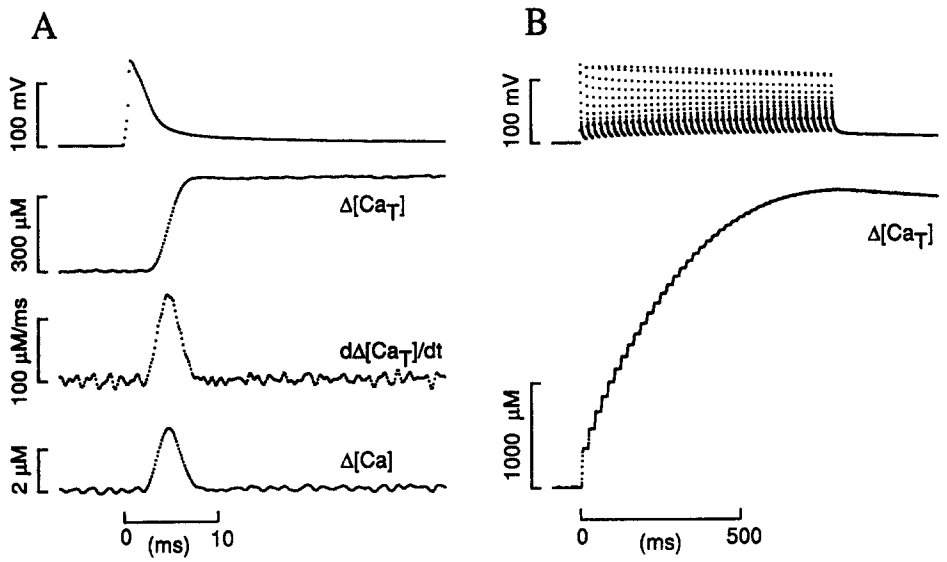

FIGURE 8. Ca signals associated with a single action potential (*A*) and a train of 40 action potentials at 50 Hz (*B*) in a fiber equilibrated with 20 mM EGTA and phenol red. (*A*) The top trace shows the action potential from Fig. 4 plotted on an expanded time scale. The second trace shows $\Delta[Ca_T]$, the change in total myoplasmic Ca concentration. This was obtained by scaling the ΔpH trace in Fig. 4 by $-\beta/2$ (Eq. A7 with β = 22 mM/pH unit) to give Δ[CaEGTA], and then using the relation $\Delta[Ca_T] \cong \Delta$[CaEGTA]. (*B*) The top and bottom traces show voltage and $\Delta[Ca_T]$, respectively, from the same fiber used in *A*. Time after saponin treatment, 99 min; holding current, −33 nA; action potential amplitude, not resolvable because of slow sampling rate; phenol red concentration at the optical site, 1.450 mM; estimated pH_R and free $[Ca]_R$, 6.885 and 0.061 μM, respectively; interval of time between data points, 0.48 ms. The time of stimulation in *A* and *B* are indicated by the first and third tick marks, respectively, in Fig. 2. See legend of Fig. 2 for additional information.

plasmic solution during this period and that the concentration of CaEGTA was essentially constant.

The third trace in Fig. 8 *A* shows $d\Delta[Ca_T]/dt$, which is taken to represent the rate of SR Ca release. The time to half-peak (after that of the action potential) was 2.89 ms, the peak amplitude was 132 μM/ms, and the half-width was 2.72 ms; the half-width is the interval of time between the half-peak on the rising phase and the half-peak on the falling phase.

The bottom trace in Fig. 8 *A* shows Δ[Ca], the estimated change in spatially aver-

aged free [Ca] in the myoplasmic solution, calculated from Eq. A8 and displayed after subtraction of the value of $[Ca]_R$, estimated to be 0.054 μM. The Δ[Ca] signal has a time course that is nearly identical to that of the $d\Delta[Ca_T]/dt$ signal; it has a time to half-peak of 2.89 ms, a peak amplitude of 2.98 μM, and a half-width of 2.76 ms. The Δ[Ca] signal is also similar to that recorded with PDAA (Fig. 1 *B*) except for the absence of an undershoot.

The peak amplitude of the Δ[Ca] signal in Fig. 8 *A* (2.98 μM) is approximately equal to $(k_1[EGTA]_R)^{-1}$ (= τ_{Ca} = 22 μs) times the peak value of $d\Delta[Ca_T]/dt$ (132 μM/ms), as expected from Eq. A10. The value of $(k_1[EGTA]_R)^{-1}$, 22 μs, was chosen so that the mean peak value of Δ[Ca] estimated with EGTA-phenol red (3.25 μM, column 10 in Table II) would be similar to that measured with PDAA (3.34 μM, column 3 in Table I). If $[EGTA]_R$ = 18.24 mM, a value of 2.5×10^6 $M^{-1}s^{-1}$ is obtained for k_1. This value lies near the upper end of the range of values that have been measured in vitro with 100 mM KCl. Harafuji and Ogawa (1980) obtained values of $1.0–3.0 \times 10^6$ $M^{-1}s^{-1}$ at 20°C and Smith et al. (1984) obtained a value of 0.9×10^6 $M^{-1}s^{-1}$ at 16°C. Harafuji and Ogawa (1980) attributed the differences among their values to the three different pH buffers that were used. Our estimate of k_1 would be smaller than 2.5×10^6 $M^{-1}s^{-1}$ if the value of $[EGTA]_R$ were greater than 18.24 mM; for example, the concentration of free EGTA might be essentially the same as that in the end pools, as seems likely after the long periods of equilibration that were used in our experiments, and an additional amount of EGTA might be bound inside the myoplasm and able to react with Ca.

Column 4 in Table II gives the peak values of $\Delta[Ca_T]$ in 12 action-potential experiments. These values progressively increase, with a small scatter, from 228 μM in the first row to 539 μM in the bottom row. The mean value is 375 μM. The progressive increase of $\Delta[Ca_T]$ is associated with a decrease in pH_R (column 2) and an increase in $[Ca]_R$ (column 3).

These changes in the amplitude of $\Delta[Ca_T]$ were not associated with any consistent changes in the action potential. In nine fibers studied with sufficient time resolution to resolve the action potential, the amplitude of the action potential was 125–139 mV and its half-width was 1.59–2.37 ms. The amplitude and half-width of the action potential showed no consistent variation with pH_R or $[Ca]_R$.

Previous estimates of the amount of Ca released by an action potential in cut fibers have been made with small concentrations of low affinity Ca indicators and only 0.1 mM EGTA in the end-pool solutions: 333 μM (SEM, 8 μM) with antipyrylazo III (high Ca calibration, Table VII in Maylie et al., 1987*c*), 317 μM with tetramethylpurpurate (SEM, 5 μM) (page 168 in Maylie et al., 1987*a*) and 294 μM (SEM, 12 μM) with PDAA (page 321 in Pape et al., 1993). These values are all somewhat smaller than the mean value in our experiments, 375 μM. The significance of this difference is uncertain, however, because a reliable estimate of SR Ca content is difficult to obtain in experiments with low affinity Ca indicators. Because the value of $\Delta[Ca_T]$ appears to be roughly proportional to SR Ca content, at least between 1,400 and 4,400 μM (see below, Fig. 10 *A*), the larger value of $\Delta[Ca_T]$ in our experiments may reflect a larger SR Ca content. On the other hand, if the SR Ca contents were similar in all of the experiments, the differences could be due to a genuine increase in SR Ca release caused by 20 mM EGTA, similar to that ob-

served with 0.5–2 mM fura-2 and attributed to a decrease in Ca inactivation of Ca release (Baylor and Hollingworth, 1988; Hollingworth, Harkins, Kurebayashi, Konishi, and Baylor, 1992; Pape et al., 1993).

A Train of 40 Action Potentials Is Able to Release Almost All of the Readily Releasable Ca from the SR

21 min after the traces in Fig. 8 *A* were obtained, the fiber was stimulated with a train of 40 action potentials at 50 Hz. The top trace in Fig. 8 *B* shows the electrical response. Since a relatively long period of recording was required for these measurements, the interval of time between experimental points was increased from 0.12 ms (Fig. 8 *A*) to 0.48 ms. As a result, the time course of the action potentials in Fig. 8 *B* cannot be resolved reliably.

The bottom trace in Fig. 8 *B* shows $\Delta[Ca_T]$. During the first part of the train, there was a rapid increase in $\Delta[Ca_T]$ after each action potential. The first action potential produced an increase of 369 μM, similar to that shown in Fig. 8 *A*, which was 366 μM. Subsequent action potentials produced smaller increases in $\Delta[Ca_T]$ until $\Delta[Ca_T]$ reached an almost steady value during the last part of the train, indicating that almost all of the readily releasable Ca had moved from the SR into the myoplasm. Accordingly, the final value of $\Delta[Ca_T]$, 2,777 μM, is taken to represent the prestimulus value of the readily releasable SR Ca content (expressed in terms of myoplasmic concentration), which is denoted by $[Ca_{SR}]_R$. After the train, $\Delta[Ca_T]$ decreased slowly (cf. Fig. 3). Traces of $d\Delta[Ca_T]/dt$ and $\Delta[Ca]$ are not included in Fig. 8 *B* because the interval of time between the experimental points was too long for reliable resolution of their time courses.

Estimates of $[Ca_{SR}]_R$ obtained with a train of action potentials, similar to that illustrated in Fig. 8 *B*, are given in column 5 of Table II. The values progressively increase, with some scatter, from 1,391 μM in the top row to 3,912 μM in the bottom row and have a mean value of 2,685 μM (SEM, 252 μM). Fig. 9 shows these values plotted as a function of $[Ca]_R$ (linear scale) and pH_R (values in parentheses, nonlinear scale). Each fiber is represented by a different small symbol; the large asymmetrical cross provides information about $[Ca_{SR}]_R$ in voltage-clamp experiments, as described below (cf. Fig. 12). The values of $[Ca_{SR}]_R$ progressively increase with $[Ca]_R$ and decrease with pH_R, similar to the situation observed with the value of $\Delta[Ca_T]$ elicited by a single action potential (column 4 in Table II). Although there is no way to establish with certainty whether the variation in $[Ca_{SR}]_R$ is due to pH_R or $[Ca]_R$ or both, the idea that $[Ca_{SR}]_R$ increases with $[Ca]_R$ is certainly plausible in view of the known ability of the SR Ca pump to accumulate more Ca inside the SR when the value of myoplasmic [Ca] is increased.

Although the value of $[Ca_{SR}]_R$ can be easily determined in an EGTA-phenol red experiment, its determination is difficult in an experiment with a low affinity Ca indicator. The reason is that, after sufficient Ca has been released to saturate the myoplasmic Ca buffers, free [Ca] increases and inhibits additional release because of Ca inactivation of Ca release (Baylor et al., 1983; Simon et al., 1985, 1991; Baylor and Hollingworth, 1988; Schneider and Simon, 1988).

A Single Action Potential Releases Only 0.13–0.17 of the Readily Releasable SR Ca Content

Fig. 10 *A* shows values of $\Delta[Ca_T]$ plotted as a function of $[Ca_{SR}]_R$, with the same symbols used in Fig. 9. With some scatter, $\Delta[Ca_T]$ increases monotonically with $[Ca_{SR}]_R$. The relation between $\Delta[Ca_T]$ and $[Ca_{SR}]_R$ is not exactly linear, but slightly curvilinear, and is expected to pass through the origin.

The value of f_1, the fraction of SR Ca content released by the first action potential, can be estimated from the value of $\Delta[Ca_T]$ divided by $[Ca_{SR}]_R$. For the experiment in Fig. 8 *B*, $f_1 = 369/2{,}777 = 0.133$. Fig. 10 *B* shows values of f_1 plotted as a

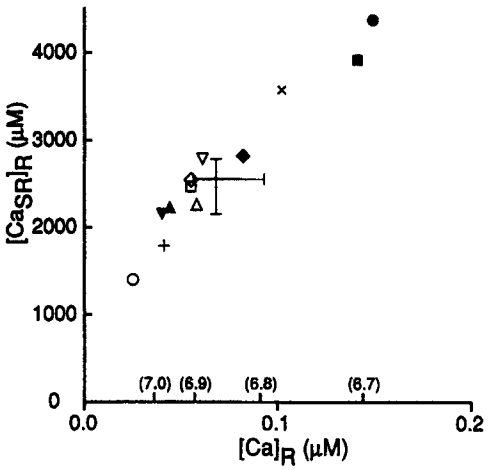

FIGURE 9. Effect of $[Ca]_R$ or pH_R on the SR Ca content. The value of $[Ca_{SR}]_R$ (expressed in terms of myoplasmic concentration), estimated from the plateau value of $\Delta[Ca_T]$ during a train of 20–40 action potentials, is plotted as a function of $[Ca]_R$ (linear scale) and pH_R (values in parentheses on a nonlinear scale), from the fibers used for Table II (which should be consulted for additional information). Each fiber is represented by a different small symbol. The intersection of the arms of the large asymmetrical cross shows the mean value of $[Ca_{SR}]_R$ obtained from 11 voltage-clamped fibers studied with long lasting depleting depolarizations (250–1,400 ms to −50 to −20 mV), plotted against the mean values of $[Ca]_R$ and pH_R; the horizontal and vertical arms of the cross indicate the range of values. For these measurements, each depleting depolarization was preceded by another depleting depolarization followed by a 5-min recovery period. Information about the voltage-clamp experiments: time after saponin treatment, 61–110 min; sarcomere length, 3.3–3.5 μm; fiber diameter, 84–160 μm; holding current, −24 to −70 nA; temperature, 13–15°C; concentration of phenol red at the optical site, 0.902–1.583 mM; pH_R, 6.795–6.904; free $[Ca]_R$, 0.056–0.093 μM. The TEA-gluconate solution was used in the central pool; the Cs-glutamate solution with 20 mM EGTA plus 1.76 mM Ca and 0.63 mM phenol red was used in the end pools.

function of $[Ca_{SR}]_R$. The values fluctuate within a small range and decrease slightly with increasing $[Ca_{SR}]_R$. Their mean value is 0.144 (SEM, 0.004).

Column 7 in Table II gives the peak values of $d\Delta[Ca_T]/dt$ and Fig. 10 *C* shows these values plotted as a function of $[Ca_{SR}]_R$. Because the derivative of a signal is expected to be noisier than the signal itself (compare the $\Delta[Ca_T]$ and $d\Delta[Ca_T]/dt$ signals in Fig. 8 *A*), the data in Fig. 10 *C* show more scatter than those in Fig. 10 *A*. Within this scatter, though, the relation between $d\Delta[Ca_T]/dt$ and $[Ca_{SR}]_R$ appears to be approximately linear.

The mean peak amplitude of $d\Delta[Ca_T]/dt$, 143 μM/ms (column 7 in Table II), is similar to and not significantly different from the values obtained with antipyrylazo

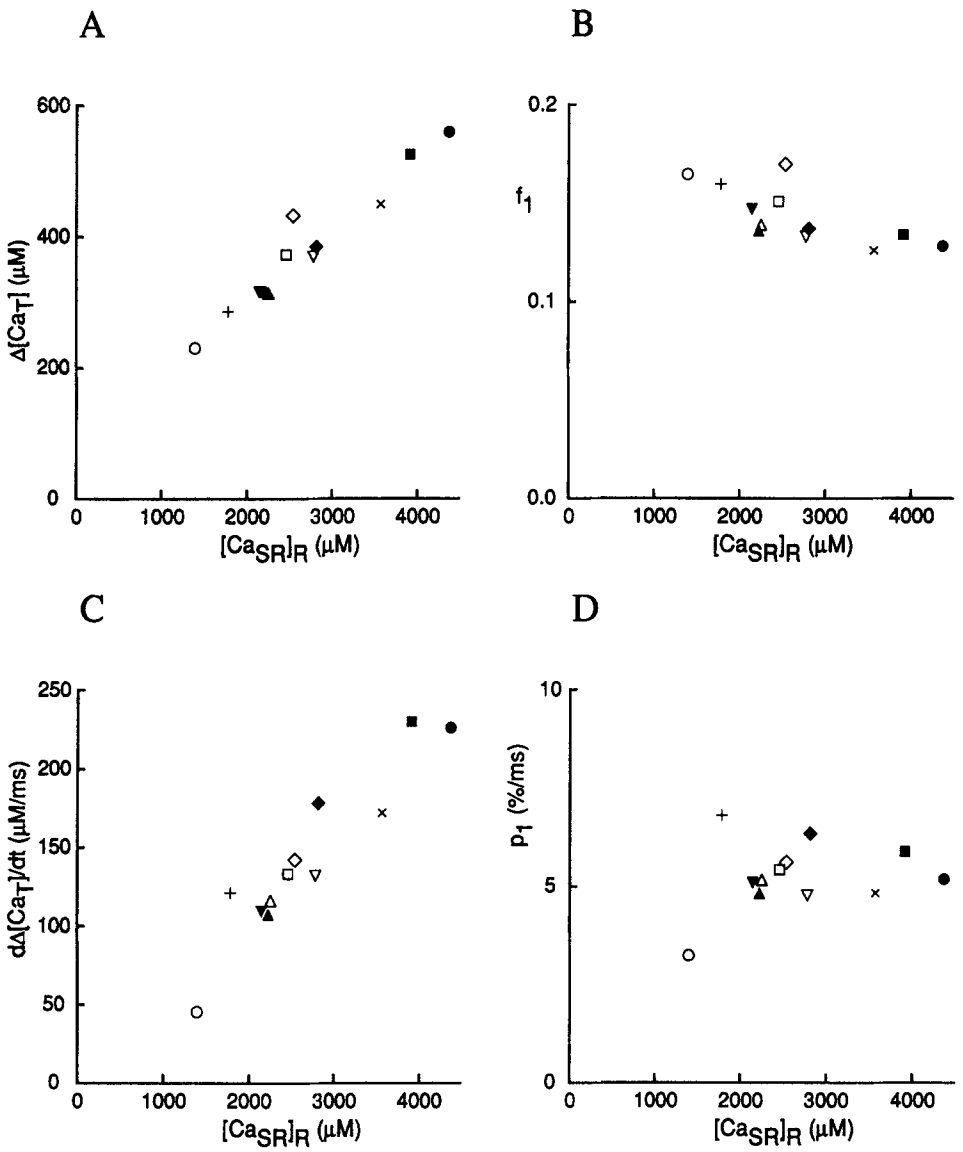

FIGURE 10. The dependence of parameters associated with SR Ca release after a single action potential on $[Ca_{SR}]_R$. (*A* and *B*) The values of $\Delta[Ca_T]$ (*A*) and f_1 (*B*) are plotted as a function of $[Ca_{SR}]_R$. (*C* and *D*) Similar to *A* and *B* except that peak values of $d\Delta[Ca_T]/dt$ and p_1 have been plotted. Each fiber is represented by the same symbol used in Fig. 9. Additional information is given in the legend of Table II.

III, tetramethylpurpurate, and PDAA in cut fibers with only 0.1 mM EGTA in the end-pool solutions (Maylie et al., 1987*a*,*c*; Pape et al., 1993). Because the values of $d\Delta[Ca_T]/dt$ depend on $[Ca_{SR}]_R$ (cf. Fig. 10 *C*), it is difficult to assign any significance to this similarity without knowing the values of $[Ca_{SR}]_R$ in the fibers with unmodified [Ca] transients.

The peak value of $d\Delta[Ca_T]/dt$ can be divided by $[Ca_{SR}]_R$ and multiplied by 100 to give p_1, the peak rate of Ca release in units of percent of SR Ca content per millisecond. Fig. 10 *D* shows the values of p_1 plotted as a function of $[Ca_{SR}]_R$. Within the scatter of the data, the values of p_1 appear to be constant, with a mean value of 5.25%/ms (SEM, 0.26%/ms).

These results are consistent with the idea that pH_R, in the range 6.7–7.1, affects the values of $\Delta[Ca_T]$ and $d\Delta[Ca_T]/dt$ mainly through an effect on $[Ca_{SR}]_R$, probably mediated through $[Ca]_R$ (preceding section).

The Temporal Waveform of $d\Delta[Ca_T]/dt$ Is Not Dramatically Affected by Equilibration with 20 mM EGTA

Column 6 in Table II gives the times to half-peak of the $d\Delta[Ca_T]/dt$ signal. Within the scatter of the data, the values show a small decrease from top to bottom, corresponding to ~2 ms/pH unit (compare values in columns 2 and 6). The mean value of the time to half-peak, 2.21 ms, is similar to and not significantly different from the corresponding values reported with antipyrylazo III, tetramethylpurpurate, and PDAA in cut fibers with only 0.1 mM EGTA in the end-pool solutions (Maylie et al., 1987*a*,*c*; Pape et al., 1993). This similarity supports the idea that EGTA tracks SR Ca release rapidly, as expected from Eq. A4. It also suggests that, similar to the results obtained with 0.5–2 mM fura-2 (Baylor and Hollingworth, 1988; Hollingworth et al., 1992; Pape et al., 1993), suppression of the increase in spatially averaged myoplasmic free [Ca] by EGTA does not affect the onset of SR Ca release.

Column 8 in Table II gives the values of the half-width of the $d\Delta[Ca_T]/dt$ signal. Within the scatter of the data, the values show a small decrease from top to bottom, corresponding to 1 ms/pH unit. The mean value of the half-width, 2.74 ms, is larger than those observed in cut fibers with only 0.1 mM EGTA in the end-pool solutions: 2.04 ms (SEM, 0.05 ms) with antipyrylazo III, 1.86 ms (SEM, 0.07 ms) with tetramethylpurpurate, and 2.05 ms (SEM, 0.14 ms) with PDAA (see references in preceding paragraph); only the differences reported for antipyrylazo III and tetramethylmurexide are statistically significant. This suggests that the duration of the $d\Delta[Ca_T]/dt$ waveform obtained with EGTA-phenol red is 0.7–0.9 ms longer than that calculated from free $\Delta[Ca]$ signals measured with low affinity Ca indicators and 0.1 mM EGTA. In intact fibers also studied with action-potential stimulation, Baylor and Hollingworth (1988) and Hollingworth et al. (1992) observed a similar prolongation with 0.5–2 mM fura-2, a finding that appeared to be correlated with an increase in the value of $\Delta[Ca_T]$.

Columns 9–11 in Table II give information about the spatially averaged myoplasmic free $\Delta[Ca]$ signal. On average, the time to half-peak was 2.20 ms (column 9), the peak amplitude was 3.25 μM (column 10), and the half-width was 2.81 ms (column 11). A fiber-to-fiber comparison of corresponding values in columns 6–8 with those in columns 9–11 shows that, in all cases, the time to half-peak and the half-width of $\Delta[Ca]$ were similar to those of $d\Delta[Ca_T]/dt$, and the peak value of $\Delta[Ca]$ was approximately equal to the peak value of $d\Delta[Ca_T]/dt$ multiplied by $(k_1[EGTA]_R)^{-1}$, with $(k_1[EGTA]_R)^{-1} = 22$ μs. As mentioned above in connection with Fig. 8 *A*, these similarities are expected from Eq. A10 and the choice of the value of $(k_1[EGTA]_R)^{-1}$.

From the results described in this and the preceding section, it seems reasonable to conclude that, under the conditions of our experiments, the main effect of pH_R in the range 6.7–7.1 was on the value of $[Ca_{SR}]_R$. Apart from this, pH appeared to have little effect on the physiological mechanisms associated with SR Ca release.

The Second Action Potential in a Train Releases Fractionally Less Ca Than the First Action Potential, Probably Because of Ca Inactivation of Ca Release

In the experiment in Fig. 8 *B*, the amount of Ca released from the SR by the second action potential was about half that released by the first action potential. The increase in $[Ca_T]$ elicited by the n^{th} action potential can be divided by the SR Ca content just preceding that action potential to give f_n, the fractional amount of Ca released by the n^{th} action potential (a generalization of the definition given above for f_1). The experiment in Fig. 8 *B* gives $f_1 = 0.133$, $f_2 = 0.076$, $f_3 = 0.075$, $f_4 = 0.069$, and $f_5 = 0.071$. The value of f_n was reduced almost twofold from $n = 1$ to 2 and then remained relatively constant from $n = 2$ to 5.

The ratio f_2/f_1 in a 50 Hz tetanus was determined in 11 of the 12 fibers listed in Table II (one fiber could not be used because it was stimulated at 10 Hz). The mean value of f_2/f_1 was 0.612 (SEM, 0.014). There was no significant effect of pH_R or $[Ca]_R$ on f_2/f_1 (not shown).

A similar but more marked reduction in SR Ca release has been inferred in other experiments in which [Ca] transients were measured with low affinity indicators in intact fibers (Baylor et al., 1983) and in cut fibers equilibrated with solutions that contained only 0.1 mM EGTA (Maylie et al., 1987*c*). Fig. 8 *B* in Pape et al. (1993) shows a cut fiber experiment in which PDAA was used to measure the [Ca] signal. In this experiment, SR Ca release was estimated to have decreased fivefold from the first to the second action potential. A likely explanation of this decrease is that Ca inactivation of SR Ca release had been elicited by the first action potential, and that this inactivation reduced the amount of Ca released by the second action potential. The finding that the mean value of f_2/f_1 in the experiments reported here was less than unity suggests that Ca inactivation of Ca release is still able to develop in fibers equilibrated with 20 mM EGTA. The following article (Jong et al., 1995) describes some of the properties of this inactivation.

Estimates of the Concentration of Ca Complexed by Troponin and Parvalbumin after a Single Action Potential

For the EGTA-phenol red method to provide a reliable estimate of SR Ca release, most of the Ca that leaves the SR and enters the myoplasm must be bound by EGTA. It therefore seemed important to estimate the concentration of Ca that is bound by troponin and parvalbumin and to compare that amount with the amount of Ca bound by EGTA.

The first three traces in Fig. 11 show the action potential, $\Delta[Ca]$, and $\Delta[Ca_T]$ from the experiment in Figs. 4 and 8 *A*. The bottom two traces show estimates of $\Delta[CaTrop]$ and $\Delta[CaParv]$, the myoplasmic concentrations of Ca bound to the Ca-regulatory sites on troponin and to the Ca,Mg sites on parvalbumin, respectively, minus their corresponding resting values. These estimates were calculated from the

spatially averaged free [Ca] signal, given by $\Delta[Ca] + [Ca]_R$, as described by Baylor et al. (1983); the values of concentrations and rate constants of troponin and parvalbumin are given in the legend of Fig. 11.

According to the Δ[CaTrop] signal in Fig. 11, 68 μM Ca was rapidly bound to troponin during the [Ca] transient. After the [Ca] transient was over, Ca dissociated from troponin with a rate constant that was approximately equal to the assumed off rate constant for troponin, 115 s^{-1}. On the other hand, the Δ[CaParv] signal shows a rapid initial increase of 38 μM. The signal remained constant for the next 20–30 ms and then began a small, slow increase.

The concentration of Ca that was bound to troponin and parvalbumin was estimated from the spatially averaged free [Ca] signal in the 12 fibers used in Table II.

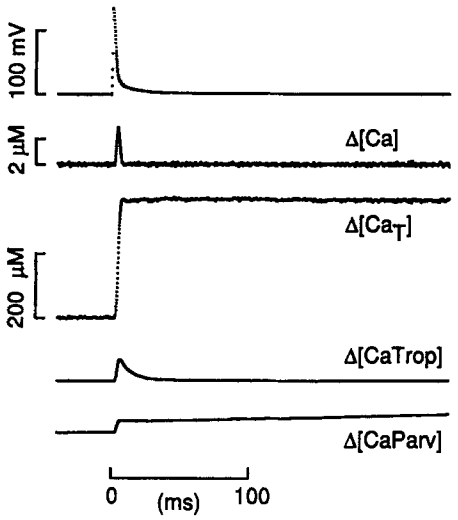

FIGURE 11. Estimated time course of Ca binding to troponin and parvalbumin after a single action potential. The first three traces show the action potential, Δ[Ca], and $\Delta[Ca_T]$ from Fig. 8 *A*, plotted on the same time scale used in Fig. 4. The time course of spatially averaged myoplasmic free [Ca], equal to Δ[Ca] plus $[Ca]_R$, was used to calculate the time courses of [CaTrop] and [CaParv]. The bottom two traces show the changes with respect to the resting values, indicated respectively by Δ[CaTrop] and Δ[CaParv]. The calculations were carried out as described by Baylor et al. (1983), model 2, except that the concentration of parvalbumin was 0.75 mM (Hou, Johnson, and Rall, 1991). The concentration of Ca-regulatory sites on troponin (two sites per molecule) was 0.24 mM and the dissociation constant was 2 μM; the forward and backward rate constants were 0.575×10^8 $M^{-1}s^{-1}$ and 115 s^{-1}, respectively. The concentration of Ca,Mg sites on parvalbumin (two sites per molecule) was 1.5 mM. The dissociation constant of the sites for Ca was 4 nM, and the forward and backward rate constants were 1.25×10^8 M^{-1} s^{-1} and 0.5 s^{-1}, respectively. The dissociation constant of the sites for Mg was 91 μM, and the forward and backward rate constants were 3.3×10^4 M^{-1} s^{-1} and 3.0 s^{-1}, respectively. $[Mg]_R$ = 1 mM; $[Ca]_R$ = 0.054 μM; $[Trop]_R$ = 233.7 μM; $[Parv]_R$ = 59 μM. The 200-μM vertical calibration bar applies to the $\Delta[Ca_T]$, Δ[CaTrop], and Δ[CaParv] traces.

Columns 1–6 in Table III give a summary of the results. Column 1 gives the fiber references arranged in the same order used in Table II. Column 2 gives the values of $\Delta[Ca_T]$ from column 4 in Table II. Columns 3 gives the peak values of Δ[CaTrop] and column 4 gives these values normalized by $[Trop]_R$, the concentration of Ca-regulatory sites that were Ca-free at rest. The values in both columns show a slight increase from top to bottom, consistent with the increase in the peak amplitude of the Δ[Ca] signal from top to bottom (column 10 in Table II). The mean values of Δ[CaTrop] and $\Delta[CaTrop]/[Trop]_R$ are 69 μM and 0.30, respectively.

Columns 5 and 6 give the values of the initial rapid increases in Δ[CaParv] and $\Delta[CaParv]/[Parv]_R$, respectively; $[Parv]_R$ represents the concentration of Ca,Mg sites that were divalent-cation-free at rest. In all but the first fiber (415911), the

[Ca] signals were sufficiently large to cause Ca to bind to more than half of the sites on parvalbumin that were divalent-cation-free at rest (column 6). Since the concentration of these sites decreases as the value of $[Ca]_R$ increases, the values of Δ[CaParv] decrease from top to bottom (column 5), especially in the last few entries in the table. The mean values of Δ[CaParv] and $\Delta[CaParv]/[Parv]_R$ are 36 μM and 0.65, respectively.

TABLE III

Estimates of the Concentration of Ca Bound to Troponin and Parvalbumin after a Single Action Potential in Fibers Equilibrated with 20 mM EGTA

(1)	(2)	(3)	(4)	(5)	(6)	(7)	(8)
Fiber reference	$\Delta[Ca_T]$	Δ[CaTrop]	$\Delta[CaTrop]/[Trop]_R$	Δ[CaParv]	$\Delta[CaParv]/[Parv]_R$	Scaling factor	−(3) × (7)
	μM	μM		μM			μM
415911	228	38	0.16	39	0.47	0.08	−2.9
O10911	299	61	0.26	40	0.58	0.31	−19.1
420921	316	61	0.26	40	0.59	−0.10	6.3
417921	309	57	0.24	37	0.57	−0.18	10.4
923911	287	57	0.24	36	0.56	−0.08	4.5
423911	370	70	0.30	42	0.66	−0.07	5.0
425911	395	75	0.31	43	0.69	0.30	−22.2
925911	366	68	0.29	38	0.65	−0.08	5.6
406921	407	76	0.33	33	0.69	−0.06	4.8
401921	455	81	0.35	30	0.73	−0.01	1.1
402921	534	91	0.40	27	0.78	−0.26	23.6
402922	539	90	0.40	24	0.79	−0.20	18.2
Mean	375	69	0.30	36	0.65	−0.03	2.9
SEM	28	4	0.02	2	0.03	0.05	3.8

Column 1 gives the fiber references arranged in the same order used for Table II. Column 2 gives the values of $\Delta[Ca_T]$ elicited by a single action potential, from column 4 in Table II. Columns 3 and 5 give the initial rapid increases in the amounts of Ca that were bound to the Ca-regulatory sites on troponin and the Ca,Mg sites on parvalbumin, respectively. These values were calculated from the free [Ca] waveform as described in the text and legend of Fig. 11. Columns 4 and 6 give the values of $\Delta[CaTrop]/[Trop]_R$ and $\Delta[CaParv]/[Parv]_R$, respectively. The values of Δ[CaTrop] and Δ[CaParv] were taken from columns 3 and 5, respectively, and the values of $[Trop]_R$ and $[Parv]_R$ were calculated from the parameters in the legend of Fig. 11 and from the values of $[Ca]_R$ in Table II. Column 7 gives the values of the scaling constant obtained from a least-squares fit of each Δ[CaTrop] trace, plus a sloping straight line, to the corresponding $\Delta[Ca_T]$ trace; the fit was done from the time when the Δ[CaTrop] trace had decayed to half its peak value to 100 ms after stimulation. Column 8 gives the negative value of the product of the values in columns 3 and 7. This represents a revised estimate of the peak amount of Ca that was bound to the Ca-regulatory sites on troponin, calculated from the amount of Ca that appeared to become complexed with EGTA during the time when Ca was expected to dissociate from troponin. See text for additional information.

Taken at face value, the mean values in columns 2, 3, and 5 indicate that a single action potential released, on average, 375 + 69 + 36 = 480 μM Ca (referred to myo-

plasmic concentration) from the SR into the myoplasm. Of this, 375/480 = 0.78 was captured by EGTA. Although such a large fractional capture of Ca by EGTA is adequate for most of the conclusions in this article, the following section shows that there is good reason to believe that the actual fraction was even larger.

The Peak Values of Δ[CaTrop] and Δ[CaParv] Estimated from Spatially Averaged Δ[Ca] Signals Are Probably Too Large

The results in columns 4 and 6 in Table III suggest that, even in fibers equilibrated with 20 mM EGTA, an action-potential stimulated free [Ca] transient is able to complex 0.30 of the Ca-regulatory sites on troponin and 0.65 of the Ca,Mg sites on parvalbumin that were divalent-cation-free at rest. Appendix D shows that these estimates of the extent of Ca complexation are probably too large because they fail to consider the spatial profile of free [Ca] inside the myoplasm.

Fig. 17 *A* shows theoretical loci of r and z that are associated with different steady state values of Δ[Ca] inside one half of an idealized cylindrical myofibril of diameter 1 μm and length 3.6 μm; the value of r varies from 0 to 500 nm and the value of z varies from 0 to 1,800 nm. Ca release was assumed to take place at a ring source at the Z-band. The value of SR Ca release was taken to be 140 μM/ms, which is similar to the mean peak value of 143 μM/ms in column 7 of Table II.

Loci of Δ[Ca] such as those in Fig. 17 *A* can be used to construct loci of different steady state values of $\Delta[\text{CaTrop}]/[\text{Trop}]_R$ and quasi-steady state values of $\Delta[\text{CaParv}]/[\text{Parv}]_R$; the loci for parvalbumin were calculated with [MgParv] = $[\text{MgParv}]_R$, which is expected to be a good approximation immediately after a brief [Ca] transient. These loci, which are shown in Fig. 17, *B* and *C*, respectively, give spatially averaged values $\Delta[\text{CaTrop}]/[\text{Trop}]_R = 0.253$ and $\Delta[\text{CaParv}]/[\text{Parv}]_R = 0.314$. These values are smaller than the mean values in Table III calculated from the spatially averaged [Ca] transients, 0.30 and 0.65, respectively. The difference is more pronounced for parvalbumin than for troponin, mainly because parvalbumin is assumed to be distributed uniformly throughout the sarcomere whereas troponin is located closer to the SR Ca release sites.

The values of $\Delta[\text{CaTrop}]/[\text{Trop}]_R$ and $\Delta[\text{CaParv}]/[\text{Parv}]_R$ associated with a brief [Ca] transient, however, are expected to be smaller than the steady state values obtained from Fig. 17, *B* and *C*. Preliminary calculations with the Δ[Ca] signal in Fig. 11 indicate that the peak value of $\Delta[\text{CaTrop}]/[\text{Trop}]_R$ should be reduced to ~0.17, which corresponds to Δ[CaTrop] = 40 μM. If the peak value of $\Delta[\text{CaParv}]/[\text{Parv}]_R$ is reduced to a similar extent, $\Delta[\text{CaParv}]/[\text{Parv}]_R = (0.17/0.253) \times 0.314 = 0.21$, which corresponds to Δ[CaParv] = 12 μM. With these revised estimates of Δ[CaTrop] and Δ[CaParv], a single action potential appears to have released, on average, 375 + 40 + 12 = 427 μM Ca into the myoplasm and EGTA appears to have successfully captured 375/427 = 0.88 of it.

For reasons that are not entirely clear, the value of 40 μM that was estimated for Δ[CaTrop] in the preceding paragraph is probably larger than the actual value. During the falling phase of the Δ[CaTrop] signal in Fig. 11, Ca is expected to have dissociated from troponin and to have been bound by EGTA. Thus, there should have been a slow secondary increase of $\Delta[\text{Ca}_T]$ (= Δ[CaEGTA]) that matches the decrease in Δ[CaTrop]. (Such an increase would be analogous to the secondary in-

crease in Δ[CaEGTA] that occurs in the presence of fura-2 when Ca dissociates from Cafura-2 and is bound by EGTA, as illustrated in the experiment in Figs. 5 and 6.) Contrary to this expectation, the $\Delta[Ca_T]$ signal was essentially constant during this period.

A possible explanation for the flat $\Delta[Ca_T]$ trace in Fig. 11 is that Ca binding by the Ca-regulatory sites on troponin is associated with a release of protons and that the stoichiometry of the release is the same as that of EGTA, 1 Ca:2 protons. In this case, a transfer of Ca from troponin to EGTA would not be expected to be associated with a change in myoplasmic pH. This possibility is considered to be unlikely because (*a*) the Ca-regulatory sites on troponin do not appear to exchange Ca for protons in the same way that EGTA does (see discussion on page 511 of Pape et al., 1990) and (*b*) the pH signal measured without EGTA is small and essentially constant during the period when Ca is expected to dissociate from troponin (Baylor, Chandler, and Marshall, 1982*a*; Irving et al., 1989; Hollingworth and Baylor, 1990). Thus, the flat $\Delta[Ca_T]$ trace suggests that little Ca dissociated from troponin during the first 200 ms after the action potential. This could be due either to an extremely slow rate of Ca dissociation or, more likely, to a reduction in the actual concentration of Ca bound to troponin.

An attempt was made to obtain an estimate of the concentration of Ca that was actually bound to troponin after an action potential. To do this, the $\Delta[Ca_T]$ trace in Fig. 11 was least-squares fitted (fit not shown) with a sloping straight line plus a scaled contribution from the Δ[CaTrop] trace. Since a decrease in Δ[CaTrop] is expected to be associated with an increase in $\Delta[Ca_T]$, the scaling constant for the Δ[CaTrop] signal is expected to be negative. The fit was carried out from the time that the Δ[CaTrop] trace had decreased to half its peak value to 100 ms after the stimulus for the action potential. The scaling factor for the Δ[CaTrop] trace was -0.083, consistent with the idea that only a small concentration of Ca, equal to $0.083 \times 68\ \mu M = 5.6\ \mu M$, had actually been bound to troponin at the time of peak binding.

Column 7 in Table III gives the values of the scaling constant obtained from a least-squares fit of each Δ[CaTrop] trace, plus a sloping straight line, to the corresponding $\Delta[Ca_T]$ trace, as described in the preceding paragraph. Column 8 gives the negative values of the product of columns 3 and 7. These represent a revised estimate of the peak value of Δ[CaTrop]. This suggests that, on average, only 2.9 μM Ca was actually complexed by troponin. With Δ[CaEGTA] = 375 μM, Δ[CaTrop] = 3 μM, and Δ[CaParv] = 12 μM (see above), it appears that EGTA was able to capture, on average, $375/(375 + 3 + 12) = 0.96$ of the Ca released from the SR.

The apparent ability of EGTA to prevent the binding of Ca to troponin is consistent with the observation of Palade and Vergara (1982) that movement artifacts are reduced considerably in cut fibers equilibrated with $\geq$3 mM EGTA. Possible explanations for the apparent failure of troponin to bind as much Ca as expected from Appendix D include (*a*) EGTA is able to spatially limit the increase in free [Ca] near the SR release sites more than predicted by Appendix D (perhaps by binding to myoplasmic sites near the SR Ca channels); (*b*) EGTA, by some other unspecified means, is able to alter the characteristics of Ca binding to troponin; (*c*) the association rate constant of Ca and troponin is smaller than the value 0.575×10^8

$M^{-1}s^{-1}$ used to calculate Δ[CaTrop]; (*d*) the amplitude or duration of the free [Ca] transient is overestimated in our experiments (and consequently overestimated in the theoretical analysis).

The Value of SR Ca Content Estimated with Voltage-clamp Depolarizations Is Similar to that Estimated with a Train of Action Potentials

Fig. 12 shows superimposed traces of voltage (*top*) and $\Delta[Ca_T]$ signals (*bottom*) from a voltage-clamp experiment in which the fiber was depolarized, in chronological order, to −50 (trace *1*), −40 (trace *2*), −30 (trace *3*), −20 (trace *4*), and −50 (trace 5) mV. A 5-min recovery interval preceeded each pulse to allow the SR to reaccumulate most of the Ca that had been released by the preceding pulse (cf. Fig. 3). The external solution was nominally Ca-free so that Ca could not enter the fiber during the prolonged depolarizations.

After depolarization, each $\Delta[Ca_T]$ signal in Fig. 12 increased to a quasi-plateau

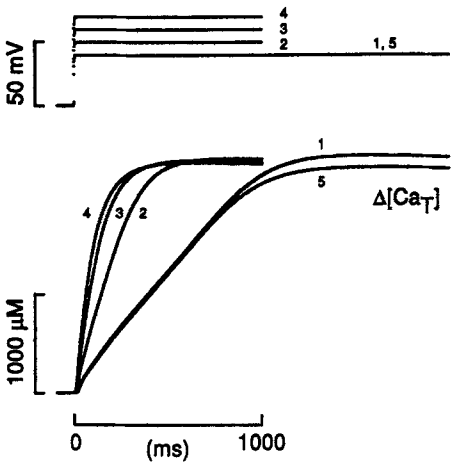

FIGURE 12. Effect of pulse potential on the amplitude of the $\Delta[Ca_T]$ signal elicted by a long lasting step depolarization. The top and bottom sets of traces show voltage and $\Delta[Ca_T]$, respectively. The measurements were made at 5-min intervals in the order indicated. Fiber reference, O15911; time after saponin treatment, 150–170 min; sarcomere length, 3.4 μm; fiber diameter, 153 μm; holding current, −51 to −52 nA; temperature, 14°C; phenol red concentration at the optical site, 1.760–1.828 mM; estimated pH_R and free $[Ca]_R$, 6.808–6.801 and 0.087–0.091 μM, respectively; interval of time between data points, 0.96 ms. The TEA-gluconate solution was used in the central pool; the Cs glutamate solution with 20 mM EGTA plus 1.76 mM Ca and 0.63 mM phenol red was used in the end pools.

value with a rate that increased with increasing voltage. The peak values of the $\Delta[Ca_T]$ traces were 2,416 μM (trace *1*), 2,385 μM (trace *2*), 2,366 μM (trace *3*), 2,345 μM (trace *4*), and 2,295 μM (trace *5*). These values are similar to one another except for a small progressive decrease of ~1% after each trial; a small progressive decrease was observed in all of our experiments and may be due, at least partially, to fiber run down. These results are generally consistent with the idea that the value of $[Ca_{SR}]_R$ can be estimated from the peak value of $\Delta[Ca_T]$ during a depleting voltage step and that this value is independent of the magnitude of the voltage step.

Values of $[Ca_{SR}]_R$ were estimated from long lasting voltage-clamp steps in 11 fibers. The mean values of pH_R and $[Ca]_R$ were 6.864 (SEM, 0.009) and 0.068 μM (SEM, 0.003 μM) respectively, and the mean value of $[Ca_{SR}]_R$ was 2,544 μM (SEM, 70 μM). These mean values are marked by the intersection of the arms of the large asymmetrical cross in Fig. 9; the range of values is marked by the horizontal and

vertical excursion of the cross. The range of values of pH_R, and therefore of $[Ca]_R$, was narrower in these voltage-clamp experiments than in the action-potential experiments, for reasons that are not known. Within this range, the values of $[Ca_{SR}]_R$ were similar in the two kinds of experiments, indicating that, with 20 mM EGTA plus 1.76 mM Ca in the end-pool solutions, the Ca content of the SR is little affected by whether K or Cs is in the internal solution or by whether Ringer's solution or the Ca-free TEA-gluconate solution is used for the external solution.

Ca Inactivation of Ca Release Is Able to Develop during Voltage-clamp Depolarizations in Fibers Equilibrated with 20 mM EGTA

Fig. 13 shows traces obtained during a 350-ms voltage-clamp depolarization to 60 mV. The top trace shows voltage and the second trace shows $\Delta[Ca_T]$. The $\Delta[Ca_T]$

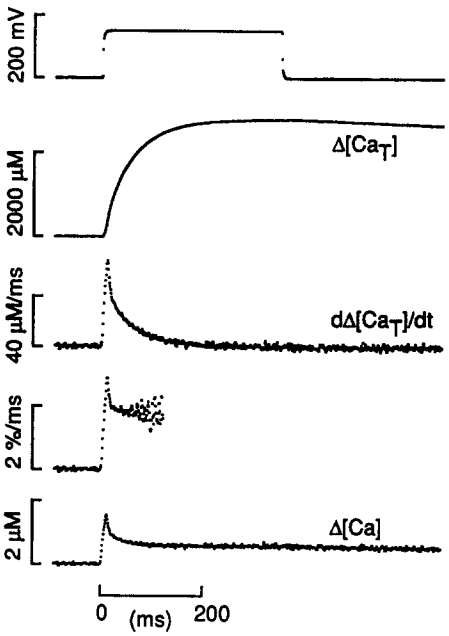

FIGURE 13. SR Ca release during a step depolarization to 60 mV. The first three traces show, from top to bottom, voltage, $\Delta[Ca_T]$, and $d\Delta[Ca_T]/dt$. The next trace shows $d\Delta[Ca_T]/dt$ after correction for SR Ca depletion; the value of $[Ca_{SR}]_R$ before depolarization was taken to be 2,779 µM, the peak value of $\Delta[Ca_T]$ during the pulse. The bottom trace shows $\Delta[Ca]$. Fiber reference, 412911; time after saponin treatment, 57 min; sarcomere length, 3.5 µm; fiber diameter, 127 µm; holding current, −32 nA; temperature, 14°C; concentration of phenol red at the optical site, 0.957 mM; estimated pH_R and free $[Ca]_R$, 6.868 and 0.066 µM, respectively; interval of time between data points, 0.96 ms. The TEA-gluconate solution was used in the central pool; the Cs-glutamate solution with 20 mM EGTA plus 1.76 mM Ca and 0.63 mM phenol red was used in the end pools.

trace started to increase soon after the depolarization and, by the end of the pulse, had reached a plateau level of 2,779 µM, which is taken to be the value of $[Ca_{SR}]_R$. After repolarization, $\Delta[Ca_T]$ slowly decreased, similar to the slow decrease observed after the train of action potentials in Fig. 8 *B*.

The third trace in Fig. 13 shows $d\Delta[Ca_T]/dt$. This signal reached a peak value of 68 µM/ms ~11 ms after depolarization. It then rapidly decreased to about half its peak value and thereafter slowly decreased to zero. Since the time course of the slow decrease was similar to that of the estimated readily releasable Ca content of the SR, given by $[Ca_{SR}] = [Ca_{SR}]_R - \Delta[Ca_T]$, it was likely due to SR Ca depletion (Schneider, Simon, and Szúcs, 1987).

The fourth trace in Fig. 13 shows $d\Delta[Ca_T]/dt$ after correction for SR Ca depletion. At each moment in time, the value of $d\Delta[Ca_T]/dt$ was divided by $[Ca_{SR}]_R -$

$\Delta[Ca_T]$ and multiplied by 100 to give units of percent per millisecond. After the early peak (2.91 %/ms), the signal rapidly decreased to a quasi-steady level (1.86 %/ms, averaged 25–54 ms after the beginning of the step), with a quasi-steady to peak ratio of 1.86/2.91 = 0.64. At later times, the trace became noisy because of the depletion correction.

The bottom trace in Fig. 13 shows the estimated time course of $\Delta[Ca]$. The peak value was 1.62 μM and the value at the end of the 350 ms pulse was 0.64 μM.

Similar results were obtained in another experiment in which a fiber was also depolarized to 60 mV. The peak value of $d\Delta[Ca_T]/dt$ was 71 μM/ms or 3.32%/ms, the quasi-steady value was 1.85 %/ms, and the quasi-steady to peak ratio was 0.56; $[Ca_{SR}]_R$ = 2,483 μM and the peak and final values of $\Delta[Ca]$ were 1.68 and 0.48 μM, respectively.

The extent of the early rapid decrease of the $d\Delta[Ca_T]/dt$ signal in both experiments is similar to, but less marked than, that inferred in previous experiments in which [Ca] transients were not modified by EGTA or any other extrinsic Ca buffer. For example, in other cut fiber experiments carried out in this laboratory with only 0.1 mM EGTA in the end-pool solutions, the quasi-steady to peak ratio of $d\Delta[Ca_T]/dt$, corrected for SR Ca depletion, was 0.2–0.3 (columns 2 and 3 in Table IIIA in Jong et al., 1993) instead of 0.64, as observed in Fig. 13, or 0.56, as observed in the other experiment. Schneider and Simon (1988) and Simon et al. (1991) showed that the decrease observed with unmodified [Ca] transients is probably due to Ca inactivation of Ca release. Because the decrease observed in Fig. 13 is qualitatively similar to that studied by Schneider and Simon (1988) and Simon et al. (1991), it seems likely that it, too, was caused by Ca inactivation of Ca release, even though the $\Delta[Ca]$ signal had been severely attenuated by equilibration of the fiber with 20 mM EGTA.

The main conclusion from these and other similar voltage-clamp experiments is that, even after equilibration with 20 mM EGTA, Ca inactivation of Ca release is able to develop during a depolarizating voltage step. A similar conclusion was reached from our action-potential experiments, based on the finding that the value of f_2/f_1 in a 50 Hz tetanus was clearly less than unity (cf. Fig. 8 *B*). Additional information about this inactivation and its reduction by EGTA is given in the following article (Jong et al., 1995).

The Peak Rate of SR Ca Release Is Larger after an Action Potential Than during a Voltage Step to 60 mV

In the fibers used for Fig. 10 *D*, the mean peak rate of SR Ca release was 5.25 %/ms after an action potential whereas, in the two experiments described in the preceding section (Fig. 13), the peak rate of release was 2.91 and 3.32 %/ms (mean value, 3.12%/ms) during a depolarization to 60 mV. The smaller peak rate during a step to 60 mV is surprising since both the amplitude of the depolarization and the time required to elicit the peak rate of release were greater with a step to 60 mV than with an action potential: (*a*) the amplitude of the individually recorded action potentials varied from 125 to 139 mV with respect to the holding potential, −90 mV, or from 35 to 49 mV with respect to 0 mV and (*b*) the time to peak rate of SR Ca re-

lease is achieved only a few milliseconds after an action potential whereas ~10 ms is required after a depolarization to 60 mV.

A possible explanation of this difference is that the SR Ca release sites were partially inactivated in the voltage-clamp experiments because Ca in the external solution had been replaced with Mg, an ionic substitution that shifts the inactivation curve of SR Ca release to more negative potentials (Brum, Ríos, and Stefani, 1988). Such inactivation cannot account for the smaller rates of release in our voltage-clamp experiments because similar small rates were observed with 1.8 mM Ca, instead of 10 mM Mg, in the external solution (Jong et al., 1995).

Several other explanations can be suggested, based on differences in the composition of the internal and external solutions in the action-potential and voltage-clamp experiments. One of these is that the membranes of the transverse tubules may be depolarized more rapidly by a regenerative Na spike during an action potential than by passive electrotonic spread during a step depolarization with TEA and TTX in the external solution. This, in turn, may allow SR Ca release to be synchronized throughout the cross section of a fiber so that the peak rate occurs simultaneously throughout the fiber before attenuation by Ca inactivation of Ca release. This explanation is consistent with the rapid speed with which Ca inactivation of Ca release is able to develop, with a time constant of 2–4 ms (Fig. 13 and Jong et al., 1995).

SR Ca Release Is Steeply Voltage Dependent When No More Than One Channel in 10^4 Is Open

Previous experiments have shown that SR Ca release is steeply voltage dependent, both in intact fibers (Baylor and Chandler, 1978; Baylor, Chandler, and Marshall, 1979, 1983; Miledi, Nakajima, Parker, and Takahashi, 1981) and in cut fibers equilibrated with only 0.1 mM EGTA (Maylie et al., 1987*b*,*c*). Near the threshold for detectable Ca signals, the amplitude of peak free [Ca] increases *e*-fold for each 2–4 mV increase in depolarization. Because the *e*-fold parameter for Ca release is ~1 mV larger than that for peak free [Ca] itself (Baylor et al., 1983), the *e*-fold parameter for SR Ca release is probably 3–5 mV. In all of these experiments, little extrinsic Ca buffer (including the indicator) was introduced into the myoplasm so that physiologically normal increases in myoplasmic free [Ca] were able to occur.

The voltage dependence of SR Ca release can also be determined with the EGTA-phenol red method, under conditions in which changes in myoplasmic free [Ca] are minimized by EGTA. As in all of the voltage-clamp experiments reported in this article, Ca was removed from the external solution and replaced with 10 mM Mg so that movements of Ca into the fiber during depolarization could not play a role in the regulation of SR Ca release—for example, by Ca-induced Ca release—or contribute directly to $\Delta[Ca_T]$.

The upper trace in Fig. 14 *A* shows a representative voltage record and the lower superimposed traces show $\Delta[Ca_T]$ signals elicited by 400-ms step depolarizations to the voltages indicated (in millivolts). In this experiment, each depolarization was followed by a 500-ms repolarization to the holding potential, after which a 600-ms pulse to −35 mV was given to deplete the SR of any remaining Ca. A recovery period of 5 min was used before each trial so that the SR would be able to reaccumu-

late almost all of the Ca released by the preceding pulse (cf. Fig. 3). The value of $[Ca_{SR}]_R$ was 2,594 μM when the first trace was taken, to the test depolarization of −72 mV. It decreased slightly with each trial during the experiment and was 2,447 μM when the last trace was taken, to −57 mV.

The $\Delta[Ca_T]$ traces in Fig. 14 *A* rise after an initial delay, which became briefer as

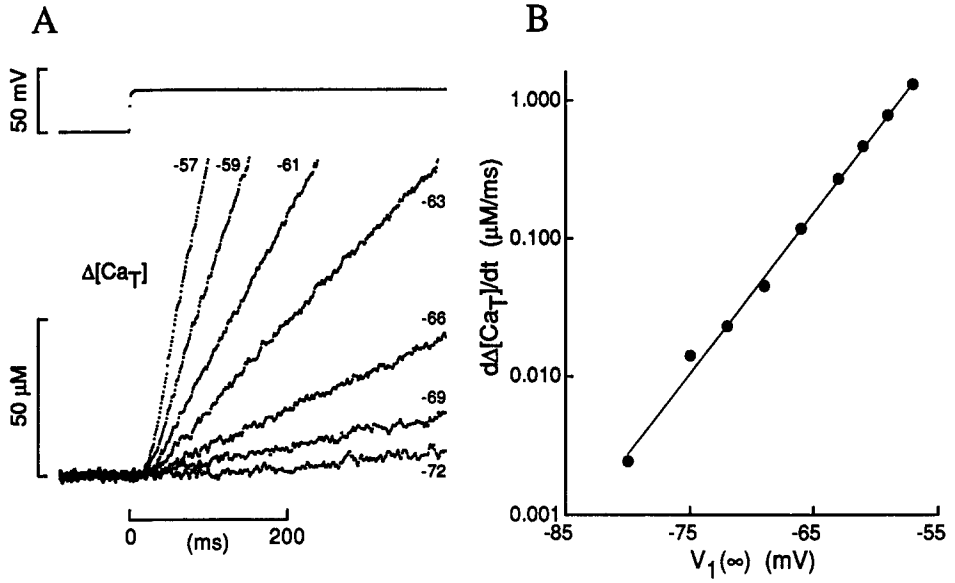

FIGURE 14. Voltage dependence of SR Ca release, from the fiber used for Fig. 12. (*A*) The top trace shows a representative voltage record. The bottom superimposed traces show $\Delta[Ca_T]$ at the voltages indicated (in millivolts). Each depolarization was followed by a 500-ms repolarization to −90 mV and a 600 ms depolarization to −35 mV (not shown), which depleted the SR of Ca. The interval between successive stimuli was 5 min. (*B*) Filled circles show the values of $d\Delta[Ca_T]/dt$ plotted semilogarithmically against $V_1(\infty)$, the steady value of potential during the pulse in the voltage-measuring end pool. The values of $d\Delta[Ca_T]/dt$ were determined from least-squares fits of straight lines to the $\Delta[Ca_T]$ traces in panel A and two other traces from the same experiment. For $V \leq -66$ mV, the traces were fitted between 150 and 400 ms. For $V \geq -63$ mV, the traces were fitted between $\Delta[Ca_T]$ = 25 and 100 μM. The straight line in B was least-squares fitted to the filled circles. Its slope corresponds to an *e*-fold increase in $d\Delta[Ca_T]/dt$ every 3.73 mV. During the course of the experiment, the voltage of the first pulse was progressively increased from −80 to −57 mV. The following list gives, in order, the first and last values of each variable: time after saponin treatment, 76–116 min; holding current, −48 to −49 nA; concentration of phenol red at the optical site, 1.098–1.572 mM; estimated pH_R and free $[Ca]_R$, 6.853–6.830 and 0.071–0.079 μM, respectively; $[Ca_{SR}]_R$, 2,594–2,447 μM; interval of time between data points, 0.96 ms. The other information is the same as that given in the legend of Fig. 12.

the voltage was made more positive. Thereafter, the slope of each $\Delta[Ca_T]$ trace became approximately constant. At voltages ≥ −63 mV, the initial slope of each curve was slightly greater than the final slope. Since the change in Ca content of the SR was ≤100 μM, corresponding to ≤4% of the value of $[Ca_{SR}]$, this change in slope is probably not due to SR Ca depletion. Rather, it is more likely due to Ca inactivation

of Ca release (Baylor et al., 1983; Simon et al., 1985, 1991; Schneider and Simon, 1988). Unfortunately, it is difficult to tell whether a similar change in slope occurred at voltages <-63 mV because of noise in the records.

A sloping straight line was least-squares fitted to each trace in Fig. 14 *A* and to two additional traces from the same experiment. The fit extended from 150 to 400 ms for $V \leqslant -66$ mV and from $\Delta[Ca_T] = 25$ to 100 μM for $V \geqslant -63$ mV. Fig. 14 *B* shows a semilogarithmic plot of the slope, $d\Delta[Ca_T]/dt$, as a function of voltage. A straight line was least-squares fitted to the data between -80 and -57 mV, as shown. It provides a good fit over a range of values of $d\Delta[Ca_T]/dt$ that span more than two orders of magnitude. At potentials more positive than -57 mV, the experimental values of $d\Delta[Ca_T]/dt$ lie below the extrapolated line (not shown). The slope of the line corresponds to an *e*-fold increase in $d\Delta[Ca_T]/dt$ every 3.73 mV. In four experiments of this type, the mean *e*-fold factor was 3.48 mV (SEM, 0.16 mV).

It is apparent in Fig. 14 that the rate of SR Ca release was steeply voltage dependent even when its value was as small as 0.01 μM/ms. This is four orders of magnitude smaller than the peak rate of Ca release, 70 μM/ms, that was observed in this fiber with strong depolarizations (not shown). The maximal rate of release that would have been observed in the absence of Ca inactivation of Ca release, with all of the SR Ca channels open, is probably >70 μM/ms (Jong et al., 1995). Furthermore, according to Eq. A10 and a value of 22 μs for $(k_1[EGTA]_R)^{-1}$, a value of 0.01 μM/ms for $d\Delta[CaEGTA]/dt$ corresponds to a value of 0.22 nM for spatially averaged myoplasmic $\Delta[Ca]$.

Thus, SR Ca release is steeply voltage dependent under conditions in which no more than one SR Ca channel in 10^4 is open and the value of spatially averaged myoplasmic free [Ca] increases by only 0.2 nM, an amount that is insignificant with respect to the value of $[Ca]_R$, 0.071–0.079 μM. These results make it very unlikely that the voltage steepness of SR Ca release depends on changes in spatially averaged myoplasmic free [Ca]. According to the ideas developed in the Discussion, if the spatial distribution of open SR Ca release sites is random, the voltage steepness of release is most likely a property of the voltage sensor in the membranes of the transverse tubular system that regulates a single release site. Such a site might consist of a single SR channel or a collection of channels that function as a singly gated unit (for example, a single voltage-gated channel and neighboring channel(s) that are slaved to it).

The EGTA-Phenol Red Method Is Able to Measure Extremely Small Rates of SR Ca Release

The EGTA-phenol red method is able to measure much smaller rates of SR Ca release than methods that rely on the free [Ca] transient measured with a low affinity Ca indicator. For example, in the experiment in Fig. 14, the rate of SR Ca release at -75 mV was ~0.01 μM/ms. If myoplasmic Ca had not been buffered by EGTA, the myoplasmic free [Ca] transient should have reached a peak within the first 100 ms of the depolarization (for example, Maylie et al., 1987*b*,*c*) and, if the rate of SR Ca release had been the same (including the delay as observed in Fig. 14 *A*), the value of $\Delta[Ca_T]$ would have been <1 μM.

The value of free Δ[Ca] is expected to have been much less than 1 μM because of Ca binding to troponin and parvalbumin. With troponin, for example, the concentration of Ca-regulatory sites is ~240 μM (Baylor et al., 1983) and their K_D is expected to be ≤2 μM (Zot and Potter, 1987). Consequently, for small values of Δ[Ca], $\Delta[Ca]/\Delta[Ca_T] < \Delta[Ca]/\Delta[CaTrop] \leq 2/240$. The presence of parvalbumin is expected to reduce the value of $\Delta[Ca]/\Delta[Ca_T]$ even more. Thus, for a value of $\Delta[Ca_T] < 1$ μM, the value of myoplasmic free Δ[Ca] is expected to be <0.01 μM. This value is much too small for a reliable estimate of SR Ca release to be obtained from the [Ca] transient measured with a low affinity Ca indicator.

DISCUSSION

The experiments reported in this article show that equilibration of cut muscle fibers with 20 mM EGTA reduces, by severalfold, both the amplitude and duration of the spatially averaged myoplasmic free Δ[Ca] signal elicited by an action potential. In spite of these reductions, many properties of SR Ca release—such as the amount of release after an action potential, the peak rate of release, and its time course—are similar in a general way to those estimated previously in cut fibers with unmodified free [Ca] transients (Maylie et al., 1987*a*,*c*; Hirota et al., 1989; Pape et al., 1993). Our voltage-clamp experiments suggest that the only important effect exerted by 20 mM EGTA on the SR Ca release mechanism is a reduction in Ca inactivation of Ca release. For example, the quasi-steady to peak ratio of $d\Delta[Ca_T]/dt$ during a step depolarization was larger in our EGTA experiments than in experiments in which the [Ca] transient was not modified. Additional information about Ca inactivation of Ca release and its reduction by EGTA is presented in the following article (Jong et al., 1995).

SR Ca Release Is Steeply Voltage Dependent Even When Each Open Channel Is Screened from the Effects of Ca from Other Open Channels

In Fig. 14, the voltage dependence of the rate of SR Ca release was found to be steeply voltage dependent when the rate of release was as small as 0.01 μM/ms. Moreover, the voltage dependence appeared to be constant over a range of values of $d\Delta[Ca_T]/dt$ that spanned more than two orders of magnitude. The only source of Ca that was available to enter the myoplasmic solution was inside the SR; Ca was omitted from the external solution so that Ca fluxes into the fiber could not contribute directly to $\Delta[Ca_T]$ or, in some unspecified way, affect the regulation of SR Ca release. Consequently, during depolarization, local increases in myoplasmic free [Ca] are expected to have developed only near the mouth of each open channel. The aim of this section is to determine how many SR Ca channels are required to give a rate of release of 0.01 μM/ms and to inquire whether neighboring open channels are able to "communicate" with one another through the local increases in [Ca] that develop near each open channel.

As described in Appendix B, if an open channel behaves as a point source of Ca flux ϕ into an isotropic infinite medium, the steady state increment in free Ca concentration, Δ[Ca], at a distance r from the mouth of the channel is given by

$$\Delta[\mathrm{Ca}] = \frac{\phi}{4\pi D_{\mathrm{Ca}} r} \cdot \exp(-r/\lambda_{\mathrm{Ca}}). \tag{B21}$$

D_{Ca} is the diffusion coefficient of Ca and λ_{Ca} is defined by

$$\lambda_{\mathrm{Ca}} = \sqrt{\frac{D_{\mathrm{Ca}}}{k_1 [\mathrm{EGTA}]_{\mathrm{R}}}}. \tag{B14}$$

λ_{Ca} represents the characteristic distance associated with the diffusion of a Ca ion before its capture by EGTA. Appendix B gives estimates of D_{Ca}, 3.0×10^{-6} cm^2/s, and $k_1(\mathrm{EGTA})_{\mathrm{R}}$, $(22\ \mu\mathrm{s})^{-1}$, that are expected to apply to a cut muscle fiber studied under our experimental conditions. These give $\lambda_{\mathrm{Ca}} = 81$ nm.

The value of ϕ, in units of number of ions per second, is given by the value of $d\Delta[\mathrm{Ca_T}]/dt$ that would be obtained if all of the channels were open, divided by the concentration of SR Ca channels referred to myoplasmic solution. Although the maximal value of $d\Delta[\mathrm{Ca_T}]/dt$ is not known, it clearly must be at least 70 μM/ms because values this large are routinely measured in fibers studied under the same conditions used in Fig. 14 (results in this article and in Jong et al., 1995). It is possible, however, that the peak value of $d\Delta[\mathrm{Ca_T}]/dt$ is attenuated by Ca inactivation of Ca release and that the actual maximal value of $d\Delta[\mathrm{Ca_T}]/dt$ is larger (Jong et al., 1995).

If the concentration of SR Ca channels is the same as that of the foot structures described by Franzini-Armstrong (1975), the concentration of SR Ca channels is ~0.27 μM (Pape, Konishi, and Baylor, 1992). A value of ≥70 μM/ms for $d\Delta[\mathrm{Ca_T}]/dt$ implies a value $\geq 2.6 \times 10^5$ ions/s for ϕ, which corresponds to a single-channel current of ≥0.083 pA. For a frog fiber with a sarcomere length of 3.6 μm, a concentration of 0.27 μM SR Ca channels corresponds to a density of ~600 channels/μm^2 in the plane of the Z-band, where the channels are located in amphibian muscle. If ρ denotes the density of open channels that corresponds to $d\Delta[\mathrm{Ca_T}]/dt = 0.01$ μM/ms, it follows that $\rho \leq (0.01/70)600 = 0.086$ channels/μm^2.

Three calculations, described below, suggest that, at this density of open channels, 20 mM EGTA is able to shield each open channel from the effects of Δ[Ca] from other open channels. An important assumption in calculations *b* and *c* is that the open channels are distributed randomly within each cross sectional area in the plane of the Z-band.

(*a*)This calculation shows that the mean increase in [Ca] in the plane of the Z-band is too small to be expected to have any appreciable influence on Ca channel activity. During SR Ca release, the mean value of Δ[Ca], $\langle\Delta[\mathrm{Ca}]\rangle$, at a distance z from the plane of the Z-band is given by

$$\Delta\langle[\mathrm{Ca}]\rangle \cong \Delta\overline{[\mathrm{Ca}]}\left(\frac{l}{\lambda_{\mathrm{Ca}}} \cdot \exp(-z/\lambda_{\mathrm{Ca}})\right). \tag{D13}$$

$\Delta\overline{[\mathrm{Ca}]}$ represents the spatially averaged value of Δ[Ca], which is equal to 0.22 nM when $d\Delta[\mathrm{Ca_T}]/dt = 0.01$ μM/ms (Eq. A10). With $l = 1{,}800$ nm (corresponding to a sarcomere length of 3.6 μm) and $\lambda_{\mathrm{Ca}} = 81$ nm, the value of $\langle\Delta[\mathrm{Ca}]\rangle$ at $z = 0$ (in the plane of the Z-band) is ~5 nM. This value is too small, especially with respect

to $[Ca]_R$, to be expected to influence channel activity. This value is a mean value, however, and larger changes in free [Ca] would be expected to occur near open channels. Calculations *b* and *c* deal with the change in free [Ca] that is expected to occur near a single open channel.

b) In the plane of the Z-band, the mean distance between an open channel and its nearest open neighbor can be shown to be given by the expression $(4\rho)^{-1/2}$. With $\rho \leq 0.086$ channels/μm^2, this distance is ≥ 1.7 μm. According to Eq. B21, the value of Δ[Ca] is negligibly small, $\leq 5 \times 10^{-17}$ M, for $r \geq 1.7$ μm. (The inequality sign for Δ[Ca] takes into account the fact that values of ρ that are ≤ 0.086 channels/μm^2 imply values of ϕ that are $\geq 2.6 \times 10^5$ ions/s.)

c) In calculation *a*, the mean value of $\langle\Delta[Ca]\rangle$ in the plane of the Z-band was estimated to be $\sim$5 nM. The aim of this calculation is to estimate the fraction of open channels that do not have another open channel sufficiently close to increase free [Ca] by some minimal amount, which will be taken to be 1 nM. According to Eq. B21, if $\phi = 2.6 \times 10^5$ ions/s (which corresponds to $\rho = 0.086$ channels per μm^2), Δ[Ca] = 1 nM at $r = 0.45$ μm. It can be shown that the fraction of open channels that do not have another open channel within a distance r is given by $\exp(-\pi\rho r^2)$. With $\rho = 0.086$ channels/μm^2 and $r = 0.45$ μm, the value of the fraction is 0.95. The same calculation carried out with $\phi \geq 2.6 \times 10^5$ ions/s (which corresponds to $\rho \leq 0.086$ channels per μm^2) gives a value of ≥ 0.95 for the fraction. Thus, if the conservative assumption is made that free [Ca] must rise by at least 1 nM to have an effect on the gating of a channel, almost all of the open channels (≥ 0.95) are shielded from the effects of Ca from their nearest open neighbors.

These three calculations, which apply to fibers equilibrated with 20 mM EGTA, are based on a rate of SR Ca release of 0.01 μM/ms and the assumption that the distribution of open channels is random. The same analysis applies if the functional unit for Ca release, which will be called a release site, consists of a single Ca channel or a collection of neighboring channels that function as a singly gated unit. A hypothetical example of such a collection can be developed along the lines proposed by Ríos and Pizarró (1988), based on the structural studies of Block, Imagawa, Campbell, and Franzini-Armstrong (1988) on muscle from toadfish swim bladder: a single voltage-gated SR channel, which is controlled by an apposing voltage sensor in the membranes of the transverse tubules, and adjacent SR channels that are not associated directly with voltage sensors but are slaved in an obligatory fashion to the voltage-gated SR channel. Coupling from the voltage-gated channel to its slaves could involve Ca, as suggested by Ríos and Pizarró (1988), or some other messenger.

Whether the release site consists of a single channel or a collection of neighboring channels that function as a singly gated unit, if the spatial distribution of open sites in the plane of the Z-band is random, it seems unlikely that the open state of any particular site could have been caused by Ca from another open site. For this reason, it seems unlikely that SR Ca release itself—by Ca-induced Ca release, by the positive feedback model proposed by Pizarró, Csernoch, Uribe, Rodríguez, and Ríos (1991), or by some other mechanism—was able to contribute to the steep voltage dependence of Ca release that was observed with small rates of release in experiments such as the one in Fig. 14. A similar conclusion is expected to apply to the

entire voltage range illustrated in Fig. 14 B because all of the data are well fitted by the same straight line. At larger depolarizations, the points lay below the extrapolated line, indicating that the voltage steepness of release never exceeds that observed with small rates of release. Since the voltage steepness of release in these fibers equilibrated with 20 mM EGTA is similar to that determined in fibers with unmodified [Ca] transients, it seems reasonable to conclude that the voltage dependence of Ca release recorded under normal physiological conditions with unmodified [Ca] transients directly reflects the voltage dependence of activation of single SR release sites by their voltage sensors in the membranes of the transverse tubular system.

The EGTA-Phenol Red Method Estimates SR Ca Release Reliably and Rapidly

A detailed description of the EGTA-phenol red method is given in the Methods and Appendix A. For the purposes of this section, the main points are (*a*) in the absence of myoplasmic Ca buffers such as troponin and parvalbumin, 20 mM EGTA is expected to capture essentially all (>99.9%) of the Ca released from the SR; (*b*) 20 mM EGTA is expected to complex the released Ca rapidly, with a time constant <0.1 ms; and (*c*) on the time scale of Ca release studied in these experiments, only two sources or sinks for protons, apart from the myoplasmic buffering power, are expected to contribute significantly to ΔpH: the exchange of protons for Ca by EGTA (with a stoichiometry of 1 Ca:2 protons) and the movement of protons into the SR that occurs during Ca release (with a stoichiometry of 1 Ca:0.2–0.3 protons).

The first additional point to consider is whether troponin and parvalbumin are able to capture an amount of Ca that is significant compared with that captured by EGTA, 375 μM on average. If the spatially averaged free [Ca] signal is used to calculate the amount of Ca bound to troponin and parvalbumin after an action potential, 105 μM Ca, on average, is estimated to have been bound by these intrinsic Ca buffers (mean values in columns 3 and 5 in Table III). As described in connection with column 8 in Table III, this estimate is almost certainly too large and, in fact, the actual value is probably ~15 μM Ca. Consequently, after a single action potential, EGTA is expected to capture ~96% of the Ca released from the SR.

The second point to consider is the accuracy of the measurements of ΔpH that are used to estimate Δ[CaEGTA]. Although approximately two thirds of the phenol red inside a fiber appears to be bound or sequestered, the ΔpH signal is expected to be reliable (see Methods). Even if it isn't, however, any inaccuracies in the estimate of ΔpH would alter, by the same relative amount, the value of Δ[CaEGTA] in both the experiments on SR Ca release and the experiments on the determination of β. Use of Eq. A7 insures that the effects of such inaccuracies are cancelled and, as a result, the primary calibration for the estimation of SR Ca release is the calibration of the Δ[Cafura-2] signals that were used for the estimates of β (Figs. 5–7).

The general conclusion of this section is that the EGTA-phenol red method provides a reliable and rapid estimate of SR Ca release. The estimated value of $\Delta[Ca_T]$, however, probably represents an underestimate. First, as much as 4% of the Ca released from the SR by a single action potential may be complexed by troponin and parvalbumin rather than by EGTA. Second, during SR Ca release, protons appear to enter the SR and balance 0.10–0.15 of the electrical charge associated with Ca re-

lease. To correct for the proton exchange, the $\Delta[Ca_T]$ signals described in this article should probably be multiplied by 1.11–1.18. Because this factor is expected to be independent of the amount or rate of SR Ca release (Pape et al., 1990), the correction is not expected to affect any conclusions about relative rates of release.

The Change in pH Produced by the Complexation of Ca and EGTA after SR Ca Release Does Not Appear to Alter the Physiological Condition of the Fiber

A possible disadvantage of the EGTA-phenol red method for the measurement of SR Ca release is that Ca complexation by EGTA decreases myoplasmic pH and this might alter the physiological condition of the fiber or the mechanism responsible for SR Ca release. As far as we can tell, however, such alterations do not occur. For example, as mentioned above in connection with Table II, the amplitude and time course of $d\Delta[Ca_T]/dt$ signals estimated with EGTA-phenol red are similar, in general, to those estimated with low affinity Ca indicators and unmodified [Ca] transients (although a quantitative comparison of amplitudes cannot be made without knowledge of the SR Ca content in the fibers with unmodified [Ca] transients). The fractional amount of SR Ca that is released by an action potential and the peak fractional rate of release appear to be relatively insensitive to pH_R between 6.7 and 7.1 and, consequently, relatively insensitive to $[Ca_{SR}]_R$ (Fig. 10, *B* and *D*). In addition, the reduction in the fractional amount of Ca released from the first to the second action potential elicted 20 ms later was insensitive to pH_R and $[Ca_{SR}]_R$ (Results).

During the course of most cut fiber experiments, the value of pH_R progressively decreased with time, regardless of whether the fiber was stimulated or not. In the fiber in Fig. 2, the values of pH_R associated with the first and last single action potentials were 6.912 and 6.878, respectively. The amplitude of the ΔpH signal associated with the first single action-potential stimulation was −0.034. This signal reduced the value of pH to 6.878, which is exactly the same as the resting value just before the second and last single action-potential stimulations. If the first decrease in pH from 6.912 to 6.878 altered the SR Ca release mechanism, the ΔpH signal associated with the second single action-potential stimulation would be expected to be different from −0.034. It was essentially the same, −0.033.

All of these findings suggest that SR Ca release in cut muscle fibers is relatively insensitive to pH in the range encountered in our experiments, 6.7–7.1 for resting values and values as low as 6.3 after a train of action potentials. This insensitivity is similar to that observed in skinned fibers by Lamb, Recupero, and Stephenson (1992). It stands in mark contrast to the results of Ma, Fill, Knudson, Campbell, and Coronado (1988) and Rousseau and Pinkos (1990), who found that ion fluxes through isolated rabbit skeletal muscle ryanodine receptors were strongly inhibited by values of pH <7.0. This difference in pH sensitivity may be due to a difference between frog and rabbit ryanodine receptors or to a difference between ryanodine receptors in an intact SR and in a bilayer.

The Value of β in Our Cut Fibers, 22 mM/pH Unit, Is Consistent with Values Obtained by Others in Intact Fibers

The mean value of β obtained in our experiments, 22 mM/pH unit, is somewhat smaller than the values that have been estimated in intact fibers, 26 to 38 mM/pH unit with a mean value of 33 mM/pH unit (Bolton and Vaughan-Jones, 1977; Aber-

crombie, Putnam, and Roos, 1983; and Curtin, 1986). This difference is probably due to a difference in the buffering power of the freely mobile myoplasmic buffers. This buffering power is expected to be about 12 mM/pH unit in intact fibers (pH = 6.8–7.18 in Table IV in Godt and Maughan, 1988; carnosine accounts for 90% of this buffering power) and only 4–5 mM/pH unit in our cut fibers (calculated at pH = 7.0 from the concentrations and pK's of MOPS, ATP, and phospho(enol)pyruvate, the main buffers in the internal solutions). When these values are taken into account, the buffering power of the immobile myoplasmic buffers is estimated to be, on average, 21 mM/pH unit in intact fibers and 17–18 mM/pH unit in our cut fibers. These values are in good agreement.

Previous estimates of the value of β in muscle have relied on measurements that took tens of seconds and sometimes even minutes to complete. This raises the concern that the value of β may have included contributions from processes other than reactions between protons and rapidly reacting buffers. Such processes include slowly reacting buffers, metabolic reactions, and movements of acid or base across internal or external membranes. The finding that the buffering power estimated for the immobile myoplasmic buffers is nearly the same in the measurements reported here (on cut fibers) as in those reported by others (on intact fibers) suggests that slow processes make little contribution to estimates of buffering power in frog muscle as long as the measurement is completed within a few minutes.

The Ability of Fura-2 to Complex Ca Is Different Inside a Muscle Fiber Than in a Calibration Solution

In the experiments reported here, the mean value of k_{-2}, the dissociation rate constant for Ca and fura-2, was 29 s^{-1} (SEM, 4 s^{-1}) at 14–15°C. This value is larger than the values estimated by Klein et al. (1988), 12 s^{-1} in cut fibers at 6–10°C, and by Hollingworth et al. (1992), 17 s^{-1} in intact fibers at 16°C. It is smaller than that measured by Kao and Tsien (1988) in a 140 mM KCl solution at 20°C, 97 s^{-1}.

Pape et al. (1993) estimated the value of k_2, the association rate constant for Ca and fura-2, in experiments on cut fibers equilibrated with fura-2 and PDAA and studied under conditions similar to those used here. The value of k_2 appeared to vary with fura-2 concentration, at least between 0.5 and 2 mM, and was 0.7×10^8 $M^{-1}s^{-1}$ with 2 mM fura-2. With $k_2 = 0.7 \times 10^8$ $M^{-1}s^{-1}$ and $k_{-2} = 29$ s^{-1}, an equation analogous to Eq. A6 gives a value of 0.41 μM for the apparent dissociation constant of Ca and fura-2. This value lies between two other estimates of the apparent dissociation constant inside muscle fibers: 0.32 μM (estimated from data obtained from cut fibers by Klein et al., 1988, after allowance for the fact that antipyrylazo III is expected to underestimate the amplitude of the [Ca] transient by a factor of about 4; see Table II in Pape et al., 1993) and 0.68 μM (estimated in intact fibers by Hollingworth et al., 1992). All of these estimates of the dissociation constant of Ca and fura-2 in myoplasm are substantially larger than that measured by Kao and Tsien (1988) in a 140 mM KCl solution at 20°C, 0.162 μM.

These differences between in vivo and in vitro values are consistent with the idea that fura-2 behaves differently inside a muscle fiber than in a calibration solution, an idea that was initially suggested by Baylor and Hollingworth (1987, 1988) and Klein et al. (1988). A likely explanation is that, in vivo, a large fraction of fura-2 is

associated with myoplasmic proteins (Baylor and Hollingworth, 1987, 1988; Konishi, Olson, Hollingworth, and Baylor, 1988). Fortunately, such differences are not expected to influence the estimates of β, and thereby the estimates of $\Delta[Ca_T]$, that are reported in this article.

APPENDIX A

This Appendix presents a detailed description of the properties of the reaction between Ca and EGTA and of the ability of the EGTA-phenol red method to measure SR Ca release rapidly and reliably.

At Neutral pH, Ca^{2+} Is Complexed by H_2EGTA^{2-} and Two Protons Are Released Almost Immediately

Ca-free EGTA is able to exist in five different states of protonation: $EGTA^{4-}$, $HEGTA^{3-}$, H_2EGTA^{2-}, H_3EGTA^{-}, and H_4EGTA. If [EGTA] denotes the total concentration of Ca-free EGTA, then [EGTA] = $[EGTA^{4-}]$ + $[HEGTA^{3-}]$ + $[H_2EGTA^{2-}]$ + $[H_3EGTA^{-}]$ + $[H_4EGTA]$. The fractional amounts of EGTA in the different states are equal to $[EGTA^{4-}]/[EGTA]$, $[HEGTA^{3-}]/[EGTA]$, $[H_2EGTA^{2-}]/[EGTA]$, $[H_3EGTA^{-}]/[EGTA]$, and $[H_4EGTA]/[EGTA]$. Their values are determined by pH and the values of the pK's associated with the different protonated states. The values of these pK's at 20°C are given in Martell and Smith (1974): $pK_1 = 9.58$, $pK_2 = 8.96$, $pK_3 = 2.76$, and $pK_4 = 2.11$ in which the subscript 1–4 denotes the number of protons of the final protonated form. These values have been corrected for the activity coefficient of protons so that they apply to the value of pH that is measured with a pH meter.

In our experiments, the values of resting myoplasmic pH were estimated to be 6.7–7.1. After stimulation, pH decreases and values as low as 6.3 were estimated. At pH = 6.3, and with the values of the pK's given above, $[EGTA^{4-}]/[EGTA]$ = 0.00000115, $[HEGTA^{3-}]/[EGTA]$ = 0.00218, and $[H_2EGTA^{2-}]/[EGTA]$ = 0.9975. The values of $[H_3EGTA^{-}]/[EGTA]$ (0.000294) and $[H_4EGTA]/[EGTA]$ (0.000000019) are small and can be ignored because Ca does not appear to react appreciably with either H_3EGTA^{-} or H_4EGTA. When the value of pH is increased from 6.3 to 7.1, the value of $[EGTA^{4-}]/[EGTA]$ is increased by a factor of 39, to 0.0000451, and the value of $[HEGTA^{3-}]/[EGTA]$ is increased by a factor of 6, to 0.01361; the value of $[H_2EGTA^{2-}]/[EGTA]$ is decreased slightly, from 0.9975 to 0.9863. Thus, [EGTA] $\cong$ $[H_2EGTA^{2-}]$ at the values of myoplasmic pH encountered in our experiments.

Ca-bound EGTA is also able to exist in different states of protonation. If [CaEGTA] denotes the total concentration of Ca-bound EGTA, [CaEGTA] = $[CaEGTA^{2-}]$ + $[CaHEGTA^{-}]$ + $[CaH_2EGTA]$. Calculations similar to those described in the preceding paragraph, with the values of pK's for Ca-bound EGTA that are given in Martell and Smith (1974), show that essentially all of the Ca-bound EGTA is nonprotonated, with $[CaEGTA^{2-}]/[CaEGTA] \geq 0.9999$. Thus, [CaEGTA] $\cong$ $[CaEGTA^{2-}]$.

Since almost all of the Ca-free and Ca-bound EGTA is divalent, the equilibrium reaction between Ca and EGTA can be written

$$Ca^{2+} + H_2EGTA^{2-} \rightleftharpoons CaEGTA^{2-} + 2H^+ . \quad (A1)$$

This reaction can occur through three different pathways: (1) Ca^{2+} can complex H_2EGTA^{2-} to form CaH_2EGTA and then two protons can dissociate to form $CaEGTA^{2-}$; (2) Ca^{2+} can complex $HEGTA^{3-}$ to form $CaHEGTA^-$ and then one proton can dissociate to form $CaEGTA^{2-}$ and another proton can dissociate from H_2EGTA^{2-} to form $HEGTA^{3-}$; and (3) Ca^{2+} can complex $EGTA^{4-}$ to form $CaEGTA^{2-}$ and then two protons can dissociate from H_2EGTA^{2-} to form $EGTA^{4-}$. Since, as mentioned above, the value of $[EGTA^{4-}]/[EGTA]$ is expected to be 0.00000115–0.0000451 in our experiments and the value of [EGTA] is expected to be 18.24 mM, the value of $[EGTA^{4-}]$ is expected to be negligibly small (<1 μM). Consequently, pathway (3) can be neglected.

Smith et al. (1984) carried out stopped-flow measurements of the kinetics of Ca complexation by EGTA and obtained information about the relative importance of pathways (1) and (2) at physiological pH. Between pH 5.8 and 7.3, the value of the apparent forward rate constant, k_1, was found to be approximately constant, 1.5×10^6 $M^{-1}s^{-1}$ at 25°C. Because the value of $[H_2EGTA^{2-}]/[EGTA]$ is also approximately constant at these pH's (≅1) and because the value of $[HEGTA^{3-}]/[EGTA]$ is expected to change sixfold (see above), Smith et al. (1984) concluded that most of the complexation of Ca by EGTA occurs through pathway 1, with Ca^{2+} complexing H_2EGTA^{2-} to form CaH_2EGTA.

Reactions that involve protons are usually very fast, so that the dissociation of CaH_2EGTA into $CaEGTA^{2-}$ and $2H^+$ is expected to occur rapidly. Two experimental observations are consistent with this expectation. First, in the stopped-flow experiments of Smith et al. (1984), the rate of Ca complexation by EGTA was determined from measurements of changes in pH whereas, in another series of stopped-flow experiments (Harafuji and Ogawa, 1980), it was determined from measurements of changes in free [Ca]. The values of k_1 that were obtained by Harafuji and Ogawa (1980), 1.0–3.0 $\times 10^6$ $M^{-1}s^{-1}$ at 20°C, are in good agreement with the value obtained by Smith et al. (1984), 1.5×10^6 $M^{-1}s^{-1}$ at 25°C, consistent with the idea that there is little delay between the complexation of Ca by H_2EGTA^{2-} and the dissociation of protons from CaH_2EGTA. Second, in the experiments of Smith et al. (1984), the change in pH began almost immediately after mixing and showed no detectable delay, also suggesting that protons dissociate from CaH_2EGTA almost immediately after Ca is complexed by H_2EGTA^{2-}.

The main conclusion of this section is that, at the values of myoplasmic pH encountered in our experiments, the reaction between Ca and EGTA effectively reduces to a single reaction in which 1 Ca is exchanged for 2 protons (Scheme A1).

In the Absence of Intrinsic Myoplasmic Ca Buffers Such as Troponin and Parvalbumin, EGTA Is Expected to Complex Almost All of the Ca Released from the SR

Because the total concentration of EGTA (= [EGTA] + [CaEGTA]) is approximately constant during a 1–3-s measurement, such as that after an action-potential or a voltage-clamp stimulation, the differential equation for reaction A1 can be written

$$d[\text{CaEGTA}]/dt = k_1[\text{Ca}][\text{EGTA}] - k_{-1}[\text{CaEGTA}] \cdot \quad \text{(A2)}$$

k_1 and k_{-1} denote, respectively, the apparent forward and backward rate constants of the net reaction between Ca and EGTA. As mentioned in the preceding section, the value of k_1 is approximately constant at the values of pH encountered in our experiments whereas, as discussed below, the value of k_{-1} depends on pH. If $[Ca_T]$ is defined by the relation $[Ca_T] = [Ca] + [CaEGTA]$, Eq. A2 can be written,

$$d[\text{CaEGTA}]/dt = k_1[\text{Ca}_T] \cdot [\text{EGTA}] - \{k_1[\text{EGTA}] + k_{-1}\} \cdot [\text{CaEGTA}]. \quad \text{(A3)}$$

After stimulation, Ca moves from the SR into the myoplasm and the values of [CaEGTA], [EGTA], $[Ca_T]$, and [Ca] at the optical site will change with respect to their resting values $[\text{CaEGTA}]_R$, $[\text{EGTA}]_R$, $[Ca_T]_R$, and $[\text{Ca}]_R$. These changes will be denoted by $\Delta[\text{CaEGTA}]$, $\Delta[\text{EGTA}]$, $\Delta[Ca_T]$, and $\Delta[\text{Ca}]$, respectively. If the resting concentrations are at equilibrium, Eq. A3 can be written,

$$d\Delta[\text{CaEGTA}]/dt = k_1[\text{EGTA}] \cdot \Delta[Ca_T] - \{k_1[\text{EGTA}] + k_1[\text{Ca}]_R + k_{-1}\} \cdot \Delta[\text{CaEGTA}]. \quad \text{(A4)}$$

Eq. A4 follows from Eqs. A2 and A3 without any approximations. The form of the equation has been selected so that, if the value of [EGTA] is large, significant changes occur only in $\Delta[\text{CaEGTA}]$ and $\Delta[Ca_T]$. This equation is analogous to Eq. 13 in Pape et al. (1993).

After release is over and the binding of Ca by EGTA has reached equilibrium, with $d\Delta[\text{CaEGTA}]/dt = 0$,

$$\Delta[\text{CaEGTA}] = \frac{[\text{EGTA}]}{[\text{EGTA}] + [\text{Ca}]_R + K_{Dapp}} \cdot [\Delta Ca_T], \quad \text{(A5)}$$

in which

$$K_{Dapp} = k_{-1}/k_1. \quad \text{(A6)}$$

K_{Dapp} represents the apparent dissociation constant of the reaction between Ca and EGTA.

In our experiments, the total amount of readily releasable Ca inside the SR was usually <3,000 μM, expressed as myoplasmic concentration. If the value of $[\text{EGTA}]_R$ was the same as that in the end pools, 18.24 mM, the value of [EGTA] after stimulation (that is, the value in Eq. A5) would be >15 mM. Since, as shown below, the value of $[\text{Ca}]_R + K_{Dapp}$ is expected to be <2 μM, $\Delta[Ca_T] > \Delta[\text{CaEGTA}] \geq 0.9999\Delta[Ca_T]$. Thus, in the absence of intrinsic myoplasmic Ca buffers such as troponin and parvalbumin, EGTA is expected to capture essentially all (≥99.99%) of the Ca released from the SR. Evidence is summarized in the Discussion that, even with troponin and parvalbumin present at myoplasmic concentrations, EGTA appears to capture ~96% of the Ca released by a single action potential.

The ability of EGTA to capture almost all of the released Ca does not depend critically on the values of $[\text{Ca}]_R$, K_{Dapp}, and [EGTA]. A 10-fold increase in the up-

per limit of the value of $[Ca]_R + K_{Dapp}$, from 2 to 20 μM, or a 10-fold reduction in the value of [EGTA] after stimulation, from >15 to >1.5 mM, would result in the inequality $\Delta[Ca_T] > \Delta[CaEGTA] \geq 0.9999\Delta[Ca_T]$ being replaced by $\Delta[Ca_T] > \Delta[CaEGTA] \geq 0.999\Delta[Ca_T]$. Thus, in the absence of intrinsic myoplasmic Ca buffers, the capture of Ca by EGTA is expected to be essentially complete even if some of the EGTA is bound or sequestered inside the myoplasm or if the myoplasmic value of K_{Dapp} is different from the in vitro values calculated below. The capture is also expected to be complete in the presence of myoplasmic gradients of free [Ca] and [EGTA] during release (Appendix B).

20 mM EGTA Is Expected to Complex Ca Released from the SR Rapidly, within <0.1 ms

Eq. A4 gives an expression for the apparent rate constant with which Δ[CaEGTA] tracks $\Delta[Ca_T]$: it is equal to $k_1[EGTA] + k_1[Ca]_R + k_{-1} = k_1([EGTA] + [Ca]_R + K_{Dapp})$. Because $[Ca]_R + K_{Dapp}$ is expected to be <2 μM (see below) and [EGTA] is expected to be >15 mM (see preceding section), $k_1([EGTA] + [Ca]_R + K_{Dapp})$ is essentially equal to $k_1[EGTA]$. With a large concentration of EGTA at the optical site, $k_1[EGTA] \cong k_1[EGTA]_R$. The value of $(k_1[EGTA]_R)^{-1}$, denoted by τ_{Ca}, represents the estimated mean time required for EGTA at its resting concentration to bind Ca. As described above, the value of k_1, and consequently that of τ_{Ca}, is expected to be independent of pH.

In our experiments on fibers equilibrated with 20 mM EGTA, a value of 22 μs was chosen for τ_{Ca} so that the Δ[Ca] signals measured with PDAA (column 3 in Table I) would have the same mean amplitude as the Δ[Ca] signals estimated from ΔpH (column 10 in Table II). The reliablity of this estimate of τ_{Ca} depends on two implicit assumptions. The first is that PDAA provides a reliable measurement of the amplitude of the spatially averaged Δ[Ca] signal. Although this appears to be the case for the measurement of unmodified (by EGTA) [Ca] transients in cut muscle fibers (Hirota et al., 1989), the presence of a small undershoot in the PDAA Δ[Ca] signal in fibers equilibrated with 20 mM EGTA (Fig. 1 *B*) might have produced a small underestimate (≤25%) of the peak amplitude of Δ[Ca] and a corresponding underestimate of the value of τ_{Ca}. The second assumption is that the actual mean amplitude of the spatially averaged Δ[Ca] signals in the experiments used for Table I was the same as that in the experiments used for Table II. This assumption seems reasonable since the same conditions, except for the presence of either phenol red or PDAA, were used in the two sets of experiments. If, for some unknown reason, one of these assumptions is seriously invalid, the value of τ_{Ca} might be considerably different from 22 μs. Although it is difficult to establish an upper limit of the value of τ_{Ca}, it seems unlikely that it could exceed two or three times 22 μs. Consequently, it seems safe to conclude that, under the conditions of our experiments, EGTA is expected to capture Ca released from the SR rapidly, within <0.1 ms.

The rapid speed with which EGTA is expected to capture Ca, and therefore track SR Ca release, may seem surprising in view of the fact that EGTA is known to react relatively slowly with Ca, at least when it is compared with many Ca indicators. To understand this apparent discrepancy, it is important to distinguish between the speed with which EGTA, or any Ca buffer, is able to track *free* Ca and the speed with

which it is able to track *total* Ca. In the first case, the apparent rate constant is given by $k_1[Ca] + k_{-1}$ (eg., Eq. 3 in Baylor, Chandler, and Marshall, 1982*b*) whereas, in the second case, it is given by $k_1[EGTA] + k_1[Ca]_R + k_{-1}$ (Eq. A4 in this article; see also Eq. 5 in Baylor et al., 1982*b*). As pointed out above, the value of $k_1[EGTA] + k_1[Ca]_R + k_{-1}$ in our experiments is essentially equal to $k_1[EGTA]$, which is expected to be at least 10^4 times that of $k_1[Ca]_R + k_{-1}$. Consequently, for changes in [Ca] that are small compared with the value of $[Ca]_R$, the speed with which EGTA is able to track *total* Ca is expected to be four orders-of-magnitude more rapid than that with which it is able to track *free* Ca.

A Change in [CaEGTA] Can Be Monitored as a Change in pH

As described above, in the absence of other myoplasmic Ca buffers, EGTA is expected to rapidly capture almost all of the Ca that is released from the SR and to exchange it for protons with a 1:2 stoichiometry (reaction A1). As a result, the myoplasmic pH should decrease by an amount that depends on the buffering power of myoplasm, β. Since ΔpH has been used to monitor Δ[CaEGTA], it is important to evaluate the contributions of sources and sinks for protons other than EGTA and the buffers that account for β.

Baylor et al. (1982*a*) and Hollingworth and Baylor (1990) measured a small positive myoplasmic ΔpH signal (0.002–0.004 pH units) with phenol red in intact fibers (without EGTA) after a single action potential. Pape et al. (1990) showed that the magnitude of this signal was increased by the injection of fura-2, which increased the amount of Ca released from the SR. The amplitude of the ΔpH signal was proportional to the amount of Ca released, with a stoichiometry of 1 Ca:0.2–0.3 protons, independent of the amount or rate of SR Ca release. They interpreted these results in terms of the idea that proton movement from the myoplasm into the SR balances 0.10–0.15 of the electrical charge associated with Ca release (see also Meissner and Young, 1980; Somlyo, Somlyo, Gonzalez-Serratos, Shuman, and McClellan, 1980; Baylor et al., 1982*a*).

Several other processes might also influence myoplasmic pH: proton release by Ca binding to intrinsic Ca buffers, ATP hydrolysis, rephosphorylation of ADP by phosphocreatine hydrolysis, and proton release by the SR Ca pump. Pape et al. (1990) considered these processes and concluded that they probably made little contribution to their ΔpH signals, at least during the first 50–100 ms after an action potential. Because the amplitude of their ΔpH signals was an order-of-magnitude smaller than those reported here with EGTA-phenol red, it seems reasonable to conclude that these other processes make a negligible contribution to the ΔpH signals in our experiments.

Thus, it appears that only two factors need to be considered in the use of ΔpH to monitor Δ[CaEGTA] during SR Ca release: the exchange of protons for Ca by EGTA (with a stoichiometry of 1 Ca:2 protons) and the movement of protons into the SR to electrically balance some of the charge carried by Ca (with a stoichiometry of 1 Ca:0.2–0.3 protons). Thus, for each 100 Ca ions that are released from the SR into the myoplasm and are captured by EGTA, 200 protons are expected to dissociate from EGTA and enter the myoplasm and 20–30 protons are expected to

leave the myoplasm and enter the SR. As a result, the net number of protons that appear in the myoplasm is 170–180 (or 0.85–0.9 times 200).

The movement of protons from the myoplasm into the SR during Ca release has been neglected in the estimates of SR Ca release reported in this article. With this simplification, ΔpH is given simply by the concentration of protons released from EGTA (= 2Δ[CaEGTA]) divided by −β, or conversely

$$\Delta[\mathrm{CaEGTA}] = -(\beta/2)\,\Delta\mathrm{pH}. \tag{A7}$$

To correct for the expected movement of protons into the SR, the values of SR Ca release estimated from Eq. A7 and reported in this article should be multiplied by 1.11–1.18 (= $0.9^{-1} - 0.85^{-1}$).

Δ[Ca] Can Be Estimated with the EGTA-Phenol Red Method

Eq. A2 can be rearranged to give an expression for [Ca],

$$[\mathrm{Ca}] = K_{\mathrm{Dapp}}\frac{[\mathrm{CaEGTA}]}{[\mathrm{EGTA}]} + (k_1[\mathrm{EGTA}])^{-1} \cdot d[\mathrm{CaEGTA}]/dt. \tag{A8}$$

The first term on the right-hand side of Eq. A8 gives the equilibrium value of [Ca] that is expected if $d[\mathrm{CaEGTA}]/dt = 0$. The second term gives an additional contribution that is proportional to the rate of SR Ca release, $d[\mathrm{Ca_T}]/dt$, because $d[\mathrm{Ca_T}]/dt \cong d[\mathrm{CaEGTA}]/dt$.

The time course of [Ca] can be estimated from Eq. A8 if the time courses of [EGTA], [CaEGTA], and K_{Dapp} are known. The time course of K_{Dapp} is calculated from pH according to

$$K_{\mathrm{Dapp}} = K_{\mathrm{D}}\left(1 + 10^{\mathrm{pK_1} - \mathrm{pH}} + 10^{\mathrm{pK_1} + \mathrm{pK_2} - 2\mathrm{pH}}\right). \tag{A9}$$

K_{D} is the dissociation constant of Ca^{2+} and $EGTA^{4-}$, and is equal to $10^{-10.97}$ M (Martell and Smith, 1974). Two terms that involve pK_3 and pK_4 have been omitted from the right-hand side of Eq. A9 since they make negligible contribution to the value of K_{Dapp} at the values of pH used in our experiments. According to Eq. A9 and the values of K_{D}, pK_1, and pK_2 given above, K_{Dapp} = 1.487 μM at pH = 6.7; 0.940 μM at pH = 6.8; 0.594 μM at pH = 6.9; 0.376 μM at pH = 7.0; 0.238 μM at pH = 7.1.

The values of $[\mathrm{EGTA}]_{\mathrm{R}}$ and $[\mathrm{CaEGTA}]_{\mathrm{R}}$ are assumed to be the same as those in the end-pool solutions, 18.24 and 1.76 mM, respectively. The value of $[\mathrm{Ca}]_{\mathrm{R}}$ is then determined from the first term on the right-hand side of Eq. A8 with [CaEGTA]/[EGTA] = 18.24/1.76. With the values of K_{Dapp} in the preceding paragraph, $[\mathrm{Ca}]_{\mathrm{R}}$ = 0.144 μM at pH = 6.7, 0.091 μM at pH = 6.8, 0.057 μM at pH = 6.9, 0.036 μM at pH = 7.0, and 0.023 μM at pH = 7.1. The value of $[\mathrm{Ca}]_{\mathrm{R}} + K_{\mathrm{Dapp}}$ is 1.631 μM at pH = 6.7. It becomes progressively smaller at larger values of pH so that the condition $[\mathrm{Ca}]_{\mathrm{R}} + K_{\mathrm{Dapp}} < 2$ μM is expected to hold in our experiments.

The Δ[CaEGTA] signal is estimated from Eq. A7. The Δ[EGTA] signal is set

equal to $-\Delta$[CaEGTA], since the total concentration of EGTA at the optical site is expected to remain constant during a 1–3-s period of measurement. The time courses of [EGTA] and [CaEGTA] are then calculated from [EGTA] = $[EGTA]_R$ + Δ[EGTA] and [CaEGTA] = $[CaEGTA]_R$ + Δ[CaEGTA]. The d[CaEGTA]$/dt$ signal is obtained by numerical differentiation. Δ[Ca] (= [Ca] − $[Ca]_R$) can then be calculated from Eq. A8 if the value of k_1 is known.

A value of 2.5×10^6 $M^{-1}s^{-1}$ was used for k_1 so that the peak value of Δ[Ca] estimated with EGTA-phenol red (3.25 μM, column 10 in Table II, calculated with $[EGTA]_R$ = 18.24 mM) would be similar to that measured with PDAA under similar conditions (3.34 μM, column 3 in Table I). We have assumed that the value of k_1 is independent of myoplasmic pH since Smith et al. (1984) found that the value of k_1 was independent of pH between 5.8 and 7.3.

Although Eq. A8 has been used for all of the estimates of Δ[Ca] described in this article, it is instructive to introduce an approximation of that equation that holds when a small amount of Ca is released rapidly from the SR, such as occurs after an action potential. In this situation, the first term on the right-hand side of Eq. A8 remains relatively constant at $[Ca]_R$ and the second term dominates. Consequently,

$$\Delta[Ca] \cong (k_1[EGTA])^{-1} \cdot d\Delta[CaEGTA]/dt. \tag{A10}$$

With this approximation, Δ[Ca] is expected to be proportional to $d\Delta$[CaEGTA]$/dt$ (or $d\Delta[Ca_T]/dt$), with a proportionality constant that is given by $(k_1[EGTA])^{-1} \cong (k_1[EGTA]_R)^{-1} = \tau_{Ca}$ (see Fig. 8 A, for example). Since the value of k_1 is expected to be independent of pH, τ_{Ca} is also expected to be independent of pH. With either Eq. A8 or A10, it is clear that the reliability of the estimate of Δ[Ca] during periods of SR Ca release depends on the reliability of the estimate of $k_1[EGTA]_R$. This estimate is considered to be good because it is based on direct measurement of Δ[Ca] with PDAA (see above).

The values of k_{-1} that apply to our experiments are small, of the order of 1 s^{-1}. For example, according to Eqs. A6 and A9, k_{-1} = 3.718 s^{-1} at pH = 6.7; 2.350 s^{-1} at pH = 6.8; 1.485 s^{-1} at pH = 6.9; 0.940 s^{-1} at pH = 7.0; 0.595 s^{-1} at pH = 7.1. One advantage of the small value of k_{-1} is that it contributes to the clear separation of the time course of Ca binding to EGTA during SR Ca release and that of Ca dissociation from CaEGTA during recovery (Figs. 4 and 8).

The main conclusion of this section is that Δ[Ca] (= [Ca] − $[Ca]_R$) can be estimated reliably with the EGTA-phenol red method, Eqs. A8 and A10.

$[Ca]_R$ Can Be Estimated with the EGTA-Phenol Red Method, But the Reliability of the Estimate Depends on the Reliability of the Value of pH_R

If our estimates of pH_R are unreliable, the estimates of K_{Dapp}, and hence those of $[Ca]_R$, are also unreliable. To correct for a possible 0.1–0.4 underestimate of pH_R (see Methods), the values of K_{Dapp} given after Eq. A9 and the values of $[Ca]_R$ in the preceding section should be multiplied by 0.63–0.16.

Another smaller source of error in the estimates of K_{Dapp} is that the values of K_D, pK_1, and pK_2 used in Eq. A9 were those determined by Martell and Smith (1974) at

20°C. At 13–16°C, the temperature of our experiments, the values of K_{Dapp} are expected to be larger, with a maximal increase of 10% at 13°C (calculated from data in Martell and Smith, 1974). Since this error is small compared with that expected from inaccuracies in the value of pH_R (preceding paragraph), the values of K_D, pK_1, and pK_2 at 20°C were used without correction for temperature.

The general conclusion of this section is that $[Ca]_R$ can be estimated with the EGTA-phenol red method but that the estimate may not be reliable because of inaccuracies in the estimates of pH_R and K_{Dapp}. In any event, any error in the estimates of pH_R and $[Ca]_R$ is expected to have little effect on the estimates of τ_{Ca} and $\Delta[Ca]$, as described in the preceding section. It should also not change the expectation that EGTA is able to bind essentially all of the Ca released from the SR, and to do so rapidly, so that the time course of Δ[CaEGTA] provides a reliable estimate of SR Ca release.

APPENDIX B

This Appendix is concerned with the changes in free [Ca], [CaEGTA], [EGTA], and pH that are expected to develop in the myoplasm near a single SR Ca channel in a fiber equilibrated with EGTA. Although the theory has been formulated with Ca and EGTA in mind, the equations for [Ca], [CaEGTA], and [EGTA] are expected to apply to other ion and buffer combinations.

The first analyses of this type were carried out by Neher (1986) and Stern (1992). They approximated a Ca channel by a point source immersed in an infinite isotropic medium. The medium is assumed to be isopotential, since the concentration of Ca ions is expected to be much smaller than that of the other ions, at least at distances greater than a few nanometers from the mouth of the channel. Under these conditions, Neher (1986) showed that any changes in [CaEGTA] and [EGTA], denoted by Δ[CaEGTA] and Δ[EGTA], are expected to be negligibly small with millimolar concentrations of EGTA. With the assumption that the changes are zero, Neher (1986) derived an equation for the value of $\Delta[Ca]$ as a function of distance from the mouth of the channel; this equation is the same as Eq. B21 below. Stern (1992) extended Neher's analysis and allowed for nonzero values of Δ[CaEGTA] and Δ[EGTA]. An equation for $\Delta[Ca]$ was derived that contained four terms. The first three terms, which are nonlinear integrals, were evaluated by an iterative computer program and found to be negligibly small under the conditions of interest. The remaining fourth term is the same as Eq. B21.

Neither Neher (1986) nor Stern (1992) gives a quantitative criterion for the use of Eq. B21 to calculate $\Delta[Ca]$, such as the minimal concentration of EGTA (or other Ca buffer) that is required for the equation to hold. Neither do they give equations, analogous to Eq. B21, for the spatial dependences of Δ[EGTA], Δ[CaEGTA], and ΔpH (or $\Delta[H^+]$). This appendix provides this information. The essential criterion for the use of Eq. B21 is that the absolute value of Δ[EGTA] must be much smaller than the resting value of [EGTA]. Under this condition, the variation of Δ[EGTA] ($= -\Delta$[CaEGTA]) with distance from the mouth of the channel is given by Eq. B22. $\Delta[H^+]$ and ΔpH are proportional to Δ[CaEGTA] with proportionality constants given by Eqs. B31 and B33. As shown in the numerical

example at the end of this appendix, the assumption that $|\Delta[\text{EGTA}]| << [\text{EGTA}]$ is expected to hold very well in our experiments.

Spatial Variation of [Ca], [EGTA], and [CaEGTA]: General Case

The steady state differential equations that relate the diffusion of Ca, EGTA, and CaEGTA and the reaction between Ca and EGTA (Eq. A2), in spherical coordinates without angular dependence, are

$$D_{\text{Ca}}\{d^2[\text{Ca}]/dr^2 + (2/r)\,d[\text{Ca}]/dr\} - \{k_1[\text{Ca}][\text{EGTA}] - k_{-1}[\text{CaEGTA}]\} = 0, \tag{B1}$$

$$D_{\text{EGTA}}\{d^2[\text{EGTA}]/dr^2 + (2/r)\,d[\text{EGTA}]/dr\} - \{k_1[\text{Ca}][\text{EGTA}] - k_{-1}[\text{CaEGTA}]\} = 0, \tag{B2}$$

$$D_{\text{CaEGTA}}\{d^2[\text{CaEGTA}]/dr^2 + (2/r)\,d[\text{CaEGTA}]/dr\} + \{k_1[\text{Ca}][\text{EGTA}] - k_{-1}[\text{CaEGTA}]\} = 0. \tag{B3}$$

r represents the distance from the center of a hemispherical source. D_{Ca}, D_{EGTA}, and D_{CaEGTA} represent the diffusion coefficients of Ca, EGTA, and CaEGTA, respectively.

At the source, as $r \to 0$, the flux of Ca ions in the solution matches that through the channel, ϕ. Consequently,

$$\phi = -\lim_{r\to 0} 4\pi r^2 D_{\text{Ca}}(d[\text{Ca}]/dr). \tag{B4}$$

The concentrations of Ca, EGTA, and CaEGTA can be expressed as a resting concentration plus a change,

$$[\text{Ca}] = [\text{Ca}]_{\text{R}} + \Delta[\text{Ca}], \tag{B5}$$

$$[\text{EGTA}] = [\text{EGTA}]_{\text{R}} + \Delta[\text{EGTA}], \tag{B6}$$

$$[\text{CaEGTA}] = [\text{CaEGTA}]_{\text{R}} + \Delta[\text{CaEGTA}]. \tag{B7}$$

The subscript R denotes resting concentrations and the prefix Δ denotes changes with respect to these concentrations.

The solution of Eqs. B1–B7 is simplified by the assumption that $D_{\text{CaEGTA}} = D_{\text{EGTA}}$. In the absence of any sources or sinks for EGTA and CaEGTA, [EGTA] + [CaEGTA] is independent of distance and equal to a constant; hence, $\Delta[\text{EGTA}] = -\Delta[\text{CaEGTA}]$. If the absolute value of $\Delta[\text{EGTA}]$ is much less than that of $[\text{EGTA}]_{\text{R}}$, which is the main assumption in this analysis, Eq. B1 gives

$$D_{\text{Ca}}\{d^2\Delta[\text{Ca}]/dr^2 + (2/r)\,d\Delta[\text{Ca}]/dr\} = \{k_1[\text{EGTA}]_{\text{R}}\Delta[\text{Ca}] + (k_1[\text{Ca}]_{\text{R}} + k_{-1})\Delta[\text{EGTA}]\}. \tag{B8}$$

The requirement that the sum of the fluxes of Ca and CaEGTA at any value of r must equal ϕ gives

$$\phi = -4\pi r^2[D_{Ca}d\Delta[Ca]/dr + D_{EGTA}d\Delta[CaEGTA]/dr], \quad \text{(B9)}$$

$$= -4\pi r^2[D_{Ca}d\Delta[Ca]/dr - D_{EGTA}d\Delta[EGTA]/dr]. \quad \text{(B10)}$$

Eq. B10 can be multiplied by $dr/4\pi r^2$ and integrated with respect to a dummy variable from r to ∞ (where $\Delta[EGTA] = \Delta[Ca] = 0$) to give

$$\Delta[EGTA] = \frac{D_{Ca}}{D_{EGTA}} \cdot \Delta[Ca] - \frac{\phi}{4\pi D_{EGTA} r}. \quad \text{(B11)}$$

Eqs. B8 and B11 can be combined to give,

$$d^2\Delta[Ca]/dr^2 + (2/r)\, d\Delta[Ca]/dr = \frac{\Delta[Ca]}{\lambda^2} - \frac{1}{\lambda_{EGTA}{}^2} \cdot \frac{\phi}{4\pi D_{Ca} r}, \quad \text{(B12)}$$

in which

$$1/\lambda^2 = 1/\lambda_{Ca}{}^2 + 1/\lambda_{EGTA}{}^2, \quad \text{(B13)}$$

$$\lambda_{Ca} = \sqrt{\frac{D_{Ca}}{k_1[EGTA]_R}}, \quad \text{(B14)}$$

and

$$\lambda_{EGTA} = \sqrt{\frac{D_{EGTA}}{k_1[Ca]_R + k_{-1}}}. \quad \text{(B15)}$$

It is easy to show that λ_{Ca} represents the characteristic distance associated with the diffusion of Ca before capture by EGTA. The mean time, $\langle t \rangle$, required for EGTA to capture Ca is given by $\langle t \rangle = (k_1[EGTA]_R)^{-1} = \tau_{Ca}$ (Appendix A). The Einstein relation gives an expression for the mean distance, $\langle x \rangle$, that a Ca ion is expected to diffuse in this time, $\langle x \rangle = (2D_{Ca}\langle t \rangle)^{1/2} = (2D_{Ca}/k_1[EGTA]_R)^{1/2} = \sqrt{2}(\lambda_{Ca})$. Thus, Ca ions are expected to diffuse about $\sqrt{2}(\lambda_{Ca})$ before they are captured by EGTA. The significance of λ_{EGTA} is analogous to that of λ_{Ca}: it provides a rough estimate of the distance that an EGTA ion will diffuse before it binds Ca.

The solution of Eq. B12 that satisfies $\Delta[Ca] = 0$ as $r \to \infty$ is

$$\Delta[Ca] = \frac{A}{r} \cdot \exp(-r/\lambda) + \frac{\lambda^2}{\lambda_{EGTA}{}^2} \cdot \frac{\phi}{4\pi D_{Ca} r}. \quad \text{(B16)}$$

The integration constant A can be evaluated from Eq. B4 with [Ca] replaced with $\Delta[Ca]$. It is given by

$$A = \frac{1 - \lambda^2/\lambda_{EGTA}{}^2}{4\pi D_{Ca}}\phi. \quad \text{(B17)}$$

Eqs. B16 and B17 can be combined to give

$$\Delta[\mathrm{Ca}] = \frac{\phi}{4\pi D_{\mathrm{Ca}} r} \cdot \{\exp(-r/\lambda) + \frac{\lambda^2}{\lambda_{\mathrm{EGTA}}{}^2} \cdot [1 - \exp(-r/\lambda)]\}, \quad \text{(B18)}$$

and Eqs. B11 and B18 can be combined to give

$$\Delta[\mathrm{EGTA}] = -\frac{\phi}{4\pi D_{\mathrm{EGTA}} r} \cdot \{1 - \exp(-r/\lambda)\} \cdot \left\{1 - \frac{\lambda^2}{\lambda_{\mathrm{EGTA}}{}^2}\right\} \cdot \quad \text{(B19)}$$

The maximal absolute value of Δ[EGTA] occurs at the source, where $r = 0$, and is given by

$$\Delta[\mathrm{EGTA}]_{r=0} = -\frac{\phi}{4\pi D_{\mathrm{EGTA}} \lambda} \cdot \left(1 - \frac{\lambda^2}{\lambda_{\mathrm{EGTA}}{}^2}\right). \quad \text{(B20)}$$

Spatial Variation of [Ca], [EGTA], and [CaEGTA]: Special Case in Which $\lambda_{Ca}/\lambda_{EGTA} \cong 0$

As described in Appendix A, the inequality $[\mathrm{EGTA}]_R >> [\mathrm{Ca}]_R + K_{\mathrm{Dapp}}$ is expected to hold in our experiments. Consequently, since the estimated values of D_{Ca} and D_{EGTA} are within a factor of two of each other (see below), $\lambda_{\mathrm{Ca}}/\lambda_{\mathrm{EGTA}} \cong 0$ (from Eqs. B14 and B15) and $\lambda \cong \lambda_{\mathrm{Ca}}$ (from Eq. B13). The relation $\lambda_{\mathrm{Ca}}/\lambda_{\mathrm{EGTA}} \cong 0$ means that, for the purpose of calculating Δ[Ca], the diffusion of EGTA is sufficiently rapid to maintain the concentrations of [EGTA] and [CaEGTA] close to their respective resting levels. Consistent with this interpretation, Eq. B18 reduces to

$$\Delta[\mathrm{Ca}] = \frac{\phi}{4\pi D_{\mathrm{Ca}} r} \cdot \exp(-r/\lambda_{\mathrm{Ca}}). \quad \text{(B21)}$$

as first derived by Neher for the case in which there were no gradients of CaEGTA and EGTA. Eqs. B19 and B20 reduce to

$$\Delta[\mathrm{EGTA}] = -\frac{\phi}{4\pi D_{\mathrm{EGTA}} r} \cdot \{1 - \exp(-r/\lambda_{\mathrm{Ca}})\} \quad \text{(B22)}$$

and

$$\Delta[\mathrm{EGTA}]_{r=0} = -\frac{\phi}{4\pi D_{\mathrm{EGTA}} \lambda_{\mathrm{Ca}}} \cdot \quad \text{(B23)}$$

In the absence of EGTA or other mobile Ca buffers, the value of Δ[Ca] is given by the well known equation

$$\Delta[\mathrm{Ca}] = \frac{\phi}{4\pi D_{\mathrm{Ca}} r} \cdot \quad \text{(B24)}$$

A comparison of Eqs. B21 and B24 shows that EGTA is able to reduce the steady state value of free Δ[Ca] by scaling the term $\phi/4\pi D_{\mathrm{Ca}} r$ by the factor $\exp(-r/\lambda_{\mathrm{Ca}})$.

Spatial Variation of pH

As Ca diffuses from a point source, it is complexed by EGTA with a rate given by $k_1[\mathrm{Ca}][\mathrm{EGTA}] - k_{-1}[\mathrm{CaEGTA}]$ (Eq. A2). Since two protons are released for each Ca that is complexed, the rate of proton release is equal to twice the rate of Ca complexation. Inside a cell such as a muscle fiber, most of the released protons are expected to be bound by the intracellular buffers. If f represents the fraction of protons that survive and appear as free $[H^+]$, the rate at which $[H^+]$ increases is given by $2f$ times the rate at which Ca complexes with EGTA.

In the steady state, the differential equation for the spatial variation of [Ca] is given by Eq. B1. An analogous equation describes the spatial variation of $[H^+]$,

$$D_{\mathrm{H,app}}\{d^2\Delta[\mathrm{H}^+]/dr^2 + (2/r)\,d\Delta[\mathrm{H}^+]/dr\} + 2f\{k_1[\mathrm{Ca}][\mathrm{EGTA}] - k_{-1}[\mathrm{CaEGTA}]\} = 0. \tag{B25}$$

$D_{\mathrm{H,app}}$ represents the apparent diffusion coefficient of protons. Eqs. B1 (with Δ[Ca] instead of [Ca] on the left-hand side) and B25 can be combined to give

$$2fD_{\mathrm{Ca}}\{d^2\Delta[\mathrm{Ca}]/dr^2 + (2/r)\,d\Delta[\mathrm{Ca}]/dr\} + D_{\mathrm{H,app}}\{d^2\Delta[\mathrm{H}^+]/dr^2 + (2/r)\,d\Delta[\mathrm{H}^+]/dr\} = 0. \tag{B26}$$

Integration gives

$$2fD_{\mathrm{Ca}}\Delta[\mathrm{Ca}] + D_{\mathrm{H,app}}\Delta[\mathrm{H}^+] = B/r, \tag{B27}$$

in which B is a constant. If Δ[Ca] is given by Eq. B21,

$$\Delta[\mathrm{H}^+] = \frac{B}{D_{\mathrm{H,app}}r} - \frac{f\phi}{2\pi D_{\mathrm{H,app}}r}\cdot\exp(-r/\lambda_{\mathrm{Ca}}). \tag{B28}$$

The value of B can be determined from the boundary condition that the flux of protons is zero at r = 0,

$$\lim_{r\to 0} 4\pi r^2 D_{\mathrm{H,app}}(d\Delta[\mathrm{H}^+]/dr) = 0. \tag{B29}$$

This gives $B = f\phi/2\pi$ and Eq. B28 becomes

$$\Delta[\mathrm{H}^+] = \frac{f\phi}{2\pi D_{\mathrm{H,app}}r}\cdot\{1 - \exp(-r/\lambda_{\mathrm{Ca}})\}. \tag{B30}$$

$\Delta[H^+]$ has the same dependence on r as Δ[CaEGTA], Eq. B22, so that

$$\Delta[\mathrm{H}^+] = \frac{2fD_{\mathrm{EGTA}}}{D_{\mathrm{H,app}}}\Delta[\mathrm{CaEGTA}]. \tag{B31}$$

The value of f can be determined from the values of $[H^+]$ and β, the buffering power for protons. It is given by

$$f = \frac{[\mathrm{H}^+]}{(\log_{10}e)\,\beta}. \tag{B32}$$

The changes in $[H^+]$ can also be expressed in terms of pH. Eqs. B31 and B32 can be used to show that

$$\Delta pH = -\frac{2D_{EGTA}}{\beta D_{H,app}}\Delta[CaEGTA] . \quad (B33)$$

Application to Myoplasmic Diffusion Near an SR Ca Channel in Muscle

The calculations described in this section were carried out with parameters appropriate for 15°C inside a cut muscle fiber. The values of $[EGTA]_R$ and $[CaEGTA]_R$ are taken to be 18.24 and 1.76 mM, respectively, the same as those in the end-pool solutions. The value of k_1, the apparent rate constant for the reaction between Ca and EGTA, is taken to be 2.5×10^6 $M^{-1}s^{-1}$ (see Results and Appendix A). The value of k_{-1}, the apparent rate constant for the dissociation of CaEGTA, is calculated from k_1 and pH_R with Eqs. A6 and A9. The value of $[Ca]_R$ is calculated from pH_R with Eqs. A8 (first term on the right-hand side) and A9. The value of D_{Ca} is taken to be 3.0×10^{-6} cm^2/s. This value was obtained from the value of 6.0×10^{-6} cm^2/s for the diffusion coefficient of Ca in dilute aqueous solution (calculated from the value of the limiting equivalent conductivity of Ca, $\lambda^\circ = 46.9$ $cm^2\Omega^{-1}equiv^{-1}$ at 15°C, Robinson and Stokes, 1959) and the assumption that the value of the diffusion coefficient in myoplasm is half of that in a dilute aqueous solution (Kushmerick and Podolsky, 1969; Konishi et al., 1988). The values of D_{EGTA} and D_{CaEGTA} are both taken to be 1.7×10^{-6} cm^2/s (see first section of Results). The value of $D_{H,app}$ is taken to be 0.5×10^{-6} cm^2/s (Irving, Maylie, Sizto, and Chandler, 1990).

With these parameters, the value of λ_{Ca} calculated from Eq. B14 is 81 nm. The value of λ_{EGTA} calculated from Eq. B15 depends on pH: $\lambda_{EGTA} = 6.5$ μm for pH = 6.7, 8.1 μm for pH = 6.8, 10.2 μm for pH = 6.9, 12.9 μm for pH = 7.0, and 16.1 μm for pH = 7.1. All of these values are two orders of magnitude larger than that of λ_{Ca}, 81 nm. Consequently, $\lambda_{Ca}/\lambda_{EGTA} \cong 0$ so that Eqs. B18–B20 reduce to Eqs. B21–B23.

The values of $\Delta[Ca]$ and $\Delta[EGTA]$ that are calculated with Eqs. B18–B24 are directly proportional to the value of ϕ. Although ϕ has not been determined for an SR Ca channel inside a muscle fiber, a lower limit is given by the ratio of the peak rate of SR Ca release and the myoplasmic concentration of SR Ca channels that was obtained in our action-potential experiments. The mean peak rate of release was 143 μM/ms or 143,000 μM/s (column 7 in Table II). Pape et al. (1992) have estimated the concentration of Ca channels, approximately 0.27 μM referred to myoplasm, on the assumption that there is one Ca channel per foot structure (Franzini-Armstrong, 1975). If all of the Ca channels were open at the time of peak rate of release, a single open channel would be expected to pass $143{,}000/0.27 \cong 5 \times 10^5$ ions per second. This value represents a lower limit of ϕ since some of the Ca channels may not have been open at the time of peak release. With $\phi = 5 \times 10^5$ ions per second, the value of $\Delta[EGTA]_{r=0}$ calculated from Eq. B23 is -4.8 μM. This value clearly meets the requirement that the absolute value of $\Delta[EGTA]$ is much smaller than the value of $[EGTA]_R$ (estimated to be 18.24 mM) as assumed in the

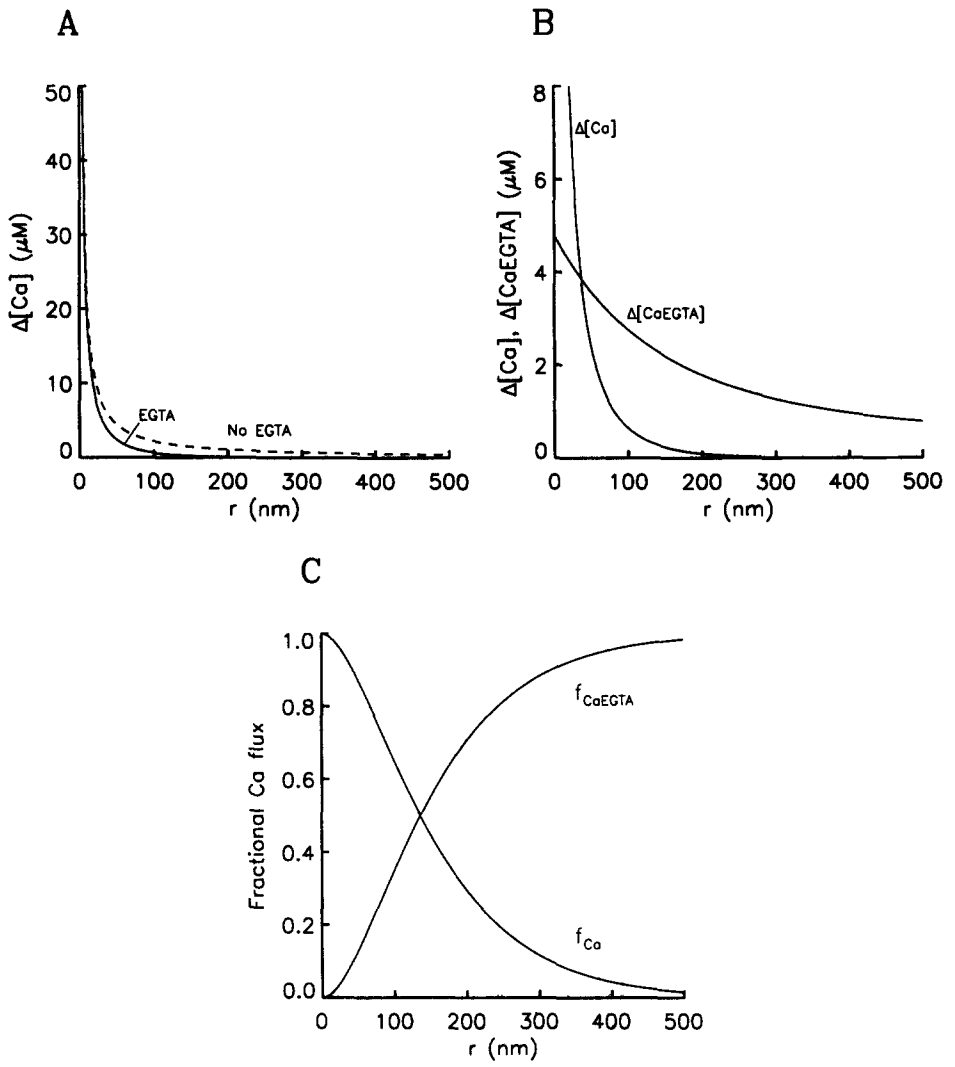

FIGURE 15. Theoretical estimates of the steady state values of Δ[Ca] and Δ[CaEGTA] plotted as a function of distance r from a single point source in an isotropic infinite medium. (*A*) The continuous curve, labeled "EGTA", was calculated from Eq. B21 with $[EGTA]_R$ = 18.24 mM. The dashed curve, labeled "No EGTA", was calculated from Eq. B24. (*B*) The curve labeled Δ[Ca] shows the curve labeled "EGTA" in A plotted with an expanded vertical scale. The curve labeled Δ[CaEGTA] was calculated from Eq. B22 with the relation Δ[CaEGTA] = −Δ[EGTA]. (*C*) The curves show the values of f_{Ca} and f_{CaEGTA} obtained from Eqs. B34 and B35, respectively. For the calculations, $D_{Ca} = 3 \times 10^{-6}$ cm²/s, $D_{EGTA} = 1.7 \times 10^{-6}$ cm²/s, $k_1 = 2.5 \times 10^6$ $M^{-1}s^{-1}$, $[EGTA]_R$ = 18.24 mM (except for the "No EGTA" curve in *A*), λ_{Ca} = 81 nm, and $\phi = 5 \times 10^5$ ions per second. See Appendix B for additional information.

derivation of Eq. B8. Even if the value of ϕ, and consequently that of $\Delta[\text{EGTA}]_{r=0}$, were ten times larger, the requirement would still be met.

Fig. 15 *A* shows Δ[Ca] plotted as a function of distance, r, from a point source of Ca flux, calculated with the values of the parameters given above. The continuous curve (labeled "EGTA") shows the values of Δ[Ca] with $[\text{EGTA}]_R$ = 18.24 mM (Eq. B21) and the dashed curve (labeled "No EGTA") shows the values with $[\text{EGTA}]_R$ = $[\text{CaEGTA}]_R$ = 0 mM (Eq. B24). At very small values of r, both curves are similar and vary inversely with r with the same proportionality constant, $\phi/(4\pi D_{Ca})$. This shows that, within a few nanometers of the point source, EGTA has little effect on the value of Δ[Ca]. At larger values of r, the curves diverge and the ability of EGTA to reduce Δ[Ca] becomes pronounced.

Fig. 15 *B* shows Δ[Ca] and Δ[CaEGTA] plotted against r on an expanded vertical scale. The curve labeled Δ[Ca] shows part of the continuous curve in *A*. The curve labeled Δ[CaEGTA] (= $-\Delta$[EGTA]), which was calculated from Eq. B22, decreases much less steeply with r than does the Δ[Ca] curve. It has a value of 4.8 μM at r = 0 nm and progressively decreases to a value of $\sim$0.8 μM at r = 500 nm. At all values of r, including the release site itself, the value of Δ[CaEGTA] is negligible compared with that of $[\text{EGTA}]_R$.

The curve for $\Delta[H^+]$ (not shown) is given by the Δ[CaEGTA] curve scaled by the factor $2fD_{\text{EGTA}}/D_{\text{H,app}}$ (Eq. B31). The value of f can be estimated from Eq. B32 and the mean value of β determined in our experiments, 22 mM/pH units = 0.022 M/pH units. For pH = 6.7–7.1, $f = 2.1-0.8 \times 10^{-5}$ and $2fD_{\text{EGTA}}/D_{\text{H,app}} = 1.4-0.6 \times 10^{-4}$. Thus, a maximal value of 4.8 μM for Δ[CaEGTA] (Fig. 15 *B*) corresponds to a maximal value of 0.7–0.3 nM for $\Delta[H^+]$. Similarly, Eq. B33 can be used to show that a maximal value of 4.8 μM for Δ[CaEGTA] corresponds to ΔpH = -0.0015 pH units. This shows that the changes in pH that are expected to occur near a Ca release site are very small and, consequently, would not be expected to influence the site.

At any value of r, the total flux of Ca is equal to the flux of free Ca plus that of CaEGTA. Under steady state conditions, which applies to this Appendix, the total flux is independent of r and equal to ϕ. Fig. 15*C* shows the fraction of total flux carried by Ca, f_{Ca}, and by CaEGTA, f_{CaEGTA}. These fractions have been evaluated from the two terms on the right-hand side of Eq. B9, with Eqs. B21 and B22. They are given by

$$f_{Ca} = (1 + r/\lambda_{Ca}) \cdot \exp(-r/\lambda_{Ca}) \tag{B34}$$

and

$$f_{\text{CaEGTA}} = 1-(1 + r/\lambda_{Ca}) \cdot \exp(-r/\lambda_{Ca}). \tag{B35}$$

At the source, all of the flux is carried by Ca. As the value of r is progressively increased, more and more Ca has a chance to be complexed by EGTA so that the value of f_{Ca} progressively decreases and that of f_{CaEGTA} progressively increases. At

r = 136 nm, the curves cross, indicating that half of the Ca has been captured by EGTA.

This Appendix allows several important conclusions to be made about the steady state changes in free [Ca], [CaEGTA], [EGTA], and [H^+] that are expected to occur near a single SR Ca channel in a fiber equilibrated with a large concentration of EGTA. First, the changes in [Ca], [CaEGTA], [EGTA], and [H^+] are directly proportional to the release flux ϕ (Eqs. B21, B22, and B30). Second, the changes in [Ca] are confined to a region within several λ_{Ca} from the release site (Eq. B21). In our experiments, the value of λ_{Ca} is estimated to be about 80 nm so that the changes are expected to be confined to within a few hundred nanometers of a release site. Third, the changes in [CaEGTA], [EGTA], and [H^+] are small and negligible compared with their respective resting values, even next to the release site itself (Eqs. B22 and B30). Fourth, these small changes spread farther away from the release site than does the change in free [Ca].

APPENDIX C

This Appendix gives the derivation of equations that describe the time course of the change in free [Ca] that is expected to develop near an SR Ca channel in a fiber equilibrated with a large concentration of EGTA. Similar to the approach used in Appendix B, an SR Ca channel is assumed to behave as a point source in an infinite medium of myoplasm. At time zero, the Ca flux through the source undergoes a step change from zero to ϕ. The analyses given in Neher (1986) and in Appendix B show that, in the steady state, [CaEGTA] $\cong$ $[CaEGTA]_R$ and [EGTA] $\cong$ $[EGTA]_R$, at least for the values of ϕ expected for SR Ca channels. Since the absolute values of Δ[CaEGTA] and Δ[EGTA] are expected to be maximal in the steady state, these approximations are also expected to hold during a transient. Consequently, the relations [CaEGTA] = $[CaEGTA]_R$ and [EGTA] = $[EGTA]_R$ have been used in the derivation in this appendix.

Under these conditions, [Ca] is expected to obey the partial differential equation,

$$\partial[Ca]/\partial t = D_{Ca}\{\partial^2[Ca]/\partial r^2 + (2/r)\partial[Ca]/\partial r\} - \{k_1[Ca][EGTA]_R - k_{-1}[CaEGTA]_R\}. \quad (C1)$$

With [Ca] = $[Ca]_R$ + Δ[Ca] (Eq. B5) and the equilibrium equation,

$$[Ca]_R = \frac{k_{-1}[CaEGTA]_R}{k_1[EGTA]_R}, \quad (C2)$$

Eq. C1 becomes

$$\partial\Delta[Ca]/\partial t = D_{Ca}\{\partial^2\Delta[Ca]/\partial r^2 + (2/r)\partial\Delta[Ca]/\partial r\} - k_1\Delta[Ca][EGTA]_R. \quad (C3)$$

Eq. C3 can be further simplified with the substitution

$$y(r,t) = \Delta[Ca]\exp(t/\tau_{Ca}) \quad (C4)$$

to give

$$\partial y/\partial t = D_{Ca}\{\partial^2 y/\partial r^2 + (2/r)\,\partial y/\partial r\}. \tag{C5}$$

As described in Appendix A, $\tau_{Ca} = (k_1[EGTA]_R)^{-1}$ represents the mean time required by EGTA at its resting concentration to complex Ca.

The Laplace transform of Eq. C5, with the initial condition $y(r,0) = 0$, is given by

$$p\bar{y} = D_{Ca}\{d^2\bar{y}/dr^2 + (2/r)\,d\bar{y}/dr\}, \tag{C6}$$

in which p represents the transform variable. The solution of Eq. C6 that is finite as $r \to \infty$ is given by

$$\bar{y} = \frac{A}{r}\exp(-r\sqrt{p/D_{Ca}}). \tag{C7}$$

The integration constant A can be evaluated from the boundary condition for $d\bar{y}/dr$ as $r \to 0$. This is given by combining Eqs. B4 and C4,

$$\phi\exp(t/\tau_{Ca}) = -\lim_{r\to 0} 4\pi r^2 D_{Ca}(\partial y/\partial r). \tag{C8}$$

The Laplace transform of Eq. C8 is given by

$$\frac{\phi}{p - \tau_{Ca}^{-1}} = -\lim_{r\to 0} 4\pi r^2 D_{Ca}(d\bar{y}/dr). \tag{C9}$$

The right-hand side of Eq. C9 can be evaluated by differentiation of Eq. C7,

$$\lim_{r\to 0} 4\pi r^2 D_{Ca}(d\bar{y}/dr) = -4\pi D_{Ca}A. \tag{C10}$$

Eqs. C7, C9, and C10 can be combined to give

$$\bar{y} = \frac{\phi}{4\pi D_{Ca} r(p - \tau_{Ca}^{-1})}\exp(-r\sqrt{p/D_{Ca}}). \tag{C11}$$

The inverse transform of Eq. C11, combined with Eq. C4, gives the solution,

$$\Delta[Ca] = \frac{\phi}{4\pi D_{Ca} r}\exp(-r/\lambda_{Ca}) \cdot F(r,t), \tag{C12}$$

in which $F(r,t)$ is given by

$$F(r,t) = 0.5\left\{\operatorname{erfc}\left(\frac{r}{\sqrt{4D_{Ca}t}} - \sqrt{t/\tau_{Ca}}\right)\right.$$
$$\left. + \exp(2r/\lambda_{Ca}) \cdot \operatorname{erfc}\left(\frac{r}{\sqrt{4D_{Ca}t}} + \sqrt{t/\tau_{Ca}}\right)\right\} \cdot \tag{C13}$$

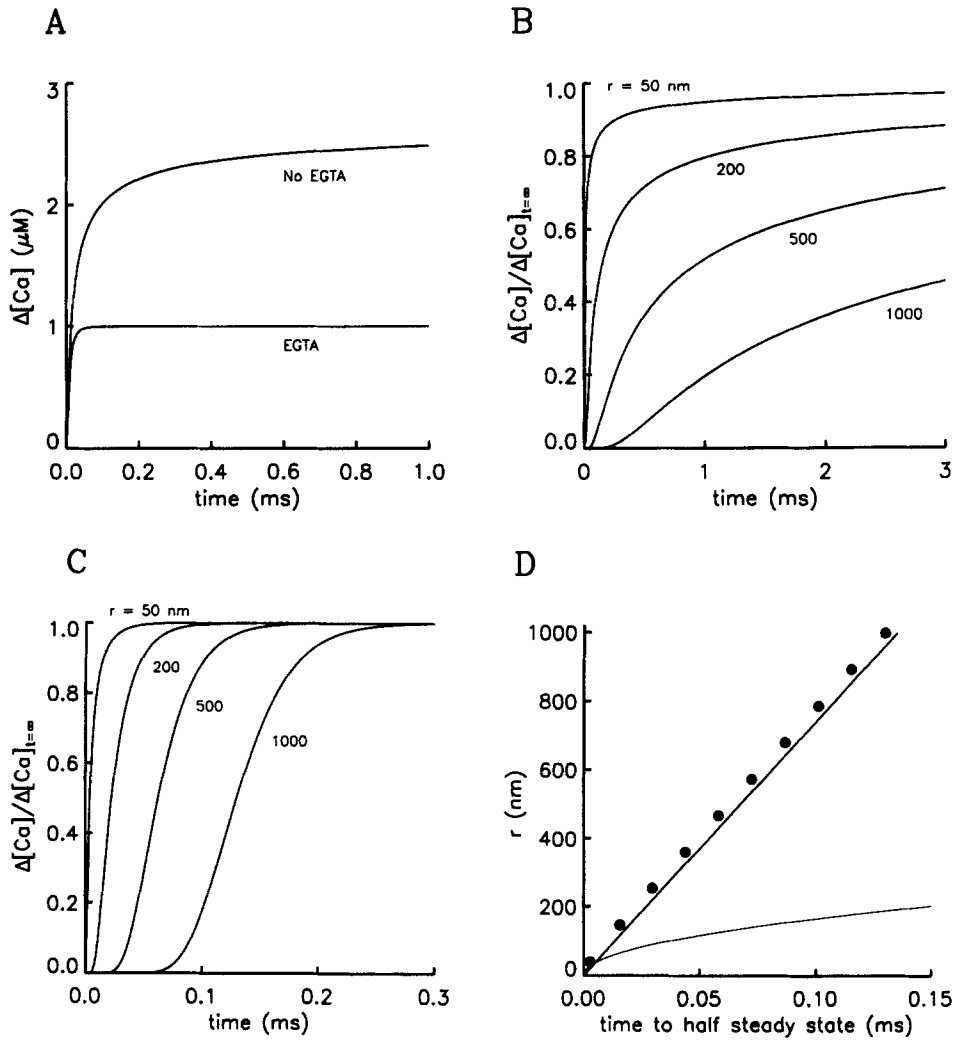

FIGURE 16. Theoretical time course of Δ[Ca] after a step change in ϕ from a single point source in an isotropic infinite medium. (*A*) The curves labeled "No EGTA" and "EGTA" were calculated from Eqs. C14 and C12, respectively, at r = 81 nm, the value of λ_{Ca} with $[EGTA]_R$ = 18.24 mM. (*B*) $\Delta[Ca]/\Delta[Ca]_{t=\infty}$ curves without EGTA were calculated from Eq. C14 at different values of r, as indicated. (*C*) $\Delta[Ca]/\Delta[Ca]_{t=\infty}$ curves with EGTA were calculated from Eq. C13 with the same values of r used in *B* and plotted on an expanded time scale. (*D*) The filled circles show values of r plotted as a function of $t_{1/2}$, from curves such as those in *C*, with EGTA. The thick straight line shows the function $r = (2\lambda_{Ca}/\tau_{Ca})t_{1/2}$. The thin line shows the function $r = 0.477(4D_{Ca}t_{1/2})^{1/2}$. The parameters for the calculations are given in the legend of Fig. 15. Additional information is given in Appendix C.

The right-hand side of Eq. C12 is equal to the steady state value of Δ[Ca] (Eq. B21) multiplied by $F(r,t)$. $F(r,t)$ gives the relative time course of Δ[Ca], starting with a value of 0 at $t = 0$ and approaching unity as $t \to \infty$.

In the special case in which there is no Ca buffer present, $[EGTA]_R = 0$, $\tau_{Ca} \to \infty$, $\lambda_{Ca} \to \infty$, and Eq. C12 reduces to

$$\Delta[Ca] = \frac{\phi}{4\pi D_{Ca} r} \cdot \operatorname{erfc}\left(\frac{r}{\sqrt{4D_{Ca}t}}\right). \tag{C14}$$

Eq. C14 is essentially the same as Eq. 2 in section 10.4 of Carslaw and Jaeger (1959).

Application to Diffusion in the Myoplasm near an SR Ca Channel in Muscle

Fig. 16 *A* shows the time course of Δ[Ca] at a distance of 81 nm from a point source, calculated with the same parameters used for Fig. 15; 81 nm is the value of λ_{Ca} estimated with $[EGTA]_R = 18.24$ mM. At $t = 0$ ms, the flux of Ca increases stepwise from 0 to ϕ. The curve labeled "EGTA" shows the values with $[EGTA]_R = 18.24$ mM and $[CaEGTA]_R = 1.76$ mM (Eq. C12). The curve labeled "No EGTA" shows the values with $[EGTA]_R = [CaEGTA]_R = 0$ mM (Eq. C14). The two curves are initially very similar, as expected because the ability of EGTA to bind Ca is not instantaneous but occurs after a delay given by τ_{Ca}. After 10–20 μs, the two curves diverge and eventually approach different final levels, as expected from Fig. 15 *A*. The "No EGTA" curve has a late slow component that is absent in the "EGTA" curve.

Fig. 16 *B* shows Δ[Ca] curves at $r = 50$, 200, 500, and 1,000 nm, as indicated. These curves were calculated for "No EGTA" (Eq. C14) and have been normalized by $\Delta[Ca]_{t=\infty}$ so that the relative time courses can be compared. The time course of Δ[Ca] becomes progressively slower as the value of r is increased.

Fig. 16 *C* shows a similar set of curves calculated with EGTA (Eq. C13), plotted on an expanded time scale. As the value of r is increased, the time course of $\Delta[Ca]/\Delta[Ca]_{t=\infty}$ becomes delayed and slower; that is, the curve is shifted to the right and the maximal slope of the rising phase is decreased. None of the curves has a late slow component similar to that observed in Fig. 16 *B*. Because the amplitude of Δ[Ca] is negligible for values of r larger than a few hundred nanometers (Fig. 15 *A*), the curves in Fig. 16 *C* show that, for all practical purposes, the spread of the Δ[Ca] signal is essentially complete within 0.1 ms. This is not surprising since Appendix A shows that EGTA is expected to complex almost all of the Ca released from the SR with a time constant τ_{Ca} equal to 22 μs.

The filled circles in Fig. 16 *D* show the value of r plotted as a function of $t_{1/2}$, the time to half steady state. Interestingly, the points lie close to the sloping straight line, determined by $r = (2\lambda_{Ca}/\tau_{Ca})t_{1/2}$. The reason for this is that, once t exceeds τ_{Ca}, the right-hand side of Eq. C13 is dominated by the first erfc function. In this case, $t_{1/2}$ corresponds approximately to the time when the argument of this function is zero, which gives $r = (4D_{Ca}/\tau_{Ca})^{1/2}t_{1/2} = (2\lambda_{Ca}/\tau_{Ca})t_{1/2}$, the equation for the straight line in Fig. 16 *D*. Thus, after a step change in ϕ in the presence of EGTA, the Δ[Ca] waveform appears to move with an approximately constant velocity of $2\lambda_{Ca}/\tau_{Ca}$. As it does so, its amplitude is attenuated (Fig. 15 *A*) and its normalized

rate of change spreads out (Fig. 16 *C*). With our standard set of parameters, the value of $2\lambda_{Ca}/\tau_{Ca}$ is equal to 7.4 μm/ms.

The thin curved line in Fig. 16 *D* shows the relation between r and $t_{1/2}$ that applies to changes in [Ca] without EGTA, Eq. C14; it was calculated from $\text{erfc}(r/\sqrt{4D_{Ca}t}) = 0.5$, which gives $r = 0.477(4D_{Ca}t_{1/2})^{1/2}$. The filled circles lie above the thin line, showing that the presence of EGTA decreases the time required for Δ[Ca] to reach its steady state value. This conclusion is exactly opposite to that reached by Simon and Llinás (1985) who concluded on page 491 that "the presence of a buffer will increase the time period for the substance to reach its steady state". The reason is that the equations used by Simon and Llinás (1985) apply to the situation in which the Ca buffer is immobile and the concentration of bound Ca at any time is directly proportional to the concentration of free Ca, a situation that does not reliably describe the properties of Ca buffering by freely diffusible buffers such as EGTA.

The main conclusion of this Appendix is that, near an SR Ca channel in a fiber equilibrated with 20 mM EGTA, changes in free [Ca] are expected to occur rapidly, within 0.1 ms, at all distances where the changes are of consequence. Since this delay is much shorter than the duration of SR Ca release, which lasts at least a few milliseconds, the relative time course of changes in free [Ca] everywhere in the myoplasm can be approximated by the time course of SR Ca release itself. This conclusion applies to a single SR release site, as considered in this Appendix, as well as to many sites, as follows from the principle of superposition.

APPENDIX D

The aim of this Appendix is to estimate the steady state profile of free Δ[Ca] that is produced by SR Ca release inside a single idealized frog myofibril. For this purpose, the shape of a myofibril is represented by a cylinder of radius a and length $2l$, the distance between two adjacent Z-bands. The radial and longitudinal distances are represented by r and z, respectively, with $z = 0$ and $2l$ corresponding to the locations of the two Z-bands. The movement of Ca from the SR into the myofibril is represented by ring sources at the two Z-bands. The flux of Ca is assumed to occur uniformly along the source rather than at discrete release sites. This assumption seems reasonable if the distance between the release sites is small compared with the value of λ_{Ca}. This is approximately the case under the conditions of the experiments reported here with large rates of SR Ca release because, as mentioned above, the value of λ_{Ca} is estimated to be about 80 nm whereas the spacing between adjacent "foot" structures that contain the SR Ca channels is about 30 nm (Franzini-Armstrong, 1975; Block et al., 1988). Radial symmetry is assumed.

Because of symmetry with other myofibrils, it is assumed that there is no flux of Ca into or out of the myofibril except at the two ring sources. Furthermore, because of symmetry within a single myofibril, it is assumed that there is no longitudinal flux of Ca midway between the two Z-bands, at $z = l$. Consequently, a single half myofibril can be represented by a cyclinder of radius a and length l, with no flux of Ca across its boundaries except for a ring source of radius a at $z = 0$.

In this situation, the concentration of Ca would be expected to increase indefinitely after release is started so that a steady state profile would never be attained.

One way to avoid this difficulty is to assume that the values of [CaEGTA] and [EGTA] are maintained constant at their prestimulus values, $[CaEGTA]_R$ and $[EGTA]_R$, respectively. This assumption seems reasonable, at least for small amounts of Ca release, since, in the case of a single SR Ca channel, the absolute values of Δ[CaEGTA] and Δ[EGTA] are expected to be extremely small compared with $[CaEGTA]_R$ and $[EGTA]_R$ (Neher, 1986; Appendix B).

The steady state equation that describes the spatial variation of [Ca] under these conditions is given by

$$D_{Ca}\{d^2[Ca]/dr^2 + (1/r)\,d[Ca]/dr + d^2[Ca]/dz^2\} - \{k_1[Ca][EGTA]_R - k_{-1}[CaEGTA]_R\} = 0. \quad \text{(D1)}$$

Eq. D1 can be combined with Eqs. B5 and C2 to give

$$D_{Ca}\{d^2\Delta[Ca]/dr^2 + (1/r)\,d\Delta[Ca]/dr + d^2\Delta[Ca]/dz^2\} - k_1\Delta[Ca][EGTA]_R = 0. \quad \text{(D2)}$$

The general solution of Eq. D2, obtained by the method of separation of variables, is given by

$$\Delta[Ca] = \sum_{n=0}^{\infty} A_n J_0(\alpha_n r)\cosh\left(\sqrt{1/\lambda_{Ca}^2 + \alpha_n^2}\,[z - l]\right), \quad \text{(D3)}$$

in which the values of α_n satisfy the equation

$$J_1(\alpha_n a) = 0. \quad \text{(D4)}$$

J_0 and J_1 represent Bessel's functions of order zero and one, respectively.

The boundary condition that $d\Delta[Ca]/dr = 0$ at $r = a$ is satisfied by $dJ_0(\alpha_n r)/dr = -J_1(\alpha_n r)/\alpha_n$ and Eq. D4. The boundary condition that $d\Delta[Ca]/dz = 0$ at $z = l$ is satisfied by the cosh terms, since $d\cosh\left(\sqrt{1/\lambda_{Ca}^2 + \alpha_n^2}\,[z - l]\right)/dz = 0$ at $z = l$ The other boundary condition, at $z = 0$, is that $d\Delta[Ca]/dz = 0$ except at $r = a$ where a total Ca flux of ϕ is introduced into the half myofibril. The values of A_n in Eq. D3 are determined by this boundary condition, which can be represented by

$$(d\Delta[Ca]/dz)_{z=0} = -\frac{\phi}{2\pi a D_{Ca}}\delta(r - a), \quad \text{(D5)}$$

in which ϕ represents the Ca flux into the half myofibril and δ represents the Dirac delta function.

Differentiation of Eq. D3 yields an expression for $(d\Delta[Ca]/dz)_{z=0}$ that can be equated with the right-hand side of Eq. D5. The value of A_n, obtained by multiplication by $rJ_0(\alpha_n r)dr$ and integration from 0 to a, is

$$A_n = \frac{\phi}{\pi a^2 D_{Ca} J_0(\alpha_n a)\sqrt{1/\lambda_{Ca}^2 + \alpha_n^2}\,\sinh\left(\sqrt{1/\lambda_{Ca}^2 + \alpha_n^2}\,l\right)}. \quad \text{(D6)}$$

Eqs. D3 and D6 can be combined to give the desired solution

$$\Delta[\mathrm{Ca}] = \frac{\phi}{\pi a^2 D_{\mathrm{Ca}}} \sum_{n=0}^{\infty} \frac{J_0(\alpha_n r)\cosh\left(\sqrt{1/\lambda_{\mathrm{Ca}}^2 + \alpha_n^2}\,[z-l]\right)}{J_0(\alpha_n a)\sqrt{1/\lambda_{\mathrm{Ca}}^2 + \alpha_n^2}\,\sinh\left(\sqrt{1/\lambda_{\mathrm{Ca}}^2 + \alpha_n^2}\,l\right)} \cdot \quad \text{(D7)}$$

The mean value of Δ[Ca] at z, weighted according to area in the r direction, is denoted by $\Delta\langle[\mathrm{Ca}]\rangle$,

$$\Delta\langle[\mathrm{Ca}]\rangle = \frac{1}{\pi a^2}\int_0^a 2\pi r\,\Delta[\mathrm{Ca}]\,dr. \quad \text{(D8)}$$

The right-hand side of Eq. D8 can be evaluated by integration of the right-hand side of Eq. D7 term by term. Because $\int r J_0(\alpha_n r)\,dr$ is equal to $r J_1(\alpha_n r)/\alpha_n$, the value of the integral from $r = 0$ to a is equal to zero for $n > 0$. Consequently, the only term on the right-hand side of Eq. D7 that contributes to $\Delta\langle[\mathrm{Ca}]\rangle$ is the first term, with $\alpha_0 = 0$. Consequently,

$$\Delta\langle[\mathrm{Ca}]\rangle = \frac{\phi\lambda_{\mathrm{Ca}}}{\pi a^2 D_{\mathrm{Ca}}} \cdot \frac{\cosh\frac{z-l}{\lambda_{\mathrm{Ca}}}}{\sinh\frac{l}{\lambda_{\mathrm{Ca}}}} \cdot \quad \text{(D9)}$$

Eq. D9 represents the solution of the equation for diffusion plus binding in only one spatial dimension, z.

The spatially averaged value of Δ[Ca] in the half sarcomere of length l is denoted by $\overline{\Delta[\mathrm{Ca}]}$,

$$\overline{\Delta[\mathrm{Ca}]} = \frac{1}{l}\int_0^l \Delta\langle[\mathrm{Ca}]\rangle\,dz \quad \text{(D10)}$$

$$= \frac{1}{k_1[\mathrm{EGTA}]_{\mathrm{R}}} \cdot \frac{\phi}{\pi a^2 l} \cdot \quad \text{(D11)}$$

Eq. D11 is essentially the same as Eq. A10. This follows because [EGTA] is assumed to equal $[\mathrm{EGTA}]_{\mathrm{R}}$ in this Appendix and because $\overline{\Delta[\mathrm{Ca}]}$ and $\phi/\pi a^2 l$ (the flux per unit volume) in Eq. D11 are analogous to Δ[Ca] and $d\Delta[\mathrm{CaEGTA}]/dt$, respectively, in Eq. A10. The equivalence of Eqs. D11 and A10 is consistent with the idea that the analysis in Appendix A, which uses spatially averaged changes in free [Ca], applies to myofibrils in which gradients of [Ca] are expected to occur.

Eqs. D9 and D11 can be combined to give

$$\Delta\langle[\mathrm{Ca}]\rangle = \overline{\Delta[\mathrm{Ca}]}\left(\frac{l}{\lambda_{\mathrm{Ca}}} \cdot \frac{\cosh\frac{z-l}{\lambda_{\mathrm{Ca}}}}{\sinh\frac{l}{\lambda_{\mathrm{Ca}}}}\right). \quad \text{(D12)}$$

Since $l >> \lambda_{Ca}$, Eq. D12 is given to an excellent approximation by

$$\Delta\langle [Ca]\rangle \cong \Delta\overline{[Ca]}\left(\frac{l}{\lambda_{Ca}} \cdot \exp\left(-z/\lambda_{Ca}\right)\right). \tag{D13}$$

This shows that the value of $\Delta\langle[Ca]\rangle$ decreases exponentially with distance from the Z-band and has a maximal value at $z = 0$ equal to $\Delta\overline{[Ca]}\,(l/\lambda_{Ca})$.

Application to Profiles of Δ[Ca] in an Idealized Myofibril

Fig. 17 A shows loci of r and z that are associated with different steady state values of Δ[Ca] (indicated in units of micromolar) in an idealized myofibril that contains 20 mM EGTA. The values of Δ[Ca] were calculated from Eq. D7. r represents the distance in the radial direction from the longitudinal axis of the idealized cylindrical myofibril. It can vary between 0 and a, the radius of the myofibril; in this example, a = 500 nm, the radius of a typical myofibril (Peachey, 1965). z represents the distance in the longitudinal direction from the Z-band, which can vary between 0 and half the sarcomere length, l. In this example, l = 1,800 nm; this corresponds to a sarcomere length of 3.6 μm, which is typical of the fibers used in our experiments. The value of ϕ corresponds to a spatially averaged rate of SR Ca release of 140 μM/ms, similar to the mean peak value obtained in our experiments with action-potential stimulation (column 7 of Table II).

The equation used to calculate Δ[Ca] in Fig. 17 *A*, Eq. D7, was derived for steady state conditions and has the property that the value of Δ[Ca] anywhere in the myofibril is expected to be directly proportional to the rate of SR Ca release, ϕ. Appendix C shows that Δ[Ca] tracks ϕ with a delay that increases with distance from the source. At distances at which the values of Δ[Ca] are of any consequence, this delay is <0.1 ms. Since this delay is short compared with the time course of SR Ca release, the steady state relation between Δ[Ca] and ϕ, Eq. D7, is expected to provide a good approximation of Δ[Ca] at any time during SR Ca release.

Each of the loci in Fig. 17 *A* extends from the horizontal axis at r = 500 nm to either the vertical axis at z = 0 nm or the horizontal axis at r = 0 nm. The direction of approach to each boundary is perpendicular, as expected since there is no flux of Ca across the boundaries of the idealized half myofibril. The values of Δ[Ca] become progressively larger as the ring source at r = 500 nm, z = 0 nm is approached. Near the source, the value of Δ[Ca] depends only on distance from the ring and not on the direction along the r or z axes. This is illustrated by the curves associated with Δ[Ca] = 100 and 30 μM being nearly perfect quarter circles. As the ring source is approached, the value of Δ[Ca] becomes progressively larger and exceeds 100 μM at distances <55 nm from the ring. Thus, EGTA does not prevent large values of Δ[Ca] from occurring near the ring source.

In Fig. 17 *A*, the value of Δ[Ca] progressively decreases away from the ring source and is 10 μM at ~200 nm and 1 μM at 372–468 nm, with the exact value depending on direction. At larger distances from the ring source, as Δ[Ca] decreases further, the loci of constant Δ[Ca] become progressively more vertical in the figure, indicating a reduction in the radial gradient of Δ[Ca].

The loci in Fig. 17 *A* can be transformed into loci of different steady state values

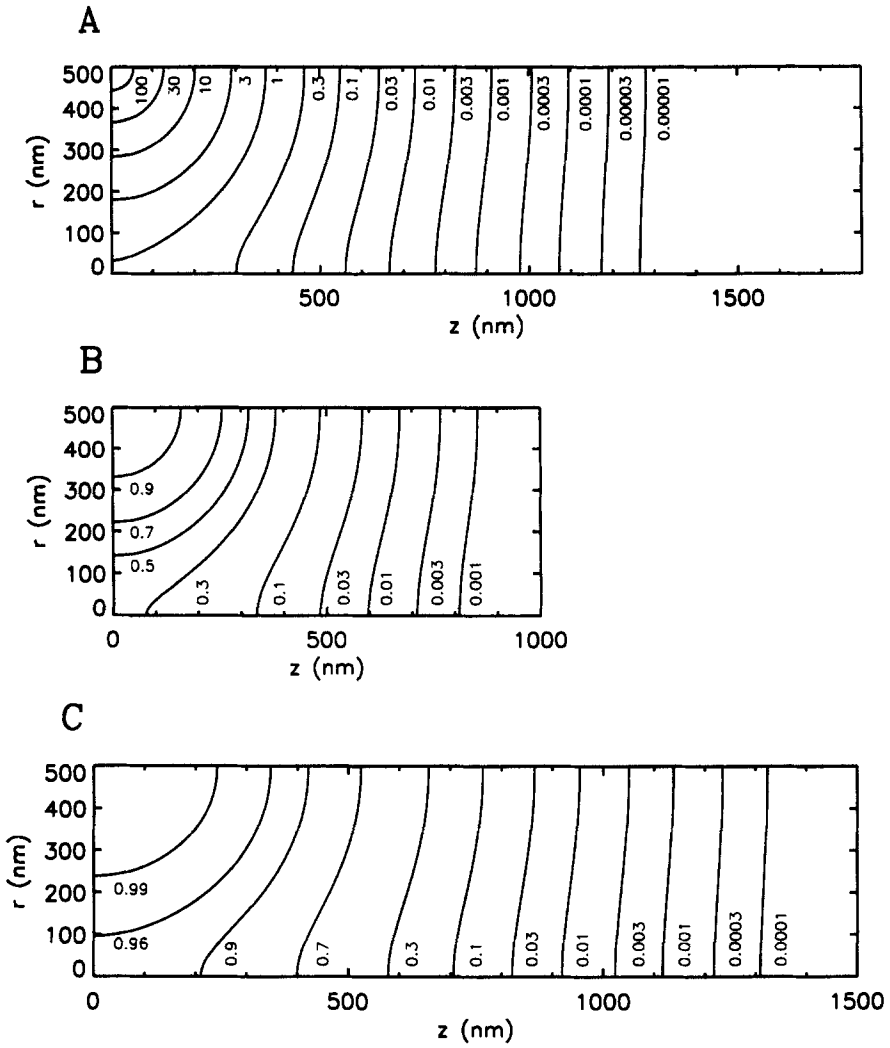

FIGURE 17. Loci of r and z associated with different steady state values of $\Delta[Ca]$ (*A*, indicated in units of micromolar) and $\Delta[CaTrop]/[Trop]_R$ (*B*), and different quasi-steady state values of $\Delta[CaParv]/[Parv]_R$ (*C*) in a idealized myofibril containing 20 mM EGTA. Ca release from the SR is represented by a ring source at the Z-band. $\Delta[Ca]$ was calculated from Eq. D7. (*A*) $\Delta[Ca]$. The mean value of $\Delta[Ca]$, denoted by $\Delta\overline{[Ca]}$ in Appendix D, is 3.07 μM. (*B*) $\Delta[CaTrop]/[Trop]_R$. The curves were calculated with a value of 2 μM for the K_D of the Ca-regulatory sites on troponin. The value of $[CaTrop]_R/[Trop]_R$, 0.027, was calculated from $[Ca]_R = 0.054$ μM. The mean value of $\Delta[CaTrop]/[Trop]_R$ from $z = 0$ to 1,025 nm, which is taken to represent the spatial distribution of troponin, is 0.253. (*C*) $\Delta[CaParv]/[Parv]_R$. The curves were calculated with a value of 0.004 μM for the K_D of Ca binding to the Ca,Mg sites on parvalbumin. The value of $[CaParv]_R/[Parv]_R$, 13.5, was calculated from $[Ca]_R = 0.054$ μM. Because diffusion of parvalbumin and changes in [MgParv] are expected to occur slowly, they were neglected in the calculations so that the curves would describe the extent of Ca complexation by parvalbumin immediately after a brief period of Ca release. The mean value of $\Delta[CaParv]/[Parv]_R$ calculated in this manner is 0.314. See Appendix D for additional information.

of Ca complexation by the Ca-regulatory sites on troponin. Troponin is assumed to be immobile and to be distributed along the thin filaments. The concentrations of Ca-bound and Ca-free sites on troponin, denoted by [CaTrop] and [Trop], respectively, are assumed to be related to the value of free [Ca] by the usual 1:1 binding equation, similar to the first term on the right-hand side of Eq. A8, with K_D = 2 μM (Baylor et al., 1983). The resting value of [CaTrop]/[Trop], $[CaTrop]_R/[Trop]_R$, was calculated from $[Ca]_R$ = 0.054 μM (from the experiment in Fig. 11) to be 0.027.

The loci in Fig. 17 *B* are associated with different values of $\Delta[CaTrop]/[Trop]_R$, as indicated; $\Delta[CaTrop]/[Trop]_R$, which does not depend on the total concentration of troponin, represents the fraction of Ca-free sites that were available at rest that become complexed by Ca. The z axis extends to only 1,025 nm, which is half the length of thin filaments in frog muscle (Page and Huxley, 1963). It is clear from the figure that, in the steady state, almost all of the Ca that is bound to the Ca-regulatory sites on troponin lies within the region $z \leq 500$ nm.

Fig. 17 *C* shows quasi-steady state loci associated with different values of $\Delta[CaParv]/[Parv]_R$. [Parv], [CaParv], and [MgParv] are used to denote, respectively, the concentrations of free, Ca-bound, and Mg-bound Ca,Mg sites on parvalbumin, and Δ and *R* have their usual meaning. In the steady state, the values of [Parv], [CaParv], and [MgParv] depend on [Ca] and [Mg]. Immediately after a brief period of Ca release from the SR, however, such as that elicited by an action potential, there is little change in the value of [MgParv]. In this situation, the value of $[CaParv]/[Parv]_R$ can be estimated from the 1:1 binding equation for Ca, similar to the first term on the right-hand side of Eq. A8, with K_D = 0.004 μM (Baylor et al., 1983). The quasi-steady state loci in Fig. 17 *C* were estimated from these values of $[CaParv]/[Parv]_R$ after subtraction of the value of $[CaParv]_R/[Parv]_R$, 13.5, which was calculated from $[Ca]_R$ = 0.054 μM. Since the calculation applies to changes produced within a few milliseconds after an action potential, parvalbumin was assumed to be immobile.

The calculated values of Δ[Ca], $\Delta[CaTrop]/[Trop]_R$, and $\Delta[CaParv]/[Parv]_R$ in Fig. 17 can be weighted according to volume (that is, multiplied by $2\pi r dr dz$), integrated along the r and z axes, and divided by the appropriate total volume ($\pi a^2 Z$ with $Z = l$ = 1,800 nm in A and C and Z = 1,025 nm in B) to give the corresponding mean values. The mean steady state value of Δ[Ca] from z = 0 to 1,800 nm that was obtained in this manner is 3.07 μM, which is the same as that obtained directly from Eq. D11 or Eq. A10. The mean steady state value of Δ[Ca] adjacent to troponin, from z = 0 to 1,025 nm, is 5.39 μM. This value is essentially equal to (1,800/1,025) times the mean value from z = 0 to 1,800, since the value of Δ[Ca] is negligibly small for $z > 1{,}025$ nm. The mean steady state values of $\Delta[CaTrop]/[Trop]_R$ and $\Delta[CaParv]/[Parv]_R$ are 0.253 and 0.314, respectively; these estimates depend implicitly on the assumption that troponin and parvalbumin are distributed uniformly along the thin filament and the entire myofibril, respectively.

We thank the staff of the Biomedical Instrumentation Laboratory of the Yale Department of Cellular and Molecular Physiology for help with the design and construction of equipment. We also thank Drs. Steve Baylor and Stephen Hollingworth for many helpful discussions and for reading the manuscript and providing useful criticism.

This work was supported by U.S. Public Health Service grant AM-37643.

Original version received 23 October 1994 and accepted version received 17 March 1995.

REFERENCES

Abercrombie, R. F., R. W. Putnam, and A. Roos. 1983. The intracellular pH of frog skeletal muscle: its regulation in isotonic solutions. *Journal of Physiology.* 345:175–187.

Baylor, S. M., and W. K. Chandler. 1978. Optical indications of excitation-contraction coupling in striated muscle. *In* Biophysical aspects of cardiac muscle. M. Morad, editors. Academic Press, Inc., New York. 207–228.

Baylor, S. M., W. K. Chandler, and M. W. Marshall. 1979. Arsenazo III signals in singly dissected frog twitch fibres. *Journal of Physiology.* 287:23–24P. (Abstr.)

Baylor, S. M., W. K. Chandler, and M. W. Marshall. 1982*a*. Optical measurements of intracellular pH and magnesium in frog skeletal muscle fibres. *Journal of Physiology.* 331:105–137.

Baylor, S. M., W. K. Chandler, and M. W. Marshall. 1982*b*. Use of metallochromic dyes to measure changes in myoplasmic calcium during activity in frog skeletal muscle fibres. *Journal of Physiology.* 331:139–177.

Baylor, S. M., W. K. Chandler, and M. W. Marshall. 1983. Sarcoplasmic reticulum calcium release in frog skeletal muscle fibres estimated from arsenazo III calcium transients. *Journal of Physiology.* 344: 625–666.

Baylor, S. M., and S. Hollingworth. 1987. Effect of calcium (Ca) buffering by fura-2 on the second component of the intrinsic birefringence signal in frog isolated twitch muscle fibres. *Journal of Physiology.* 391:90P. (Abstr.)

Baylor, S. M., and S. Hollingworth. 1988. Fura-2 calcium transients in frog skeletal muscle fibres. *Journal of Physiology.* 403:151–192.

Baylor, S. M., and S. Hollingworth. 1990. Absorbance signals from resting frog skeletal muscle fibers injected with the pH indicator dye, phenol red. *Journal of General Physiology.* 96:449–471.

Blatter, L. A., and J. R. Blinks. 1991. Simultaneous measurement of Ca^{2+} in muscle with Ca electrodes and aequorin. Diffusible cytoplasmic constituent reduces Ca^{2+}-independent luminescence of aequorin. *Journal of General Physiology.* 98:1141–1160.

Block, B. A., T. Imagawa, K. P. Campbell, and C. Franzini-Armstrong. 1988. Structural evidence for direct interaction between the molecular components of the transverse tubule/sarcoplasmic reticulum junction in skeletal muscle. *Journal of Cell Biology.* 107:2587–2600.

Bolton, T. B., and R. D. Vaughan-Jones. 1977. Continuous direct measurement of intracellular chloride and pH in frog skeletal muscle. *Journal of Physiology.* 270:801–833.

Brum, G., E. Ríos, and E. Stefani. 1988. Effects of extracellular calcium on calcium movements of excitation-contraction coupling in frog skeletal muscle fibres. *Journal of Physiology.* 398:441–473.

Carslaw, H. S., and J. C. Jaeger. 1959. Conduction of heat in solids. 2nd edition. Oxford University Press, London, UK.

Chandler, W. K., A. Hirota, D.-S. Jong, and P. C. Pape. 1993. Measurement of calcium release from the sarcoplasmic reticulum into the myoplasm of frog cut muscle fibers. *Japanese Journal of Physiology.* 43:S77–S81.

Chandler, W. K., D.-S. Jong, and P. C. Pape. 1992. Measurement of sarcoplasmic reticulum (SR) calcium release in frog cut muscle fibers with EGTA and phenol red. *Biophysical Journal.* 61:A130. (Abstr.)

Chandler, W. K., D.-S. Jong, and P. C. Pape. 1994. Measurement of the rapidly available proton buffering power in frog cut muscle fibers. *Biophysical Journal.* 66:A86. (Abstr.)

Colquhoun, D. 1971. Lectures on biostatistics. Oxford University Press, Oxford.

Colquhoun, D., and F. J. Sigworth. 1983. Fitting and statistical analysis of single-channel records. *In* Single-Channel Recording. B. Sakmann and E. Neher, editors. Plenum Publishing Corp, New York. 191–263.

Coray, A., C. H. Fry, P. Hess, J. A. S. McGuigan, and R. Weingart. 1980. Resting calcium in sheep cardiac tissue and in frog skeletal muscle measured with ion-seletive micro-electrodes. *Journal of Physiology.* 305:60–61P. (Abstr.)

Csernoch, L., V. Jacquemond, and M. F. Schneider. 1993. Microinjection of strong calcium buffers suppresses the peak of calcium release during depolarization in frog skeletal muscle fibers. *Journal of General Physiology.* 101:297–333.

Curtin, N. A. 1986. Buffer power and intracellular pH of frog sartorius muscle. *Biophysical Journal.* 50: 837–841.

Endo, M., M. Tanaka, and S. Ebashi. 1968. Release of calcium from sarcoplasmic reticulum in skinned fibers of the frog. *Proceedings of the International Congress of Physiological Sciences.* 7:126. (Abstr.)

Fabiato, A. 1984. Dependence of the Ca^{2+}-induced release from the sarcoplasmic reticulum of skinned skeletal muscle fibres from the frog semitendinosus on the rate of change of free Ca^{2+} concentration at the outer surface of the sarcoplasmic reticulum. *Journal of Physiology.* 353:56P. (Abstr.)

Ford, L. E., and R. J. Podolsky. 1968. Force developement and calcium movements in skinned muscle fibers. *Federation Proceedings.* 27:375. (Abstr.)

Franzini-Armstrong, C. 1975. Membrane particles and transmission at the triad. *Federation Proceedings.* 34:1382–1389.

Godt, R. E., and D. W. Maughan. 1988. On the composition of the cytosol of relaxed skeletal muscle of the frog. *American Journal of Physiology.* 254:C591–C604.

Grynkiewicz, G., M. Poenie, and R. Y. Tsien. 1985. A new generation of Ca indicators with greatly improved fluorescence properties. *Journal of Biological Chemistry.* 260:3440–3450.

Hammes, G. G. 1974. Investigations of rates and mechanisms of reactions. Part II. *In* Temperature Jump Methods. G. G. Hammes, editor. John Wiley and Sons, New York. 147–185.

Harafuji, H., and Y. Ogawa. 1980. Re-examination of the apparent binding constant of ethylene glycol bis(β-aminoethyl ether)-N,N,N′,N′-Tetraacetic Acid with calcium around neutral pH. *Journal of Bichemistry.* 87:1305–1312.

Harkins, A. B., N. Kurebayashi, and S. M. Baylor. 1993. Resting myoplasmic free calcium in frog skeletal muscle fibers estimated with fluo-3. *Biophysical Journal.* 65:865–881.

Hille, B., and D. T. Campbell. 1976. An improved Vaseline gap voltage clamp for skeletal muscle fibers. *Journal of General Physiology.* 67:265–293.

Hirota, A., W. K. Chandler, P. L. Southwick, and A. S. Waggoner. 1989. Calcium signals recorded from two new purpurate indicators inside frog cut twitch fibers. *Journal of General Physiology.* 94:597–631.

Hollingworth, S., and S. M. Baylor. 1990. Changes in phenol red absorbance in response to electrical stimulation of frog skeletal muscle fibers. *Journal of General Physiology.* 96:473–491.

Hollingworth, S., A. B. Harkins, N. Kurebayashi, M. Konishi, and S. M. Baylor. 1992. Excitation-contraction coupling in intact frog skeletal muscle fibers injected with mmolar concentrations of fura-2. *Biophysical Journal.* 63:224–234.

Hou, T.-T., J. D. Johnson, and J. A. Rall. 1991. Parvalbumin content and Ca^{2+} and Mg^{2+} dissociation rates correlated with changes in relaxation rate of frog muscle fibres. *Journal of Physiology.* 441:285–304.

Irving, M., J. Maylie, N. L. Sizto, and W. K. Chandler. 1987. Passive electrical and intrinsic optical properties of cut frog twitch fibers. *Journal of General Physiology.* 89:1–40.

Irving, M., J. Maylie, N. L. Sizto, and W. K. Chandler. 1989. Simultaneous monitoring of changes in magnesium and calcium concentrations in frog cut twitch fibers containing antipyrylazo III. *Journal of General Physiology.* 93:585–608.

Irving, M., J. Maylie, N. L. Sizto, and W. K. Chandler. 1990. Intracellular diffusion in the presence of mobile buffers. Application to proton movement in muscle. *Biophysical Journal.* 57:717–721.

Jacquemond, V., L. Csernoch, M. G. Klein, and M. F. Schneider. 1991. Voltage-gated and calcium-gated calcium release during depolarization of skeletal muscle fibers. *Biophysical Journal.* 60:867–873.

Jong, D.-S., P. C. Pape, W. K. Chandler, and S. M. Baylor. 1993. Reduction of calcium inactivation of sarcoplasmic reticulum calcium release in voltage-clamped cut twitch fibers with fura-2. *Journal of General Physiology.* 102:333–370.

Jong, D.-S., P. C. Pape, S. M. Baylor, and W. K. Chandler. 1995. Calcium inactivation of calcium release in frog cut muscle fibers that contain millimolar EGTA or fura-2. *Journal of General Physiology.* 106:337–388.

Kao, J. P. Y., and R. Y. Tsien. 1988. Ca binding kinetics of fura-2 and azo-1 from temperature-jump relaxation measurements. *Biophysical Journal.* 53:635–639.

Klein, M. G., B. J. Simon, G. Szúcs, and M. F. Schneider. 1988. Simultaneous recording of calcium transients in skeletal muscle using high- and low–affinity calcium indicators. *Biophysical Journal.* 53: 971–988.

Klein, M. G., B. J. Simon, and M. F. Schneider. 1990. Effects of caffeine on calcium release from the sarcoplasmic reticulum in frog skeletal muscle fibers. *Journal of Physiology.* 425:599–626.

Konishi, M., S. Hollingworth, A. B. Harkins, and S. M. Baylor. 1991. Myoplasmic calcium transients in intact frog skeletal muscle fibers monitored with the fluorescent indicator furaptra. *Journal of General Physiology.* 97:271–301.

Konishi, M., A. Olson, S. Hollingworth, and S. M. Baylor. 1988. Myoplasmic binding of fura-2 investigated by steady-state fluorescence and absorbance measurements. *Biophysical Journal.* 54:1089–1104.

Kovács, L., E. Ríos, and M. F. Schneider. 1983. Measurement and modification of free calcium transients in frog skeletal muscle fibres by a metallochromic indicator dye. *Journal of Physiology.* 343: 161–196.

Kurebayashi, N., A. B. Harkins, and S. M. Baylor. 1993. Use of fura red as an intracellular calcium indicator in frog skeletal muscle fibers. *Biophysical Journal.* 64:1934–1960.

Kushmerick, M. J., and R. J. Podolsky. 1969. Ionic mobility in muscle cells. *Science.* 166:1297–1298.

Lamb, G. D., E. Recupero, and D. G. Stephenson. 1992. Effect of myoplasmic pH on excitation-contraction coupling in skeletal muscle fibres of the toad. *Journal of Physiology.* 448:211–224.

Lisman, J. E., and J. A. Strong. 1979. The initiation of excitation and light adaptation in Limulus ventral photoreceptors. *Journal of General Physiology.* 73:219–243.

Ma, J., M. Fill, C. M. Knudson, K. P. Campbell, and R. Coronado. 1988. Ryanodine receptor of skeletal muscle is a gap junction-type channel. *Science.* 242:99–102.

Martell, A. E., and R. M. Smith. 1974. Critical Stability Constants. Vol. 1. Amino Acids. Plenum Publishing Corp., New York. 469 pp.

Maylie, J., M. Irving, N. L. Sizto, G. Boyarski, and W. K. Chandler. 1987*a*. Calcium signals recorded from cut frog twitch fibers containing tetramethylmurexide. *Journal of General Physiology.* 89:145–176.

Maylie, J., M. Irving, N. L. Sizto, and W. K. Chandler. 1987*b*. Comparison of arsenazo III optical signals in intact and cut frog twitch fibers. *Journal of General Physiology.* 89:41–81.

Maylie, J., M. Irving, N. L. Sizto, and W. K. Chandler. 1987*c*. Calcium signals recorded from cut frog twitch fibers containing antipyrylazo III. *Journal of General Physiology.* 89:83–143.

Meissner, G., and R. C. Young. 1980. Proton permeability of sarcoplasmic reticulum vesicles. *Journal of Biological Chemistry.* 255:6814–6819.

Melzer, W., E. Ríos, and M. F. Schneider. 1984. Time course of calcium release and removal in skeletal muscle fibers. *Biophysical Journal.* 45:637–641.

Melzer, W., E. Ríos, and M. F. Schneider. 1987. A general procedure for determining the rate of calcium release from the sarcoplasmic reticulum in skeletal muscle fibers. *Biophysical Journal.* 51:849–863.

Miledi, R., S. Nakajima, I. Parker, and T. Takahashi. 1981. Effects of membrane polarization on sarcoplasmic calcium release in skeletal muscle. *Proceedings of the Royal Society of London, Series B.* 213:1–13.

Neher, E. 1986. Concentration profiles of intracellular calcium in the presence of a diffusible chelator. *In* Calcium Electrogenesis and Neuronal Functioning. U. Heinemann, M. Klee, E. Neher, and W. Singer, editors. Springer-Verlag, Berlin, Heidelberg. 80–96.

Page, S., and H. E. Huxley. 1963. Filament lengths in striated muscle. *Journal of Cell Biology.* 19:369–390.

Palade, P., and J. Vergara. 1982. Arsenazo III and antipyrylazo III calcium transients in single skeletal muscle fibers. *Journal of General Physiology.* 79:679–707.

Pape, P. C. 1990. pH in cut frog muscle fibers. *Biophysical Journal.* 57:347*a*. (Abstr.)

Pape, P. C., D.-S. Jong, and W. K. Chandler. 1994. Voltage dependence of sarcoplasmic reticulum (SR) calcium release in frog cut muscle fibers equilibrated with 20 mM EGTA. *Biophysical Journal.* 66:A87. (Abstr.)

Pape, P. C., D.-S. Jong, W. K. Chandler, and S. M. Baylor. 1993. Effect of fura-2 on action-potential stimulated calcium release in cut twitch fibers from frog muscle. *Journal of General Physiology.* 102: 295–332.

Pape, P. C., M. Konishi, and S. M. Baylor. 1992. Valinomycin and excitation-contraction coupling in skeletal muscle fibres of the frog. *Journal of Physiology.* 449:219–235.

Pape, P. C., M. Konishi, S. Hollingworth, and S. M. Baylor. 1990. Perturbation of sarcoplasmic reticulum calcium release and phenol red absorbance transients by large concentrations of fura-2 injected into frog skeletal muscle fibers. *Journal of General Physiology.* 96:493–516.

Peachey, L.D. 1965. The sarcoplasmic reticulum and transverse tubules of the frog's sartorius. *Journal of Cell Biology.* 25:209–231.

Pizarró, G., L. Csernoch, I. Uribe, M. Rodríguez, and E. Ríos. 1991. The relationship between Q_γ and Ca release from the sarcoplasmic reticulum in skeletal muscle. *Journal of General Physiology.* 97:913–947.

Rakowski, R. F., P. M. Best, and M. R. James-Kracke. 1985. Voltage dependence of membrane charge movement and calcium release in frog skeletal muscle fibres. *Journal of Muscle Research and Cell Motility.* 6:403–433.

Ríos, E., and G. Pizarró. 1988. Voltage sensors and calcium channels of excitation-contraction coupling. *News in Physiological Sciences.* 3:223–227.

Robinson, R. A., and R. H. Stokes. 1959. Electrolyte Solutions. Butterworth and Co., Ltd., London. 559 pp.

Rousseau, E., and J. Pinkos. 1990. pH modulates conducting and gating behaviour of single calcium release channels. *Pflügers Archiv.* 415:645–647.

Schneider, M. F., and B. J. Simon. 1988. Inactivation of calcium release from the sarcoplasmic reticulum in frog skeletal muscle. *Journal of Physiology.* 405:727–745.

Schneider, M. F., B. J. Simon, and G. Szúcs. 1987. Depletion of calcium from the sarcoplasmic reticulum during calcium release in frog skeletal muscle. *Journal of Physiology.* 392:167–192.

Simon, S. M., and R. R. Llinás. 1985. Compartmentalization of the submembrane calcium activity

during calcium influx and its significance in transmitter release. *Biophysical Journal.* 48:485–498.

Simon, B. J., M. G. Klein, and M. F. Schneider. 1991. Calcium dependence of inactivation of calcium release from the sarcoplasmic reticulum in skeletal muscle fibers. *Journal of General Physiology.* 97: 437–471.

Simon, B. J., M. F. Schneider, and G. Szúcs. 1985. Inactivation of sarcoplasmic reticulum calcium release in frog skeletal muscle is mediated by calcium. *Journal of General Physiology.* 86:36*a.* (Abstr.)

Smith, P. D., G. W. Liesegang, R. L. Berger, G. Czerlinski, and R. J. Podolsky. 1984. A stopped-flow investigation of calcium ion binding by ethylene glycol bis(β-aminoethyl ether)-N,N′-tetraacetic Acid. *Analytical Biochemistry.* 143:188–195.

Somlyo, A. P., A. V. Somlyo, H. Gonzalez-Serratos, H. Shuman, and G. McClellan. 1980. The sarcoplasmic reticulum and its composition in resting and in contracting muscle. *In* Muscle Contraction: Its Regulatory Mechanisms. S. Ebashi, K. Maruyama, and M. Endo, editors. Japan Scientific Societies Press, Tokyo. 411–420.

Stern, M. D. 1992. Buffering of calcium in the vicinity of a channel pore. *Cell Calcium.* 13:183–192.

Tsien, R. Y. 1980. New calcium indicators and buffers with high selectivity against magnesium and protons: design, synthesis, and properties of prototype structures. *Biochemistry.* 19:2396–2404.

Zot, H. G., and J. D. Potter. 1987. Calcium binding and fluorescence measurements of dansylaziridine-labelled troponin C in reconstituted thin filaments. *Journal of Muscle Research and Cell Motility.* 8:428–436.